Alma Mater Studiorum – Università di Bologna

DOTTORATO DI RICERCA IN

BIOLOGIA CELLULARE E MOLECOLARE

Ciclo XXVII

Settore Concorsuale di afferenza: 05/E2
Settore Scientifico Disciplinare: BIO/11

TITOLO TESI

Structural and functional characterization of Group B *Streptococcus* pilus 2b

Presentata da: **Maddalena Lazzarin**

Coordinatore Dottorato

Chiar.mo Prof.
Davide Zannoni

Relatore

Dott.ssa
Daniela Rinaudo

Tutor Dottorato

Chiar.mo Prof.
Vincenzo Scarlato

Esame finale anno 2015

The aim of my PhD project was the study of the sortase-mediated assembly mechanism of *Streptococcus agalactiae* pilus 2b and the contribution of this pilus type to host infection.

The research work done during this PhD project lead to the following patent application and publications:

- Maione D., Cozzi R., Rinaudo D., **Lazzarin M.**, Zerbini F., Margarit Y Ros I. 2013. Pilus proteins and compositions. WO2013/124473(PCT/EP2013/053644), filed February 23, 2013 and issued August 29, 2013

- Cozzi R., Malito E., **Lazzarin M**., Nuccitelli A., Castagnetti A., Bottomley M. J., Margarit I., Maione D, Rinaudo CD. Structure and assembly of Group B *Streptococcus* pilus 2b backbone protein. SUBMITTED

- **Lazzarin M**., Cozzi R., Malito E., Martinelli M., D'Onofrio M., Maione D, Margarit I., Rinaudo CD. Assembly and cell-wall anchoring of Group B *Streptococcus* pilus type 2b by class C sortases. IN PREPARATION

- **Lazzarin M**., Mu R., Rinaudo CD., Margarit I., Doran KS. Funcional characterization of Group B *Streptococcus* pilus 2b in mouse models. IN PREPARATION

Table of Contents

Abstract

Group B *Streptococcus* or GBS (also referred as *Streptococcus agalactiae*) is a Gram-positive human pathogen representing one of the most common causes of life-threatening bacterial infections such as sepsis and meningitis in neonates and infants. Covalently polymerized pilus-like structures have been discovered in GBS as important virulence factors as well as vaccine candidates. Pili are protein polymers that form long and thin filamentous structures protruding from bacterial cells, mediating adhesion and colonization to host cells and other activities involved in the virulence of the bacterium. Gram-positive bacteria, including GBS, build pili on their cell surface via a class C sortase-catalyzed transpeptidation mechanism from pilin protein substrates that are the backbone protein (BP) forming the pilus shaft and two ancillary proteins (APs). Also the cell-wall anchoring of the pilus polymers made of covalently linked pilin subunits is mediated by a sortase enzyme. GBS expresses three structurally distinct pilus types (type 1, 2a and 2b). Although the mechanisms of assembly and cell wall anchoring of GBS types 1 and 2a pili have been investigated, those of pilus 2b are not understood until now. Pilus 2b is frequently found in ST-17 strains that are mostly associated with meningitis and high mortality rate especially in infants.

In this work the assembly mechanism of GBS pilus type 2b has been elucidated by dissecting through genetic, biochemical and structural studies the role of the two pilus-associated sortases. The most significant findings show that pilus 2b assembly (in terms of pilin subunits polymerization and cell-wall anchoring of the pilus polymers) appears “non-canonical”, differing significantly from the current model of pilus assembly in Gram-positive pathogens. Only one pilus-related sortase (SrtC1-2b) is involved in pilin polymerization, while the second sortase (SrtC2-2b) does not act as a pilin polymerase, but it is involved in cell-wall pilus anchoring by using the minor ancillary subunit as anchor protein. Our findings provide new insights into pili biogenesis in Gram-positive bacteria. Moreover, the role of this pilus type during host infection has been investigated. By using a mouse model of meningitis we demonstrated that type 2b pilus contributes to pathogenesis of meningitis *in vivo*.

Chapter 1. Introduction

1.1 *Streptococcus agalactiae* (Group B *Streptococcus*, GBS)

Group B *Streptococcus* or GBS (also referred to as *Streptococcus agalactiae*) is an encapsulated Gram-positive bacteria. It generally grows in pairs or in long chains of spherical bacteria, less than 2 μm in size (Fig. 1A). It displays beta-hemolysis when cultured on blood agar plates and produces zones of hemolysis that are only slightly larger than the colonies themselves (Fig. 1B) (1). GBS strains are classified into ten serotypes according to immunogenic characteristics of the capsule polysaccharides that surround its surface (Ia, Ib, II, III, IV, V, VI, VII, VIII and IX) (2). Approximately, 10% of serotypes are non-typeable (3).

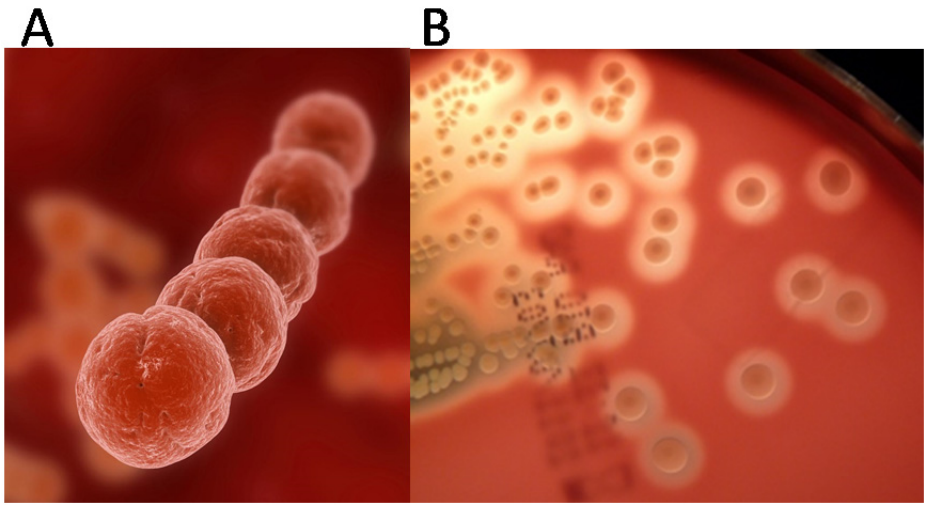

Figure 1. *Streptococcus agalactiae.* (A) Scanning Electron Microscopy (SEM) of *Streptococcus agalactiae.* (B) Colonies of *Streptococcus agalactiae* on a blood agar plate. Note the zone of clear haemolysis.

Consistent with other streptococcal species, *Streptococcus agalactiae* is present on the mucosal surfaces of animals and humans (4). In fact, GBS can usually colonize asymptomatically as a normal commensal the intestinal and genitourinary tract but also the pharyngeal mucosa of human healthy adults (5,6) and 20–40% of healthy women carry GBS (5,7,8). GBS can also cause serious bacterial infections in newborns and young infants leading to pneumonia, sepsis

and meningitis. To cause meningitis GBS has to interact and penetrate the blood-brain barrier (BBB) to gain access to the central nervous system (CNS). The BBB is mainly composed by a monolayer of specialized human brain microvascular endothelial cells (hBMEC), and it separates the brain from the circulating blood, thus regulating the flow of nutrients and also preventing circulating bacteria to permeate it (9,10). GBS has many surface virulence factors important for host infection and among them, pili have been recently implicated in mediating attachment to many different human epithelial cells (11), and among them also to brain microvascular endothelial cells (12).

GBS is not only one of the most common causes of life-threatening bacterial infections in neonates, but can cause severe infections in elderly and immune-compromised patients (13,14). Moreover *Streptococcus agalactiae* is also associated to a number of postpartum sequelae, such as urinary tract infections, amnionitis and endometritis (15).

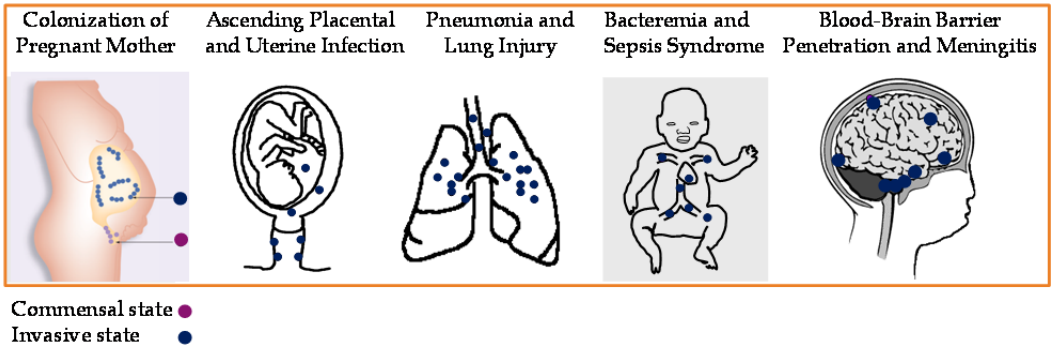

Figure 2. GBS cause serious bacterial infections in newborns and young infants. GBS commensal colonization of the rectovaginal tract of 10-30% of healthy women can be the cause of the 50-70% of children that will become colonized after delivery. The infection incidence is 1 out of 1200 live births per year.

GBS disease in newborns has been divided in early-onset disease (EOD) and late-onset disease (LOD) depending on the infants' age and disease manifestation. Early-onset disease manifests in the first week of life and the neonate is usually infected by exposure to GBS during birth. The transmission from mothers to newborns usually occurs when the neonate aspirates contaminated amniotic and vaginal fluids before or during delivery (16). Early-onset disease can progress as

pneumonia and the bacteria can spread into the bloodstream resulting in septicaemia, meningitis and osteomyelitis (17-19).

Infants who present late-onset disease do not show signs of infection in the first 6 days of life. LOD (7–90 days) is less frequent than EOD and the mortality rate is lower but morbidity is high, as around 50% of neonates that survive to GBS infection suffer complications, including mental retardation, hearing loss and speech and language delay (15,18,20).

Vaccination represents the most attractive strategy for GBS disease prevention. Effective vaccines would stimulate the production of functionally active antibodies that could cross the placenta and provide protection against neonatal GBS infection. During the last years, polysaccharide-based vaccines against GBS have been extensively studied, but also several promising protein antigens have been identified leading to the potential development of universal protein-based vaccines (21-24).

1.1.1 The hypervirulent clone ST-17

Population genetics methods have been applied to GBS strains to investigate genotypes associated with disease, assess genetic variation within genotypes, and examine the role of recombination in the generation of new genotypes. Several methods have identified specific GBS genotypes to be associated with neonatal disease. Multilocus sequence typing (MLST), which uncovers sequence variation among conserved housekeeping genes, has classified GBS strains into numerous clones, or sequence types (STs) (25). In this system, fragments (459 to 519 bp) of seven housekeeping genes are amplified by PCR for each strain and sequenced. The combination of alleles at the seven loci provided an allelic profile or sequence type (ST) for each strain. The majority of analyzed isolates causing neonatal diseases belongs to the ST-17 clone and is serotype III. This ST appeared to be associated with the late-onset disease (LOD) and meningitis in infants after the first week of life (26,27) (25). So the ST-17 serotype III strains were defined "highly virulent" clones since they were strongly associated with neonatal invasive infections (28) as reported from studies performed in Canada (29), in

Israel (30), Sweden (31), the United Kingdom (32), Portugal (33), France (34) and the United States (35).

By following phylogenetic analyses STs were grouped together into clusters or clonal complexes (CCs) and seven clusters have been identified to include the majority of the circulating clinically relevant GBS strains (30,36). The distribution of CCs has been shown to vary in colonizing and invasive strains (30,32,35,36). Different genomic studies showed that the ST-17 hypervirulent clone is a homogeneous group of strains that displays a conserved combination of secreted/surface proteins, including the pilus type 2b (37).

1.1.2 Identification of novel genomic islands coding for pilus-like structures in *Streptococcus agalactiae*

In the last decade, the exponential growth of genome sequence information has led to the identification in several Gram-positive organisms, including GBS, of covalently polymerized pilus-like structures that were remained largely unknown until then. Pili are protein polymers that form long and thin filamentous structures extending out from the bacterial cells, mediating adhesion and colonization to host cells, biofilm formation or other activities involved in the virulence/pathogenesis of the bacterium (38,39). Moreover, pili contribute to BBB penetration and meningitis development (40). It has been reported that these surface structures are involved in GBS adhesion and invasion of the host. Specifically, pili mediate the initial bacterial attachment to the host, binding to extracellular matrix (ECM) components and thus facilitating the bacterial uptake by host cells (41,42).

Additionally, a recent study provided evidence for an active role of *S. agalactiae* pilus proteins in the paracellular translocation through the epithelial barrier, during host colonization (43). Gram-positive pili could be considered important virulence factors for several diseases (44), in particular infections of the urinary, genital and gastrointestinal tracts and particularly in GBS they have been identified as promising vaccine candidates (23,24,45).

In 2005, characterization studies of protective antigens by a multiple genome approach aiming at the development of an effective vaccine against GBS

infections, revealed for the first time in a streptococcal species the existence of high-molecular-weight (HMW) polymers, visible by electron microscopy as pilus-like structures extending out from the bacterial surface (6;11;12).

Subsequently, comparative analysis of the eight published genome sequences have permitted the discovery in GBS of three genomic pilus islands (PIs), named PI-1, PI-2a and PI-2b (13). The overall organization of the three islands is similar to pilus gene clusters identified in other Gram-positive bacteria (9;14) (Fig. 3). Each of the GBS PIs encodes three structural pilus components, corresponding to the major pilus subunit (known as the backbone protein, BP) forming the pilus shaft and the two ancillary proteins (named ancillary protein 1, AP1 and ancillary protein 2, AP2). These structural subunits harbour a (L/I)PXTG sorting motif that is typical of cell wall-anchored proteins. In addition, the pilus clusters contain at least two genes coding for pilus-associated class C sortase enzymes (SrtC1 and SrtC2) catalyzing pilus protein polymerization (11;13).

PI-1 consists of an approximately 16 kbp-long DNA region flanked by 11 bp of direct repeats, and it has been found in ≈ 70% of the GBS strains that have been analyzed (24,46). In addition to the pilus genes, the genomic island contains a gene that encodes an AraC-type transcriptional regulator (Fig. 3A).

PI-2a and PI-2b represent two variants of Pilus Island 2 since they are alternatively present in the same genomic locus and define an approximately 11 kb region flanked by identical conserved genes. In addition to the genes coding for the three pilus structural subunits and two sortases, upstream of the *ap1* gene, the PI-2a region contains a gene coding for a *rogB* type transcriptional regulator (15). PI-2b lacks the transcriptional regulator but contains a gene that encodes for a protein similar to the LepA-type signal peptidase of Gram-negative bacteria (Fig. 3B).

The three pilus islands in GBS are similar in organization but poorly conserved among different isolates. Extensive genome analysis of pili distribution and conservation in large collection of GBS clinical isolates showed that all strains analyzed carried at least one of the islands, and 94% of these isolates expressed pili on their surface (24). In particular PI-1 is never found alone, but always in combination with one of the two variants of PI-2 (47).

Interestingly, a correlation was observed between the presence of a particular

combination of PIs and the capsule (CPS) type. All serotype III isolates (the most epidemiologically relevant serotype) carried a combination of two pilus islands: 30% of the strains contained PI-1 and PI-2a, while 70% carried PI-1 and PI-2b. Moreover, the highly virulent sequence type 17 (ST-17) seemed to be strongly associated with PI-1 plus PI-2b pattern (37(48,49)) suggesting the importance of this pilus type in bacterial virulence.

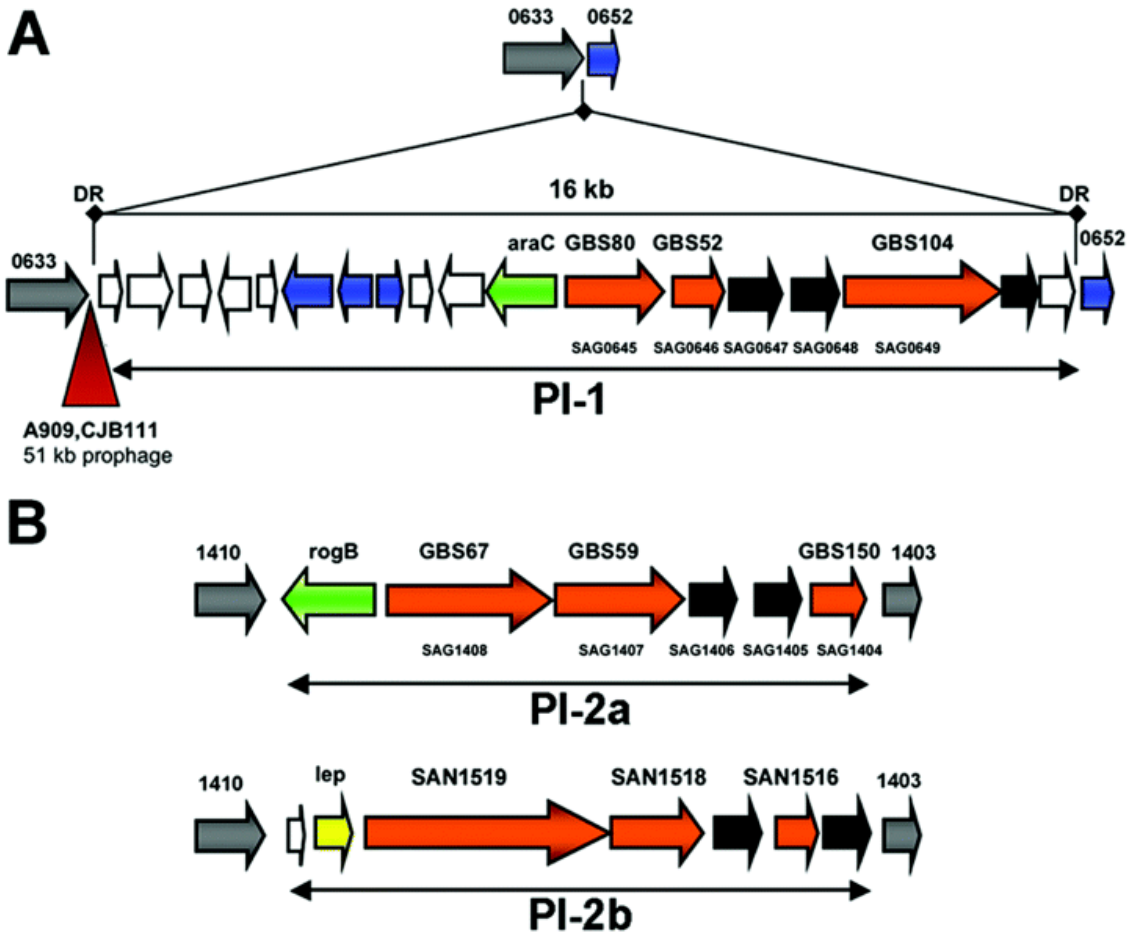

Figure 3. Schematic representation of GBS pilus-island regions. A) pilus island 1; B) pilus island 2. Genes coding for LPXTG-containing proteins are represented with orange arrows, whereas transcriptional regulators are in green and conserved flanking genes are in grey. At least two sortases are present in each PI (black arrows), while a signal peptidase is present in PI-2b (yellow arrow). For PI-1 and PI-2a, gene numbers are relative to the database annotation for strain 2603 V/R, while for PI-2b, gene numbers are relative to COH1 strain. DR: direct repeat (50).

1.2 Structure and assembly of Gram-positive pili

The best-known and characterized pili are those of Gram-negative bacteria: the Type I and Type P pili of Escherichia coli, and the Type IV pili of Neisseria species (51), which form rod-like bundles of non-covalently assembled subunits. In contrast, the pili on Gram-positive bacteria are basically different. They are long (2–5 μm) but extremely thin (about 3 nm), assembled by enzymes called sortases, and they are exceptional examples of covalent polymers (Fig. 4).

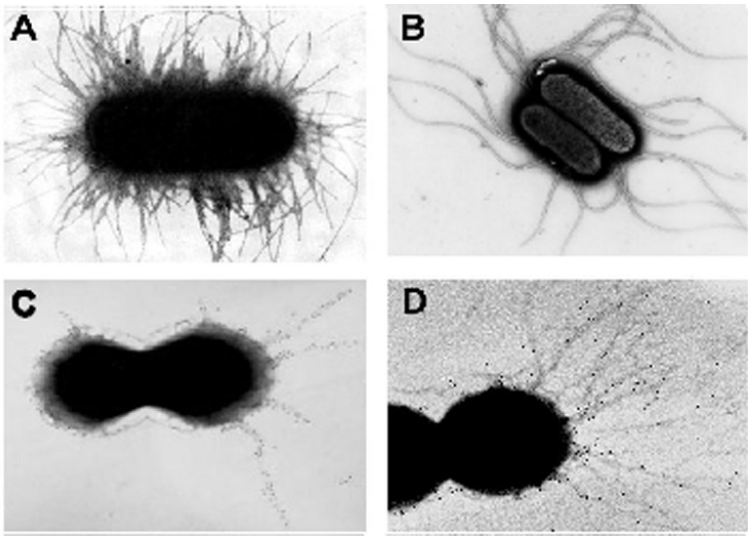

Figure 4. Different examples of pilus-like structures in Gram-negative and Gram-positive bacteria. Electron micrographs of fimbriae in Gram-negative organisms : *E. coli* (A) and *Salmonella enterica* (B). Electron microscopy of two different types of pili in Gram-positive bacteria: fibrils in *Streptococcus salivarius* (C) and pili in *Streptococcus agalactiae* (D) stained by immunogold labeling (52).

Despite many years of studies on Gram-positive bacteria, their pili remained largely ignored until very recently (53). The identification and the characterization of pilus structures in different Gram-positive microorganisms in a very short time (from 2005 to date) represent an example of the amazing impact of genomics in accelerating the discovery of previously unknown functions. (53). Pili can be visualized on the bacterial surface by negative staining, or, more specifically, by immunogold electron microscopy (IEM), which can reveal the localization of a

protein within the pilus structure using pilin specific antisera (Fig. 5B-D-F). Gram-positive pili are composed of multiple copies of a single pilin called backbone protein (BP), and of other two additional proteins associated with the shaft (called major and minor ancillary proteins).

However, the expression of pilus structures can be generally detected by immunoblot assays using total cell proteins separated by SDS-PAGE and probed with antisera anti pilin subunit. A protein that is part of a pilus will appear as a high molecular weight (HMW) ladder (Fig. 5A-C-E).

The backbone protein has been demonstrated to be very important for pilus polymerization and function. Indeed it has been reported that no pilus structures can be detected on the bacterial cell surface if the *BP* gene is deleted, suggesting the backbone protein is required for incorporating other two ancillary proteins into the pilus structure (50). In fact antisera specific for the backbone protein stain the whole length of the pilus structure (52), while, antisera specific for ancillary protein 1 (AP1) detect this pilin subunit at the pilus tip and along the pilus shaft (50). The minor ancillary pilus component, AP2, is thought to be the terminal pilus subunit, located at the pilus base (54) (55). Ancillary proteins (APs) are not required for backbone protein polymerization but might function as adhesins or in anchoring to the cell wall (55).

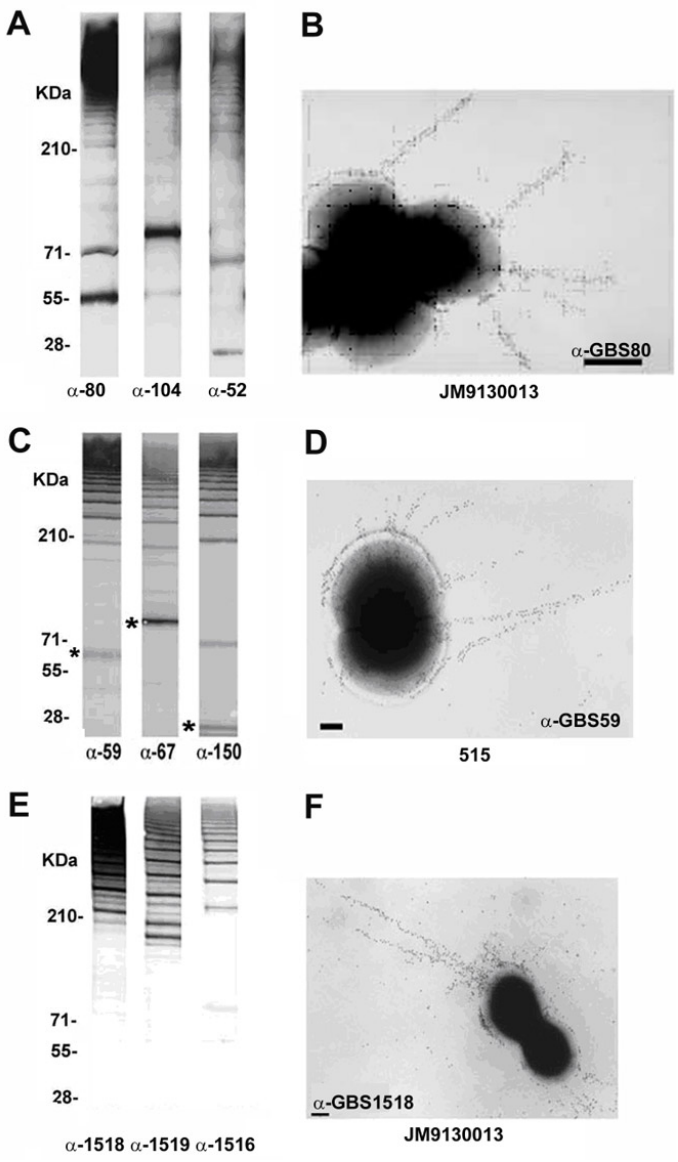

Figure 5. GBS PI-1, 2a and 2b pili. (A) Immunoblots of total protein extracts from GBS JM9130013 strain probed with antisera specific for PI-1 proteins GBS80 (α-80), GBS104 (α-104) and GBS52 (α-52). **(B)** Immunogold labeling and transmission electron microscopy of GBS80 in strain JM9130013, showing long pilus-like structures.**(C)** Immunoblots of total protein extracts from GBS 515 strain probed with antisera specific for PI-2a proteins GBS59 (α-59), GBS67 (α-67) and GBS150 (α-150). Asterisks (*) indicate the monomeric form of GBS59, GBS67 and GBS150. **(D)** Immunogold electron microscopy of 515 strain incubated with sera raised against GBS59 protein and labeled with secondary antibodies conjugated with 10nm gold particles. **(E)** Immunoblots of total protein extracts from GBS JM9130013 strain probed with antisera specific for PI-2b proteins SAN1518 (α-1518), SAN1519 (α-1519) and SAN1516 (α-1516). **(F)** Immunogold electron microscopy of JM9130013 wt strain incubated with sera raised against GBS1518 protein and labeled with secondary antibodies conjugated with 10nm gold particles (50).

The three pilus proteins together with genes coding for sortases, that are required for pilus assembly, are encoded in a small gene cluster within pathogenicity islands which are known as Pilus Islands (PIs). The genes are transcribed in the same direction, indicating that they are part of an operon. The three pilus components are characterized by the presence of an N-terminal signal peptide together with a C-terminal cell-wall sorting signal (CWSS) that is found in many surface proteins and is required for the attachment to the peptidoglycan of the cell wall. The CWSS comprises the amino acid sequence "LPXTG" (where X denotes any amino acid) or a variation of this motif followed by a hydrophobic membrane-spanning domain and a positively charged tail.

This motif is targeted by sortase enzymes, which are membrane-bound transpeptidases catalysing the covalent linkage of LPXTG motif proteins. During pilus formation, specific pilus-related sortases catalyse the covalent attachment of the pilin subunits to each other or to the peptidoglycan cell wall (52).

The first insights into the assembly mechanism of Gram-positive pili were provided by a study performed on *Corynebacterium diphteriae* (50, 60).

Initially, the three pilus components containing an LPXTG motif are secreted in a Sec-dependent way (52). Each component remains anchored to the cell membrane, owing to the presence of the C-terminal hydrophobic transmembrane domain.

The second step involves a sortase-dependent reaction in which the membrane-anchored proteins are cleaved at the LPXTG motif, between the threonine (T) and glycine (G) residue. This reaction leads to the formation of acyl-enzyme intermediates in which a covalent thioester bond is formed between the thiol group of the cysteine residue located in the catalytic pocket of the sortase and the carboxyl group of the threonine residue in the LPXTG motif of the pilin protein (52). Because sortases are membrane-associated enzymes, the acyl-enzyme derivatives that are formed are retained on the external side of the membrane (Fig. 6).

The following steps of the assembly process involve the oligomerization of the pilus protein subunits and the anchoring of the oligomerized structure to the cell wall.

These steps require the nucleophilic attack of the thioester bond in the acyl-enzyme intermediate. During pilus polymerization the nucleophile is provided by

the ε-amino group of a specific lysine (K) residue within the "pilin motif", WXXXVXVYPKN (where X denotes any amino acid), which has been found in most of the pilin subunits that have been characterized (55).

The nucleophilic attack results in cleavage of the thioester bond and concomitant formation of an amide bond between the carbonyl-group carbon of the threonine residue of the pilin subunit (present in the catalytic pocket of the sortase) and the lysine side-chain (ε-amino group) of the pilin motif of the neighboring pilin subunit. This leads to the formation of a membrane-associated covalently linked dimer with a pilin motif that can interact with other sortase- associated pilin subunits, forming an elongated pilus fiber.

According to this model, pilus growth occurs by subunit addition at the base of the pilus (Fig. 6), and the length of the pilus depends on the relative abundance of the pilus subunits that are coupled to the membrane-associated sortases (52). Finally, the association of the membrane-proximal pilus subunit with the cell wall occurs when the thioester bond between the subunit and the sortase is subject to nucleophilic attack by the amino group in the cross-bridge of the peptidoglycan precursor lipid II (56), and this leads to the formation of an amide bond between the basal subunit and the bacterial cell wall.

In conclusion, pilus assembly in Gram-positive bacteria seems to occur by a universal mechanism of ordered cross-linking of precursor proteins, whose multiple conserved features are recognized by designated sortase enzymes (55,57). Also GBS pili are covalently linked structures that follow this biphasic assembly mechanism (58). SortaseC-polymerized backbone protein (BP) units constitute the pilus scaffold and ancillary proteins 1 and 2 are located respectively at the tip and the base of the pilus. Polymerized pili are anchored to the cell wall by the housekeeping sortase A (SrtA) and protrude from the bacterial cell surface. No detectable role in pilus polymerization for the housekeeping SrtA was found in GBS (50,59).

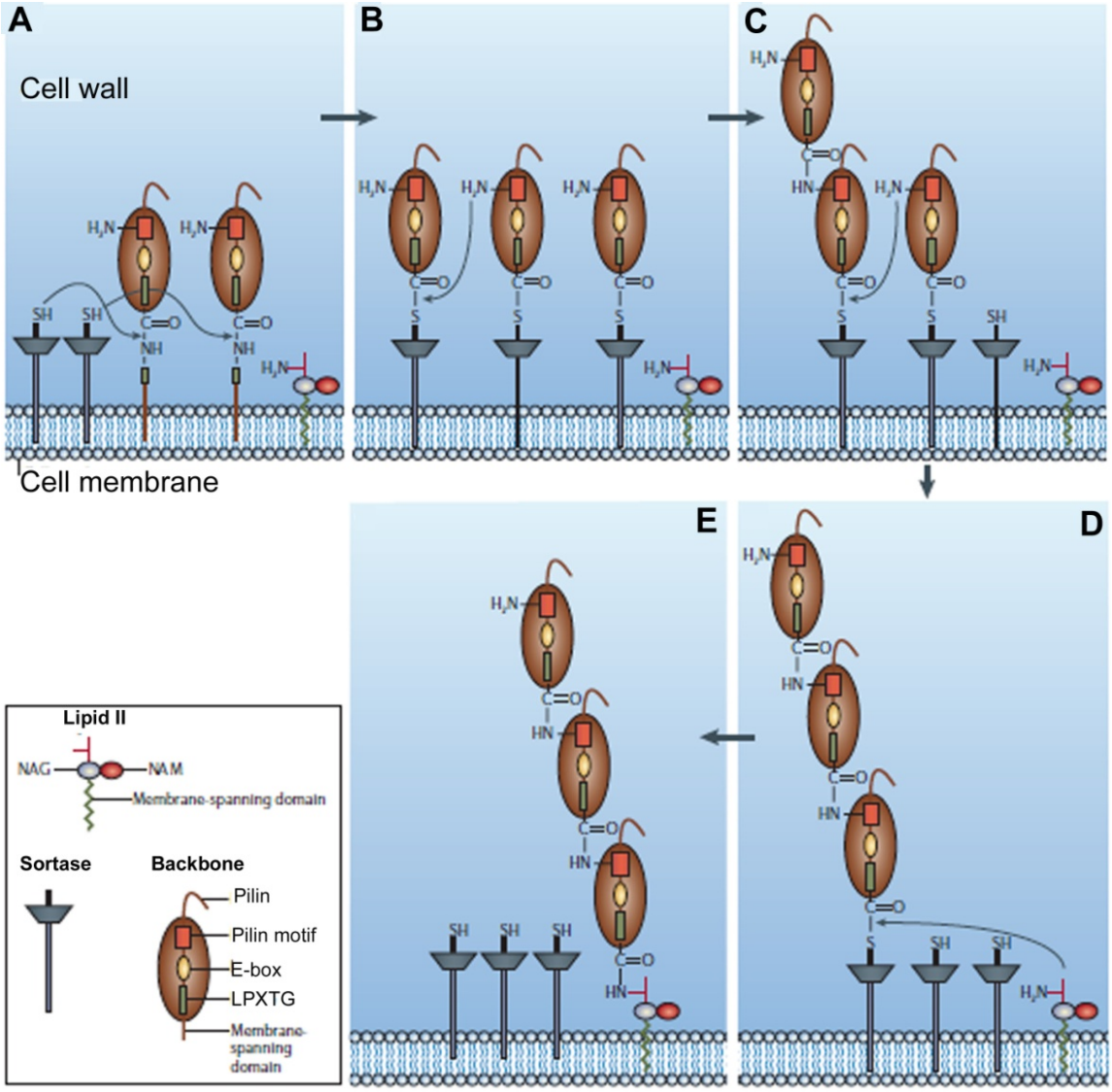

Figure 6. General model for pilus assembly in Gram-positive bacteria (52). (A) In the first step, proteins that contain the amino-acid motif LPXTG are targeted to the cell membrane by Sec-dependent secretion (not shown). This is followed by a sortase-mediated reaction (indicated by the arrows) in which the LPXTG motif is cleaved between the threonine (T) and glycine (G) residues. **(B)** The reaction leads to the formation of an acyl-enzyme intermediate in which a covalent thioester bond is formed between the thiol group of a cysteine residue in the sortase and the carboxyl group of the pilin threonine residue. **(C)** Oligomerization occurs after the nucleophilic attack provided by the e-amino group of the lysine residue in the pilin motif on the cysteine residue of the sortase. **(D)**The thioester bond between the pilin subunit and the sortase is targeted by the amino group of the pentapeptide of lipid II, the precursor of peptidoglycan. **(E)** This leads to the formation of an elongated pilus covalently linked to the cell wall peptidoglycan. NAG, *N*-acetyl glucosamine; NAM, N-acetyl muramic acid (52).

1.3 Sequence and structure of pilin subunits

The current model proposed for pilus assembly in Gram-positive bacteria as already described above, is based on a transpeptidation mechanism of pilins (58). Sortases recognize specific sequence elements and/or residues in the pilin subunit that are essential for pilus assembly, and well conserved among pilin-subunits in different bacteria. Briefly, these main motives include:

- the pilin motif (consensus WxxxVxVYPK), wherein the lysine residue (K) participates in sortase-catalysed amide bond formation by reaction with the C terminus of the next subunit molecule during polymerization;
- a cell wall sorting signal (CWSS) containing the sortase recognition site LPxTG motif, typical of cell wall-anchored proteins;
- the E-box motif (consensus YxLxETxAPxGY), important for the proper folding of pilin proteins and subsequently necessary for pilus polymerization (60-62). Moreover, several X-ray crystal structures of backbone pilins have shown that a specific E-box residue is involved in the formation of intramolecular isopeptide bonds and that these linkages confer higher stability to the monomeric subunit (63-65).

Despite low sequence similarities, pilin subunits of Gram-positive bacteria show very similar tridimensional structure comprising immunoglobulin G (IgG)-like domains of shared evolutionary origin. These domains are all stabilized by intramolecular isopeptide bonds commonly formed by Lys-Asn residues (although Lys-Asp bonds also exist) located in a largely hydrophobic pocket comprising several aromatic residues, including a bond-catalyzing aspartyl or glutamyl residue.

Intriguingly, in the backbone protein of GBS pilus 2a (BP-2a) and in other major pilins this glutamate is the same conserved residue present in the E-box motif (50,62).

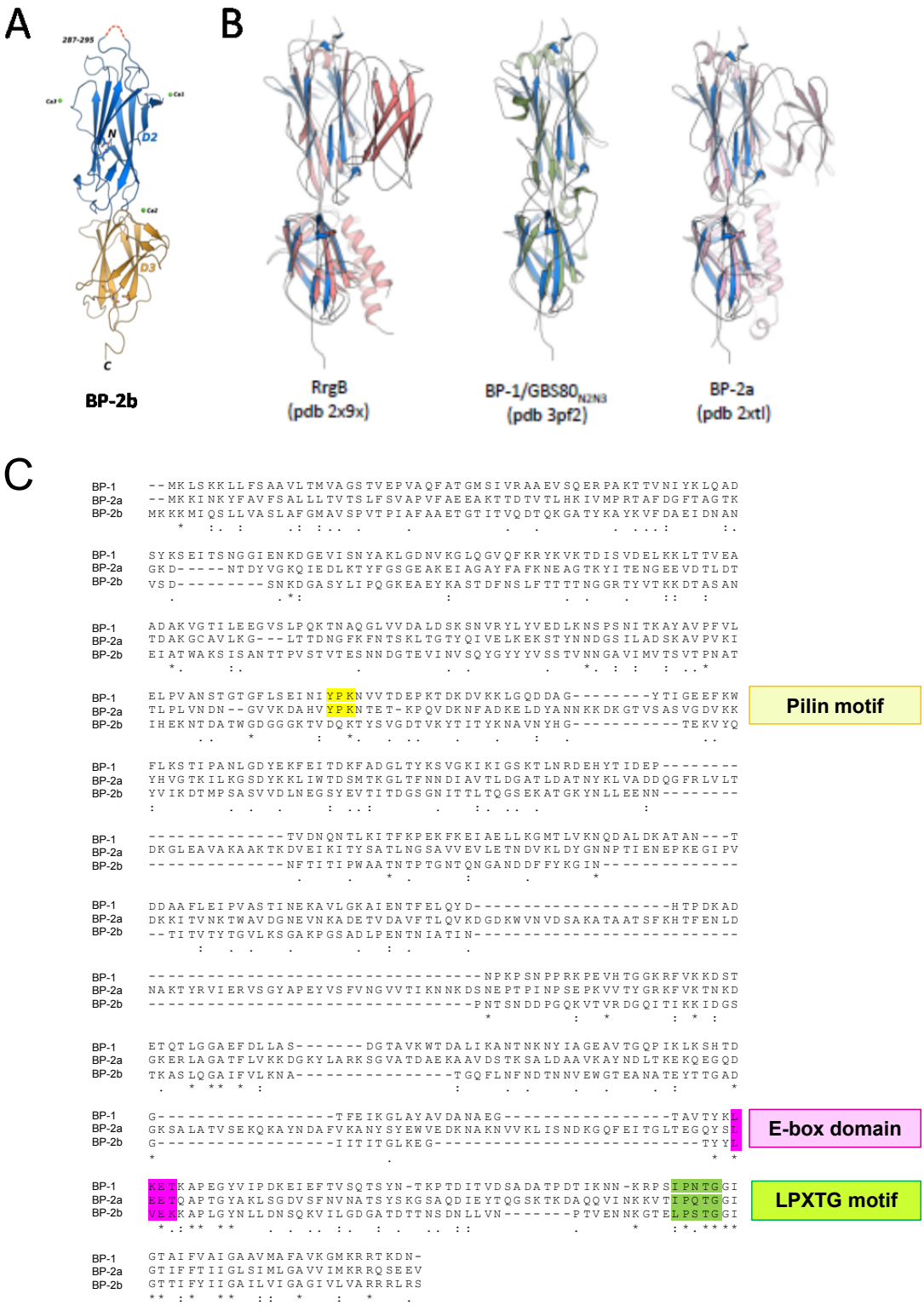

Figure 7. Comparisons of BP-2b with other pilus backbone proteins. A) The structure of BP-2b is depicted with light blue and orange cartoons for domains D2 and D3. B) BP-2b (blue cartoon) is shown overlaid onto: the pilus backbone protein RrgB (pdb 2x9x, red cartoon, left), the major pilin protein GBS80 (GBS-PI-1) (pdb 3pf2, green cartoon, middle), and on the major pilin protein BP-2a (pdb 2xtl, pink cartoon, right). C) Primary sequence alignment of BPs of the three PI in GBS.

In recent years, the X-ray crystal structures of several Gram-positive pilin proteins from *Corynnebacteium diphtheriae* (66,67), *Actinomyces species* (68,69), *Streptococcus pyogenes* (65), *Streptococcus pneumoniae* (70-74), *Streptococcus agalactiae* (45,75-77) and *Bacillus cereus* (78) have been described.

Also BP-2b X-ray structure was solved encompassing domains D2 and D3 (Fig. 7A). Both domains revealed an IgG-like fold organization, typical of the pilin subunits, and the presence of internal isopeptide bonds in each domain. Nevertheless, except for the typical C-terminal cell wall sorting signal BP-2b does not contain the canonical conserved primary sequence motives described for pilus polymerization in Gram-positive bacteria, suggesting a different mechanism of assembly of this pilus type. BP-2b indeed does not harbor a canonical E-box domain neither a conserved pilin motif (Fig. 7C).

1.4 Sortase enzymes in Gram-positive bacteria

Sortases are a family of membrane-associated enzymes, known especially to catalyze the covalent anchoring of surface proteins to the cell wall envelope in Gram-positive bacteria (79,80). These enzymes are cysteine transpeptidases, which recognize a conserved carboxylic CWSS followed by a hydrophobic stretch of amino acids and a short positively charged tail (57,80,81).

Sortases are positioned at the cytoplasmic membrane via a membrane anchor located either at the N- or C-terminus, contain the active site, LxTC motif (80), of which cysteine is essential for the sortase activity (82) and recognize their substrate proteins via a common C-terminal pentapeptide sequence, which acts as a cell wall sorting signal. So far, more than 700 putative sortase substrates encoded by more than 50 different prokaryotic genomes have been identified (83). Although they are not essential for bacterial viability when cells are grown in rich media, sortases can be important virulence factors as they display surface proteins that mediate bacterial adhesion to host tissues, host cell entry, evasion and suppression of the immune response and acquisition of essential nutrients.

Multiple sortases are often found in the same genome in different bacterial species and can be grouped into six classes based on their primary sequences, membrane topology, genomic localization, and specificity for amino acid sequence motifs

(84,85). These six families include class A to F enzymes (Fig. 8) (84) (11). Experimental and bioinformatics analyses indicate that members of each group recognize distinct CWSSs in which the LPXTG sequence is diverse (hereafter called sorting signal motifs).

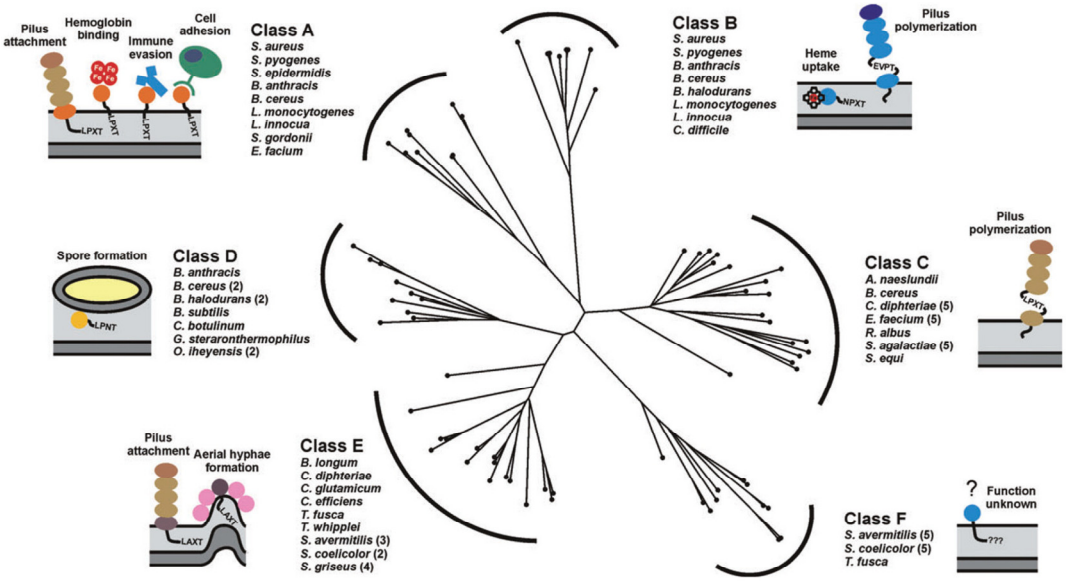

Figure 8. Phylogenic tree showing the relationships among the six classes of sortases from Gram-positive bacteria. A multiple sequence alignment based on pairwise constraints of a selected set of 73 sortase proteins was generated using the program COBALT and a phylogenetic tree constructed using the neighbour joining method (86). The analysed sortases can be partitioned into six distinct subfamilies based on their primary sequences. It should be noted that the class D and E enzymes described here are collectively referred to as a class D enzymes by Bierne and colleagues (85). Class D and E enzymes have also previously been referred to as subfamily-4 and -5 enzymes (84). The bacterial species associated with the enzyme classes A–F are listed and schematic representations of the main biological function of their corresponding sortase substrates are illustrated (79).

Class A enzymes appear to perform a housekeeping role in the cell as members of this group are able to anchor a great number of functionally different proteins to the cell wall. The sorting reaction catalyzed by the sortase A protein from *Staphylococcus aureus* (SrtA) is the best understood and begins when a full-length precursor protein containing an amino terminal leader peptide is exported from the cytoplasm through the secretory pathway. The C-terminal CWSS is then processed by SrtA. The C-terminal charged tail presumably retards export,

positioning the protein for processing by the extracellular membrane associated SrtA enzyme. Then a highly conserved active site cysteine residue in SrtA nucleophilically attacks the backbone carbonyl carbon of the threonine residue in the LP*X*TG motif, breaking the threonine and glycine peptide bond and creating a sortase-protein complex in which the components are linked via a thioacyl bond. The protein is then relocated by SrtA to the cell wall precursor lipid II, when the amino group in this molecule nucleophilically attacks the thioacyl linkage to create an isopeptide linked protein-lipid II product. Transglycosylation and transpeptidation reactions synthesize the cell wall and then incorporate this product into the peptidoglycan, where it is covalently linked to the cross-bridge peptide. Other sortases catalyse a similar transpeptidation reaction, but join remarkably different LPXTG motifs and amino groups.

Most surface proteins attached by class A enzymes contain a canonical LPXTG motif within their CWSS and have diverse functions that can promote bacterial adhesion, nutrient acquisition, host cell invasion, and immune evasion.

Class A enzymes have attracted significant interest as potential drug targets because a number of clinically important pathogens use these sortases to display virulence factors and they are attenuated in their virulence if their *srtA* gene is eliminated (*S. aureus, L. monocytogenes, Streptococcus pyogenes* and *Streptococcus pneumoniae* among others) (87) (88).

Class B enzymes can have distinct functions. Some members of this group attach haem-receptors to the peptidoglycan, while others assemble pili especially during iron starvation conditions.

Class C enzymes are broadly distributed in Gram-positive bacteria and function as pilin polymerases that construct pili.

Class D enzymes predominate in Bacilli and in *Bacillus anthracis;* this type of enzyme anchors proteins to the cell wall that facilitate sporulation.

Actinobacteria contain class E and F enzymes whose functions are largely unknown. In *Corynebacterium diphtheriae* a class E enzyme appears to perform a housekeeping function similar to class A enzymes (55), while class F enzymes have yet to be studied.

Sortases are also present in a few Gram-negative and archaebacterial species, but the functions of these enzymes are still unknown (84,89,90).

1.4.1 Class C sortases

The class C sortases, also called pilus-specific sortases, represent the biggest and most heterogeneous group of enzymes and are encoded by genes clustered together with the genes coding for the pilus structural subunits in genomic islands inserted in specific loci of the genome. The overall organization of these pilus islands is similar among Gram-positive bacteria.

In GBS, sequence comparison by multiple alignment and phylogenetic analysis allowed the identification of 3 major clusters, corresponding to class C sortases of PI-1, PI-2a, and PI-2b, with amino acid identities ranging from 15 to 60% (Fig. 9).

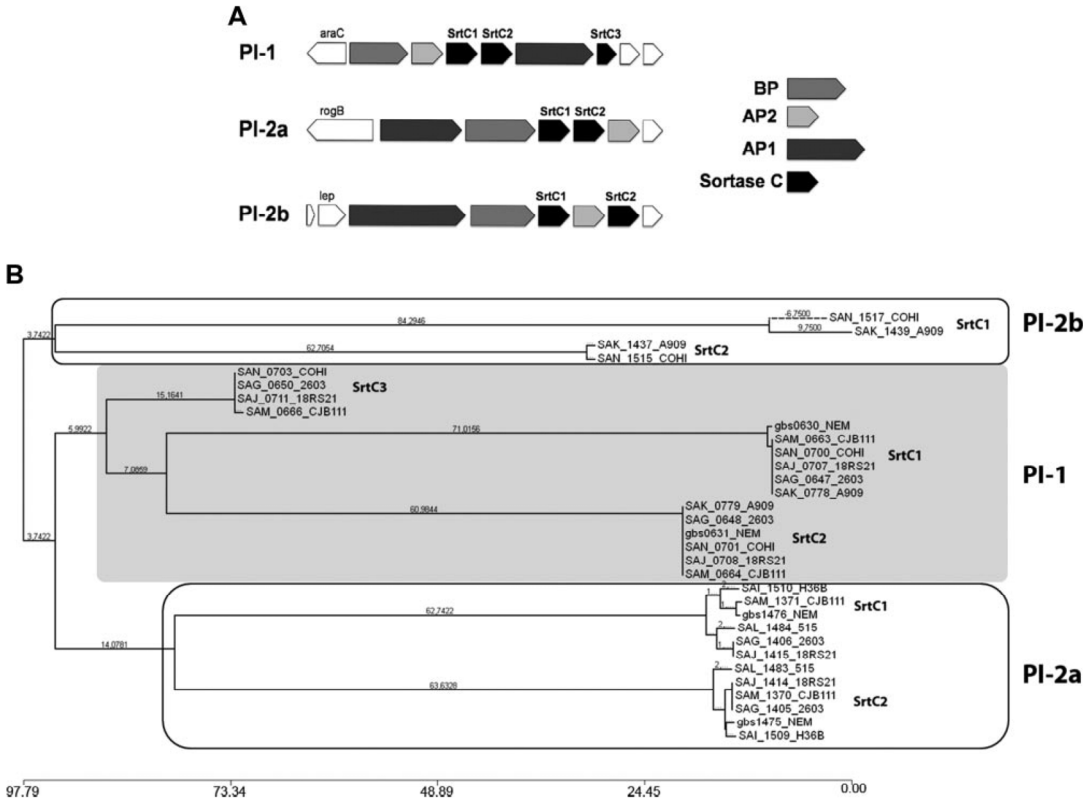

Figure 9. Class C sortases in PIs of GBS. (A) Schematic representation of GBS PIs. **(*B*)** Phylogenetic tree inferred from the alignment by the neighbor-joining distance-based method of C sortases from the available genomes of GBS. Single sortases are indicated by TIGR annotation. The 3 major clusters, highlighted in the boxes, include C sortases of each PI (91).

Although the assembly mechanism and cell wall anchoring of GBS type 1 and 2a pili have been investigated, those of pilus type 2b are not understood. In GBS pilus 1 and 2a two class C sortases (SrtC1 and SrtC2) are involved in the pilin proteins polymerization and the assembly mechanism occurs following the classical biphasic model (56).

Genetic studies showed that (50) SrtC1 and SrtC2 from pilus 1 and 2a can both efficiently polymerize the backbone proteins and were found to be specific in terms of ancillary proteins incorporation (50). The cell wall anchoring of pilus type 2a is mediated by the housekeeping SrtA through the use of the minor ancillary pilin as anchor protein as clearly demonstrated both by genetic (59) and biochemical studies (92).

The available crystal structures of class A and C sortases from different Gram-positive pathogens revealed similar overall folding. They share a common catalytic domain, based on a β-barrel core and a highly conserved catalytic triad made of histidine, cysteine, and arginine residues (91,93-98). Recently, a wide characterization of pilus-associated sortases from *Streptococcus pneumoniae* pilus 1 (SrtC-1, SrtC-2, and SrtC-3) was performed, and the X-ray structures of all 3 SrtC enzymes have been solved (94) (99). Also in this case the overall fold of the three enzymes is very similar to other known sortases, with a β-barrel core composed of eight anti-parallel β-strands linked by multiple helices. The conserved catalytic triad within the substrate binding region is encapsulated by the so-called lid that is an N-terminal flexible loop, which maintains the active site in a closed and inactive conformation in the absence of substrate. This loop anchors the active site through multiple interactions with the key catalytic residues (93,94). While the catalytic triad of Cys, His, and Arg side chains within the active site cleft is absolutely conserved among different classes of sortases (100) (101), including SrtA from *Staphylococcus aureus*, the region corresponding to the lid is found only in pilus-related C sortases of Gram-positive bacteria (93) (102).

The crystal structures of several other pilin-related class C sortases, including AcSrtC-1 from *Actinomyces oris* (97), SrtC1 from *S. suis* (98) and GBS (91,96,103), have been reported. These structures all reveal a core 8-stranded β-barrel, with the catalytic triad (His, Cys, Arg) situated in the active site at the end of a groove along one side of the β-barrel. *S. suis* SrtC1 structure was determined

with the active-site in the 'open' conformation, while the other structures showed the active site occluded by the lid.

The lid in SrtC1 from GBS PI-2a (SrtC1-2a) and *Actinomyces oris* SrtC2 has been demonstrated to be dispensable for sortase activity *in vivo* (91,104) suggesting a regulatory role for the enzyme activity.

1.4.2 Structural and functional characterization of sortases C of GBS PI-1 and 2a

The crystal structures of GBS C sortase from PI-2a (SrtC1-2a) and PI-1 (SrtC1-1 and SrtC2-1) have been determined (Fig.10 and 11).

The ectodomain of sortase SrtC1 of PI-2a was crystallized and the structure was solved by molecular replacement (91).

The overall fold of SrtC1-2a is highly similar to the structure of previously studied pilus-associated sortases. A β-barrel made of 9 antiparallel β-strands forms the core of the enzyme; a so-called roof made of 3 α-helices is positioned above the β-barrel and a loop (known as the "mobile lid") covers the active site (Fig. 10A), placed on one inner side of the β-barrel core and made of the catalytic triad His157-Cys219-Arg228. The lid of SrtC1-2a harbors 3 residues, Asp84, Pro85, and Tyr86, which make interactions with residues of the active site and surroundings. The aromatic benzene ring of Tyr86 is close enough to the catalytic Cys219 side chain to make an aromatic-sulfur interaction (91). As shown previously, this sulfur-aromatic interaction is conserved in other sortases suggesting a general mechanism of anchoring the lid within the active site (105) (Fig. 10B). This sulfur-aromatic interaction has been hypothesized to strengthen the anchoring of the lid within the active site (94). This network of interactions between catalytic residues and those located on the lid (Asp84 and Try86) is postulated to regulate the movement of the lid and therefore the access of LPXTG substrates to the active site (91,99).

Through site-directed mutagenesis and *in vivo* complementation studies, it has been demonstrated that each residue in the conserved catalytic triad of SrtC1-2a (Fig. 10) is essential for pilus polymerization; these data confirm the relationship between GBS C sortases and other members of sortase family.

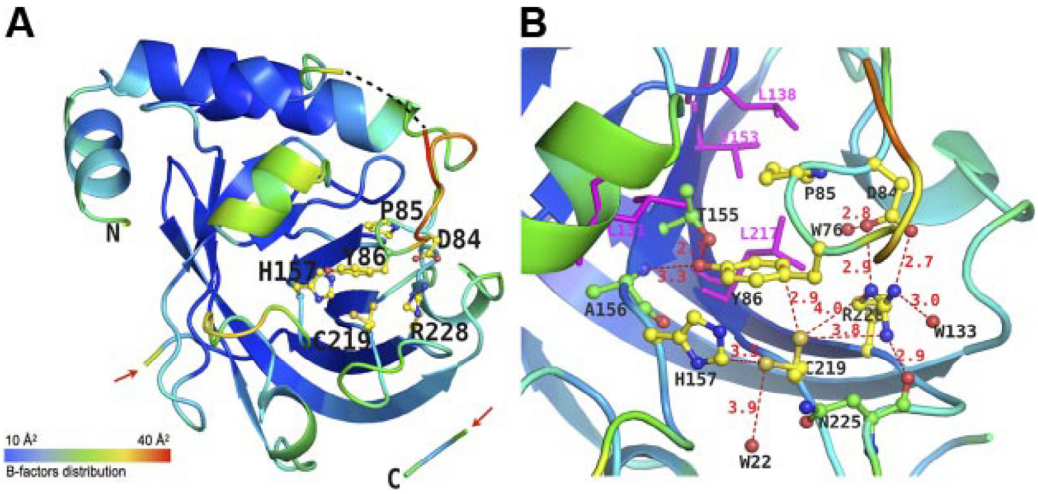

Figure 10. Overall folding of SrtC1-PI-2a and active site organization. *A*) Overall folding and *B* factors of SrtC1-PI-2a. SrtC1-PI-2a is represented as a cartoon, colored according to *B*-factor distribution, from low (blue) to high (red). Residues forming the mobile lid and the active site are shown as balls and sticks and are labeled. N and C termini are labeled. Carbon, oxygen, an nitrogen atoms are depicted in yellow, red, and blue, respectively. Position of residues 92–93 of the mobile lid, missing from the model because of poor electron density, is indicated by black dashes. Red arrows indicate the gap in the C-terminal region, fragment of residues 240–249. *B*) Active site of SrtC1-PI-2a. Residues forming the mobile lid (Asp84, Tyr86) and the active site (His157, Cys219, Arg228) are shown as balls and sticks, with carbon, oxygen, and nitrogen atoms in yellow, red, and blue, respectively. Conserved surrounding and interacting residues (Thr155, Ala156, Asn225) are shown as balls and sticks, with carbon, oxygen, and nitrogen atoms in green, red, and blue, respectively. Conserved hydrophobic residues are shown as magenta sticks and labeled in magenta. Distances between atoms are labeled and shown as red dashes. Water molecules are shown as red spheres. Background cartoon representation of SrtC1-PI-2a is colored according to *B* factors as in panel *A* (91).

Structural and biochemical data indicated that the lid maintains the enzyme in an inactive and closed conformation and that, for the enzyme activation, the lid needs to move. Accordingly, the deletion of the lid region does not abrogate pilus protein polymerization because its role is not catalytic; rather, it is a catalytic cleft-blocking loop, and only its movement can activate the enzyme *in vivo* (91). Based on these analyses, the SrtC enzymes can be considered as having two functional domains: one involved in enzyme regulation and probably specificity; and an enzymatic region, the β-barrel core that contains the catalytic triad (95). Moreover, the predicted C- and N-terminal TM domains of GBS SrtC1-2a are

absolutely required for sortase biological function (91). The importance of TM domains for the enzyme activity has been recently reported by Ton-That and co-workers (106) who showed that the predicted C-terminal TM domain of pilus-associated sortase SrtA is essential for efficient pilus polymerization in *C. diphtheriae*.

Open main questions are to understand how this movement can be regulated by the interaction with the pilus proteins and to identify which are the residues involved in stabilizing the active open lid conformation of the enzyme.

.

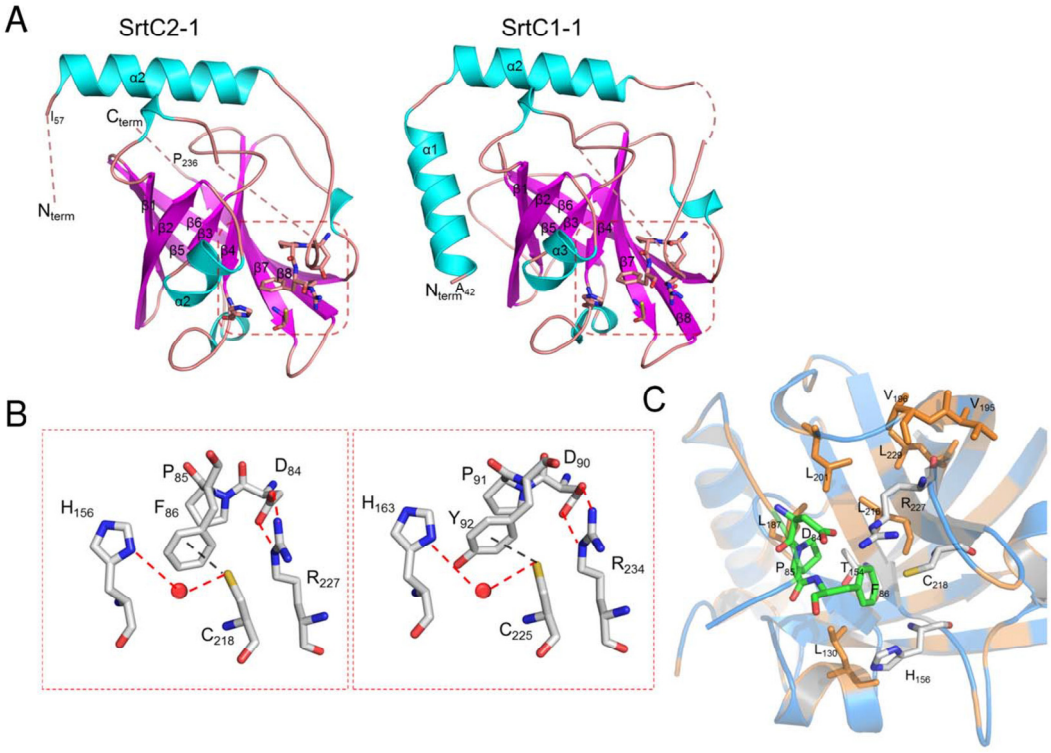

Figure 11. Overall fold of GBS PI-1 SrtC1 and SrtC2 and active site organization. (A) Overall fold of SrtC2 and SrtC1. Residues linking the mobile lid to the second helix and to the first beta-strand are missing in the final structures because of poor electron density, and are shown here as dashed lines. (B) Active sites of SrtC2 and SrtC1. Residues forming the mobile lid (Asp84-Phe86 in SrtC2 and Asp90-Tyr92 in SrtC1) and the active site (H156, C218, R227 in SrtC2 and H163, C225, R234 in SrtC1) are shown as sticks where sulfur, oxygen, and nitrogen atoms, are depicted as yellow, red, and blue, respectively. Water molecules are shown as red spheres. (C) The DPX motif is proximal to the catalytic triad of SrtC2, which is surrounded by conserved hydrophobic residues shown as sticks, where carbon, oxygen, and nitrogen atoms, are depicted as salmon, red, and blue, respectively (95).

The crystal structures of GBS PI-1 SrtC2 and SrtC1 were also determined (Fig.11). In both structures, the catalytic residues are not accessible to pilin substrates, suggesting that the enzymes cannot bind substrates in this conformation.

Also, these sortase C enzymes contain an additional N-terminal extension of approximately 50 residues, composed of one or two α-helices and a lid that blocks the access of substrates to the active site, further supporting the already proposed regulatory role played by the lid in restricting the access of the pilin substrates to the catalytic cleft (91,93,94).

Both class A and class C sortases cleave LPXTG-like motifs, but only sortase C can polymerize the pilus proteins to form high molecular weight structures.

In vitro and *in vivo* complementation studies revealed that both GBS PI-1 sortases C cleaved all the LPXTG-like peptides tested and exhibited a functional promiscuity for pilin subunit incorporation into pili, although each enzyme predominantly incorporates into pili one of the two ancillary subunits.

Multiple sequence alignment of all GBS sortase C enzymes and structural homology modeling, showed that, in contrast with the highly similar SrtC enzymes of PI-1 and PI-2a, the pilus-associated sortases of PI-2b are shorter.

In addition, even if the catalytic triad is conserved, SrtC1 from pilus 2b does not contain the conserved motif DPY(F/W) in the lid, and SrtC2 completely lacks this region and the C-terminal TM domain.

PI-2b in GBS has a similar genetic organization to group A *Streptococcus* (GAS) FCT-3 pilus, and like GAS, it contains the *LepA* gene required in GAS for pilus polymerization (107).

1.5 Aim of the thesis

Assembly and anchoring mechanisms of Gram-positive bacteria pili, including GBS pilus 1 and 2a types have already been characterized.

In these assembly mechanisms pilin subunits are covalently linked by a transpeptidation mechanism by class C sortases and subsequently polymerized pili are anchored to the cell wall peptidoglycan by the housekeeping sortase A through the minor ancillary protein. The resulting protruding pili are then involved in the interaction with the host, mediating the bacterial initial attachment.

The aim of this thesis work is to investigate the mechanism of GBS pilus 2b biogenesis unknown until now and also to elucidate its role during host interaction. By using a multidisciplinary approach including structural, biochemical and genetic studies, such as site-directed mutagenesis and complementation of KO GBS strains lacking the genes for each sortase (*SrtC1* and *SrtC2*) we unraveled the specific role of the two sortases and identified the key residues/motifs essential for pilus assembly and sortases activity.

We also elucidated pilus 2b importance during host interaction using both *in vitro* cell models and *in vivo* mouse meningitis model.

Chapter 2. Results

2.1 Pilus 2b assembly

2.1.1 PI-2b backbone protein characterization

The backbone protein of GBS Pilus Island 2b (BP-2b) is 502 residues long and carries a C-terminal cell wall sorting signal (CWSS) with the typical sortase recognition site LPSTGG. The protein shows low sequence identity ranging from 12 to 16% with other known backbone pilin subunits from either GBS or other Gram-Positive bacteria.

To confirm the essential role of this protein during pilus 2b assembly we generated a mutant strain lacking the gene for the pilus 2b backbone protein (Δ*BP-2b*). The presence of covalently-linked pili on the GBS surface was detected by SDS-PAGE immunoblot analysis of cell-wall preparations through the identification of a ladder of high-molecular-weight (HMW) bands. Western blotting analysis, performed with total protein prepared from the KO Δ*BP-2b* strain confirmed the key role of BP-2b in pilus 2b assembly, since the typical HMW laddering could not be observed as in the wild type strain. Complementation of Δ*BP-2b* with a plasmid expressing the wild type gene (pAM_*BP-2b*) restored the pili expression.

To identify the specific residues and motives required for pilus 2b protein polymerization we used site-directed mutagenesis and complementation studies in GBS KO strains. To confirm the key role of the sortase-recognition LPSTGG motif of the BP-2b protein in pilus assembly, this region was entirely deleted in the complementation plasmid pAM_*BP-2b* by site-directed mutagenesis. The new plasmid pAM-*BP-2b*$_{\Delta LPSTG}$ expressing the C-terminally truncated backbone subunit was used to complement the GBS mutant strain (Δ*BP-2b*). Western blotting analysis, performed with total protein extracts from the complemented strain (Δ*BP-2b*/pAM_*BP*$_{\Delta LPXTG}$) and probed with a BP-2b specific antiserum, confirmed the expression of the protein only in the monomeric form, demonstrating that its polymerization into HMW structures was completely abolished (Fig. 12).

The BP-2b primary sequence does not contain a "canonical" pilin motif, and four different lysine residues were identified in the N-terminal domain as putative pilin motif candidates involved in mediating the cross-linking between two monomeric subunits. To assess the role of each residue in pilus polymerization, each lysine was replaced individually by an alanine. By site-directed mutagenesis we generated four new complementation plasmids (pAM_*BP-2b*$_{K77A}$, pAM_*BP-2b*$_{K82A}$, pAM_*BP-2b*$_{K118A}$, pAM_*BP-2b*$_{K175A}$) and used them to transform the KO-strain Δ*BP-2b*. The complemented strains expressing mutated forms of BP-2b were analyzed for their ability to assemble HMW structures by immunoblotting analysis. We observed that the mutation of lysine 77, 82 and 118 into alanine did not affect pilus protein polymerization, while mutation of lysine 175 (K175A) led to the abrogation of pilus polymerization (Fig. 12).

In the BP-2b sequence, a canonical "LXET" E-box motif could not be identified; however, BP-2b crystal structure (155) showed that Glu423 (which is part of the motif LVEK) is favourably positioned towards the isopeptide bond between Lys358 and Asn462, suggesting a possible role as for other E-box motives. To functionally characterize the role of this residue in pilus 2b polymerization, we constructed the plasmid pAM_*BP-2b*$_{E423A}$ to complement the KO Δ*BP-2b*. The expression of the backbone protein carrying the mutation E423A in the complemented strain abolished protein polymerization (Fig. 12), demonstrating the key role of residue E423 in pilus 2b assembly, although present in a non-canonical E-box motif.

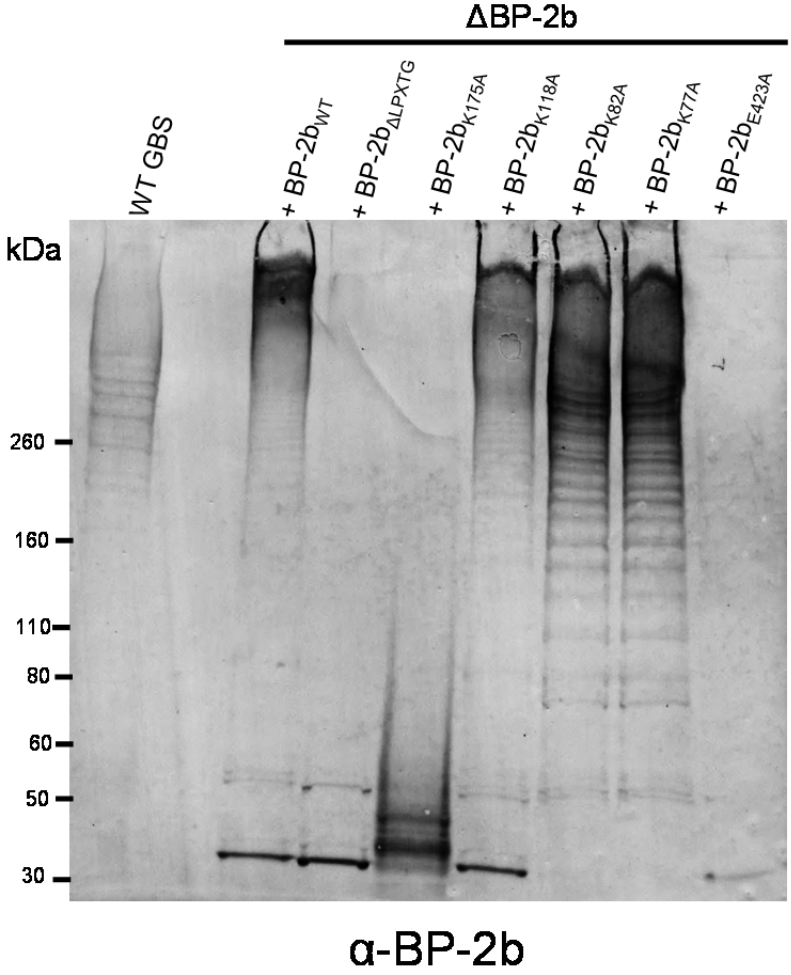

Figure 12. Lys 175, Glu 423 and the sorting motif LPSTG are involved in BP-2b polymerization in GBS. Immunoblot analysis of total protein extracts from GBS mutant strain lacking the pilus 2b backbone protein gene (Δ*BP-2b*) complemented with plasmids expressing the wild-type BP-2b protein (WT) or BP-2b mutants carrying a deletion of the C-terminal sorting signal (BP-2b$_{\Delta LPXTG}$), alanine substitutions of the putative pilin motif lysine (BP-2b$_{K175A}$, BP-2b$_{K118A}$, BP-2b$_{K82A}$,BP-2b$_{K77A}$) or of the E-box E423 residue (BP-2b$_{E423A}$). Nitrocellulose membrane was probed with a mouse antiserum raised against the recombinant BP-2b protein (α-BP–2b).

2.1.2 Class C sortases in GBS Pilus Island 2b

The genomic locus corresponding to GBS Pilus Island 2b (PI-2b) presents an overall organization similar to the other known pilus islands, carrying three genes coding for the structural subunits and two genes (*srtC1* and *srtC2*) expressing for class C sortase enzymes (Fig. 13).

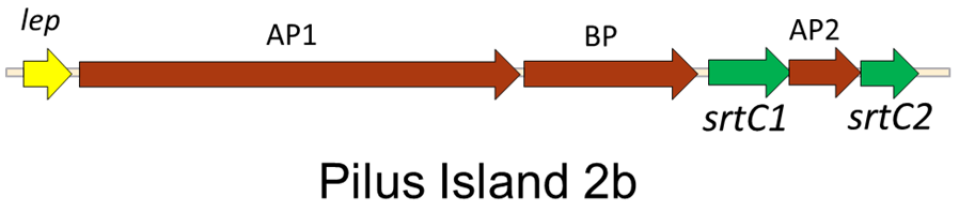

Figure 13. Schematic representation of GBS pilus island 2b. The genomic island is composed of three structural proteins that are the backbone protein (BP) that constitutes the scaffold of pilus structure, and ancillary proteins 1 and 2 located at the tip and the base respectively. These genes coding for structural subunits are represented by red arrows. In the genomic island are also present two genes coding for two class C sortases (in green) and also a signal peptidase *Lep* gene (yellow arrow), that is not present in the other GBS PIs.

As previously reported (91), by multiple sequence alignment with other class C sortases performed using ClustalW, SrtC1 and SrtC2 of PI-2b revealed a very low percentage of amino acid identity (Fig. 14).

SrtC1-2b and SrtC2-2b proteins consist of 291 and 199 residues, respectively. Prediction of transmembrane (TM) helices using their primary sequences revealed that SrtC1 carries two TM regions at the N-terminal (residues 7-29) and at the C-terminal (region 246-268), while the SrtC2 protein lack the predicted C-terminal trans-membrane (TM) helix, showing only a N-terminal TM (residues 4-27).

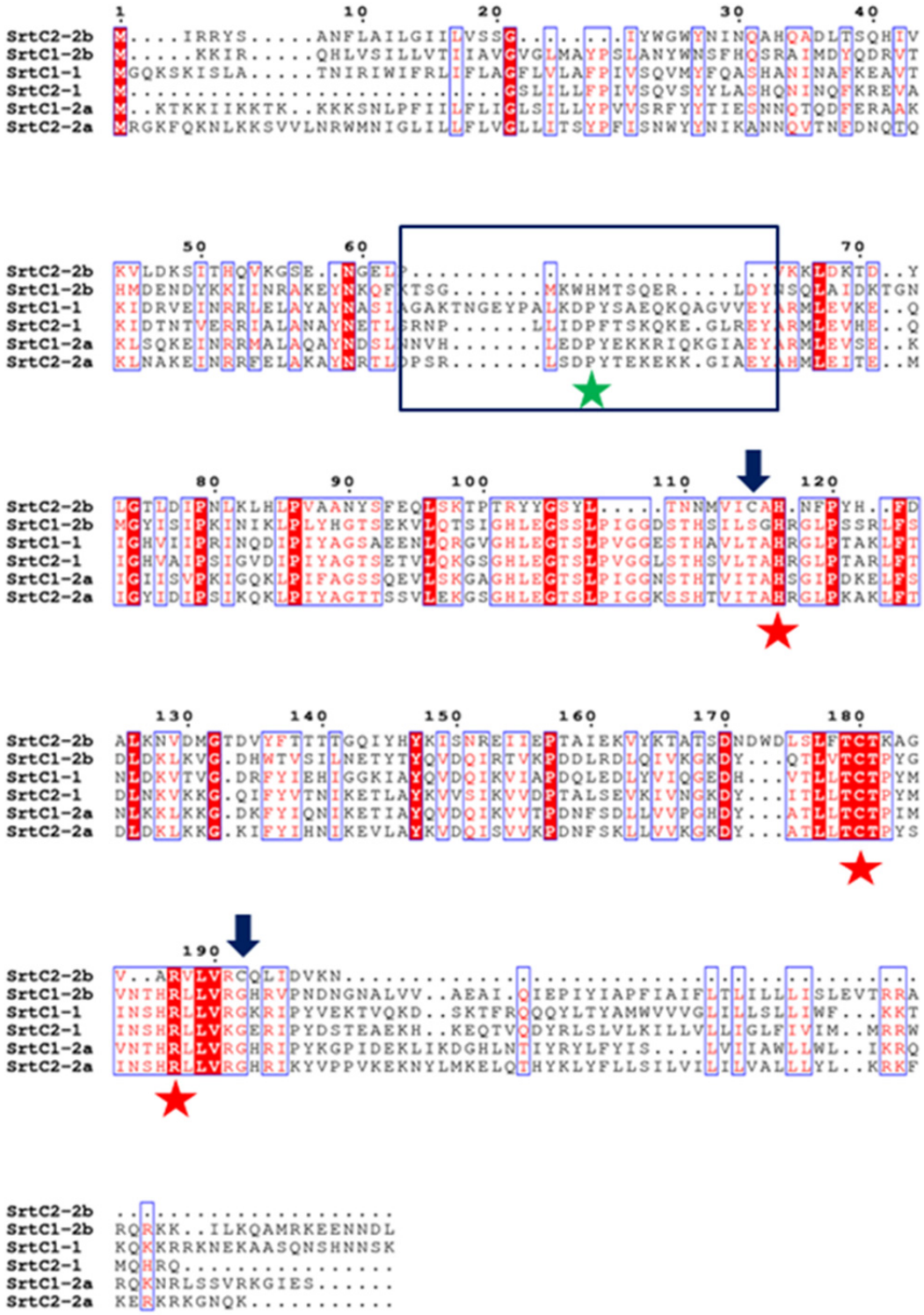

Figure 14. PI-2b Sortases C do not contain the canonical lid motif. Sequence alignment of all GBS class C sortases. Sequences corresponding to the lid region of sortases are highlighted in a blue box with a green star. Red stars are indicating the catalytic triad residues. PI-2b SrtC2 is also lacking the C-terminal transmembrane domain.

2.1.3 Generation of GBS mutant strains lacking sortase genes

To functionally characterize the role of the two sortases C in pilus 2b assembly, we generated two knock-out (KO) mutant strains (Δ*srtC1* and Δ*srtC2*) carrying in-frame deletions for each sortase gene using Splicing by Overlap Extension (SOE) PCR in a GBS strain (ABC020017623) containing only the genomic pilus island 2b (Suppl. Table 1). Sequence analysis of PI-2b in this strain confirmed 100% gene conservation with respect to the entire locus sequences of GBS strain COH1 whose complete genome is available in the public databases.
Δ*srtC1* KO strain resulted in the *srtC1* gene deletion of the region corresponding to amino acid residues 11 to 259, while Δ*srtC2* mutant resulted in the deletion of SrtC2 amino acid residues 14 to 190. Confirmation of these in-frame deletions were obtained by sequence analysis.

2.1.4 SrtC1 is the only pilus 2b-associated sortase involved in pilin subunit polymerization

To assess the role of each sortase in pilus protein polymerization, total proteins were extracted from each mutant strain and analyzed by immunoblot analysis with antisera specific for each structural subunit (the backbone and the ancillary subunits). As expected, total proteins from the wild type strain revealed the canonical HMW laddering indicative of pilus-like structures, while unexpectedly, only the deletion of sortase C1 affected pilin proteins polymerization, completely abrogating it, whereas Δ*srtC2* KO strain was able to express and assemble HMW pilus-like structures, as well as the wild type strain (Fig. 15A-B-C).

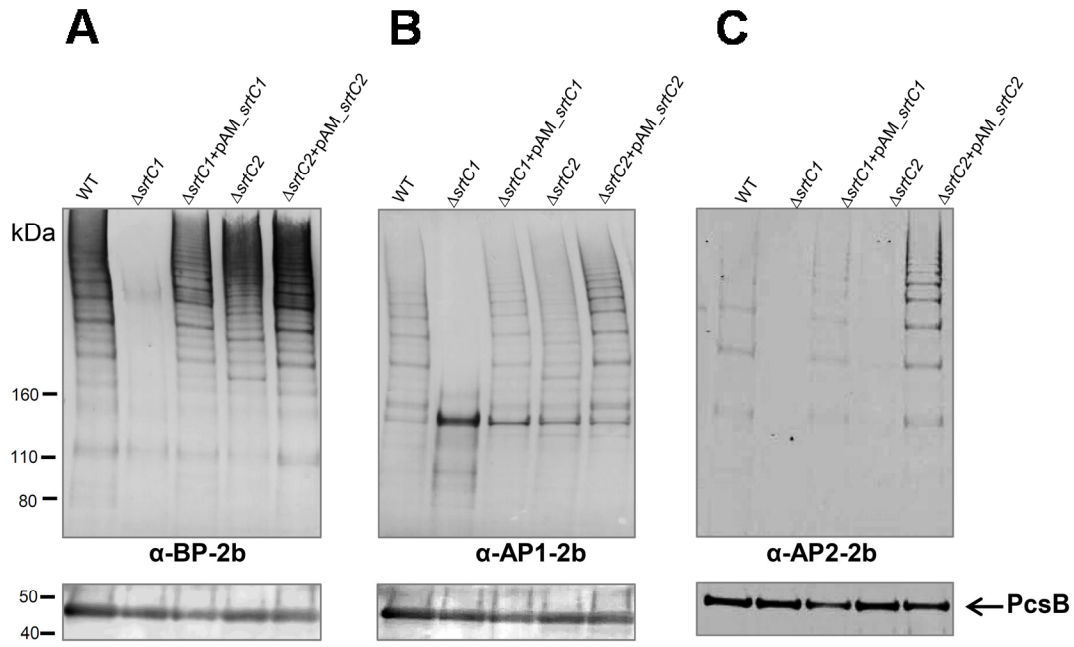

Figure 15. Only SrtC1-2 is essential to polymerize the pilin proteins into high molecular weight (HMW) structures. Immunoblotting analysis of total protein extracts from ABC020017623 wt and mutant strains lacking *srtC1-2b* and *srtC2-2b* genes (Δ*SrtC1* and Δ*SrtC2*) or mutants complemented by plasmids expressing SrtC1-2b or SrtC2-2b (Δ*srtC1*+pAM_*srtC1* and Δ*srtC2*+pAM_*srtC2*). Nitrocellulose membranes were probed with antisera raised against the backbone protein of pilus 2b (α-BP-2b), the major ancillary AP1 protein (α-AP1–2b) and the minor ancillary AP2 protein (α-AP2–2b). The equal amount loaded in each well was verified by probing the same gel with a control antiserum that recognizes the constitutive protein PcsB of 47 kDa (in the lower panels indicated by a black arrow).

Interestingly, the deletion of *srtC2* gene did not cause any effect on the backbone protein polymerization (Fig. 15A) and on the incorporation of the major ancillary protein (AP1) into pili (Fig. 15B), while the incorporation into pili of the minor ancillary protein (AP2) resulted significantly reduced (almost totally abrogated) (Fig. 15C). Complementation of the *srtC1* gene restored proteins polymerization to levels comparable to those of the wild type strain (Fig. 15A-B-C) as well as the complementation of the *srtC2* gene into the Δ*srtC2* mutant restored the AP2 incorporation into the pili as well as the wild type strain (Fig. 15C). These data clearly indicate that only the sortase C1 is involved in pilus 2b formation, while the sortase C2 appears to be dispensable for the backbone protein polymerization and it could play a role in the AP2 incorporation into pili.

2.1.5 The lack of SrtC2 induces release of polymerized pili in the culture supernatant

Since it is known that the minor ancillary subunit is involved in the cell-wall anchoring of other pili, including GBS pilus type 2a (59,92), we hypotized that sortase C2, not affecting the process of pilus protein polymerization, could be involved in pilus anchoring to the cell-wall through the use of the AP2 protein. To investigate this hypothesis, we analyzed the presence of pili released into the culture supernatant of the mutant strains deleted of *srtC2* and *ap2* genes. Thus, we also generated the knock-out (KO) mutant strain (*Δap2*) carrying in-frame deletion for *ap2* gene (Suppl. Table 1). Thus, both mutants were cultured in chemically defined medium so that levels of pilus found in the extracellular and cell-associated fractions could be directly compared.

Total proteins from the cell-wall and supernatant fractions were extracted and equal amounts were analyzed by immunoblot with an antiserum specific for the backbone protein. As shown in figure 16, in the wild type strain almost all the polymerized pili were detectable only in the cell-associated fraction. Whereas no pilus proteins were detected in the extracellular fraction of the wild-type strain, by contrast, significant amounts of pili were released in the culture supernatants of *ΔsrtC2* and *Δap2* mutant strains, which revealed a highly comparable phenotype (Fig. 16). Protein profiles comparable to those of the wild type were restored upon complementation of *ΔsrtC2* and *Δap2* mutants with vectors expressing the corresponding wild type genes (Fig. 16). These data indicate, therefore, that in the absence of SrtC2 or AP2 protein, polymerized pili structures were produced at levels comparable to those of the wild type strain, but then they were lost from the bacterial cell surface and released into the culture supernatant, suggesting that SrtC2 could be involved in pilus anchoring process by using the minor ancillary protein 2 (AP2) as anchor protein.

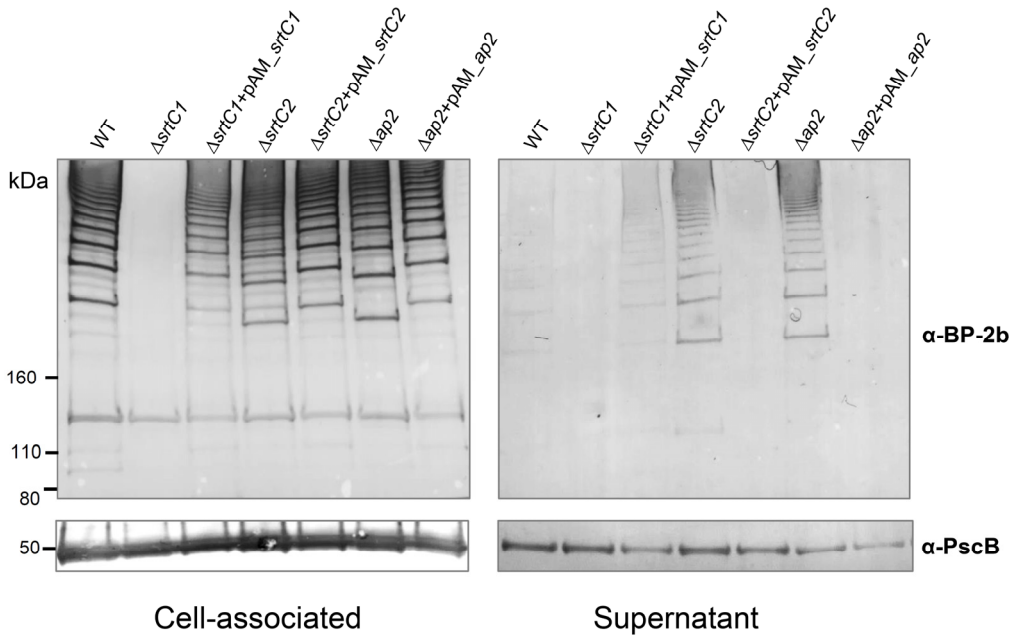

Figure 16. Pili are mostly released in the culture media of the mutant strains Δ*srtC2* and Δ*ap2*. Proteins were collected from RPM1 culture supernatants (right panel) or extracted from cell pellets (left panel) of GBS wild-type strain (WT), or mutant strains deleted of *srtC1*, *srtC2* or *ap2* genes (Δ*srtC1*, Δ*srtC2* and *Δap2,* respectively) and mutant strains complemented with the plasmids expressing SrtC1, SrtC2 or AP2-2b proteins (Δ*srtC1*+pAM_*srtC1*, Δ*srtC2*+pAM_*srtC2* and Δ*ap2*+pAM_*ap2*, respectively). Protein fractions were analyzed by immunoblot stained with antibody specific for the backbone protein BP-2b (α-BP-2b, in the upper panels), and as a quantitative control of equal amount of proteins loaded in each well with the serum against the constitutive protein PcsB (in the lower panels).

2.1.6 Biochemical characterization of SrtC2-2b

To further investigate the role and the specificity of sortase C2 in pilus 2b assembly we performed a biochemical characterization of the enzyme. We first cloned and expressed in *E. coli* the catalytic domain of SrtC2 enzyme (residues 32-199) as an N-terminal His-tagged recombinant protein lacking the N-terminal hydrophobic region and the leader sequence. The soluble protein (rSrtC2) was then purified by immobilized metal affinity chromatography (IMAC) followed by size-exclusion chromatography (SEC). The purified enzyme ($SrtC2_{32–199}$) showed >90% purity by SDS-PAGE. Gel filtration revealed that in the analyzed peak the protein was mono-disperse with an apparent molecular weight (MW) of

25 kDa, consistent with the theoretical MW of 23.9 kDa of the monomeric protein (Fig. 17).

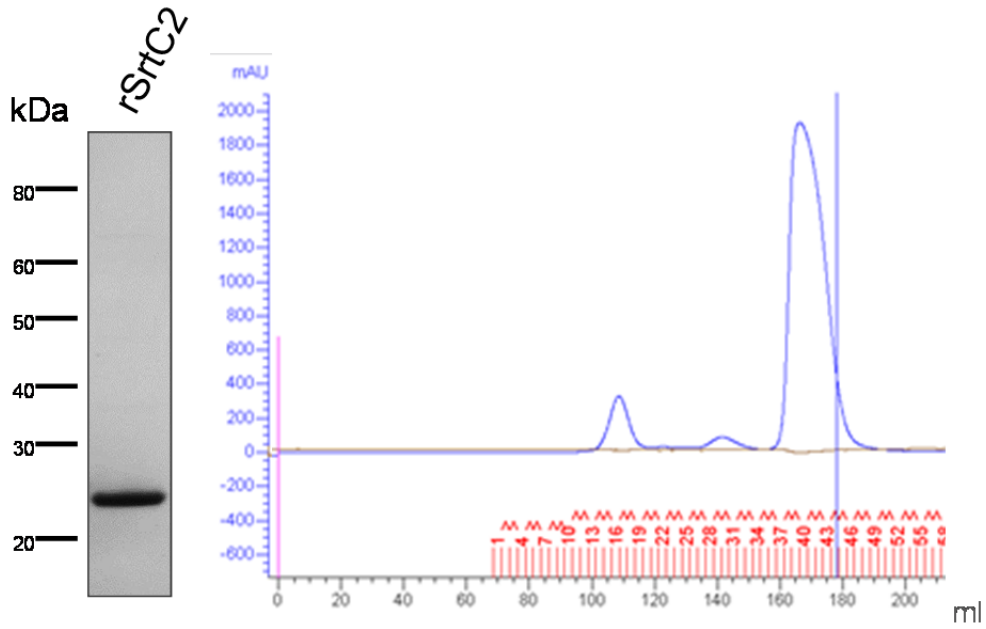

Figure 17. SrtC2 purification. Recombinant SrtC2 was cloned expressed and purified. SDS-PAGE of the purified enzyme after last purification step by size-exclusion chromatography (SEC). The corresponding SEC graph is also reported, where the blue peak corresponds to the purified protein fraction.

2.1.7 Recombinant SrtC2 specifically recognizes and cleaves the sorting motif of the AP2-2b protein

As a precondition to evaluate the enzymatic activity of the produced sortase, we verified the folding of the enzyme by Nuclear Magnetic Resonance (NMR) spectroscopy using a purified ^{15}N-labeled recombinant SrtC2. The ^{1}H-^{15}N-HSQC NMR spectrum provides amino acid-specific information, showing signals from all HN groups of the protein, including backbone amide groups as well as a number of side chains. Therefore, it is a valuable tool to evaluate protein folding, as the secondary and tertiary structures determine unique chemical environments of amide groups, which are reflected by significant signal dispersion in both the nitrogen and proton dimensions. An unfolded protein displays poor signal dispersion because all amide atoms are in similar chemical environments (for example exposed to the solvent). The ^{1}H-^{15}N-HSQC spectrum of SrtC2-2b

showed a significant dispersion of peaks in both the proton and nitrogen frequency dimensions (spanning ~ 5 ppm and ~ 30 ppm respectively) indicating that the enzyme was correctly folded (Fig. 18).

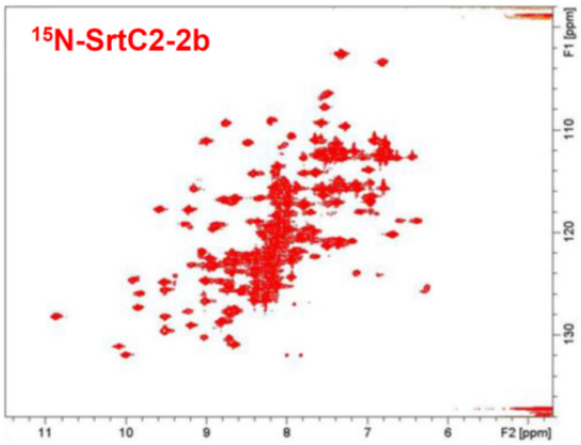

Figure 18. Recombinant SrtC2 is correctly folded. Recombinant SrtC2 was cloned expressed and purified, and the correct folding was checked by NMR to verify the correct folding of the protein. NMR spectroscopy of the purified recombinant ^{15}N-labelled-SrtC2-2b. The ^{1}H-^{15}N-HSQC spectrum of the protein was recorded in 50 mM phosphate buffer, pH 6.5 and acquired at 25°C. The signals of the residues are consistent with a folded protein.

To evaluate its *in vitro* enzymatic activity we performed a Fluorescence Resonance Energy Transfer (FRET) based assay using synthetic fluorogenic peptides mimicking the LPXTG-like sorting motives of pilin proteins. FRET analysis is a commonly used method to follow cleavage reaction of specific substrates by specific enzymes, such as sortases. When the peptide is cleaved by the sortase, the EDANS fluorophore group is separated from the DABCYL quencher group, resulting in an enhanced fluorescence signal. We first tested synthetic peptides carrying the LPXTG-like motifs of the three pilus 2b structural proteins (Table 3). The LPSTGG-motif of the backbone protein (BP-2b) overlaps with the motif of the major ancillary protein (AP1-2b), and differs from the sorting signal LPFTGQ of the minor ancillary protein (AP2-2b). A significant increase of the fluorescence signal (normalized against the fluorescence values of the peptide alone) was observed only when the rSrtC2 sortase was incubated with the AP2-2b peptide, indicating that this enzyme specifically recognizes and

cleaves only this peptide (Fig. 19A). By contrast, rSrtC2 was not able to cleave neither the BP-2b/AP1-2b peptide nor the peptide containing the LPKTGM motif of the AP2 protein of pilus 2a (AP2-2a) used as control (Fig. 19A). We have chosen this peptide as control since we had previously demonstrated that it is the substrate target of the GBS housekeeping sortase A (SrtA), which is responsible of the cell-wall anchoring of pilus 2a through the AP2-2a subunit that is at the base of the pilus and acts as the pilus anchor protein (92). To confirm the cleavage specificity of rSrtC2 *vs* the AP2-2b peptide, we verified if the AP2-2b peptide was also recognized and cleaved by the housekeeping SrtA. Thus, we expressed in, and purified from *E. coli* the SrtA, as an N-terminal His-tagged recombinant protein, and performed an *in vitro* FRET assay by incubating 5µM of rSrtA with 64 µM of the fluorescent AP2-2b peptide or the AP2-2a peptide used as positive control (92). We observed that the rSrtA enzyme cleaved specifically only the AP2-2a peptide as expected, but was not able to cleave the AP2-2b motif, confirmed that the AP2 protein of pilus 2b was the specific substrate of SrtC2 (Fig. 19B).

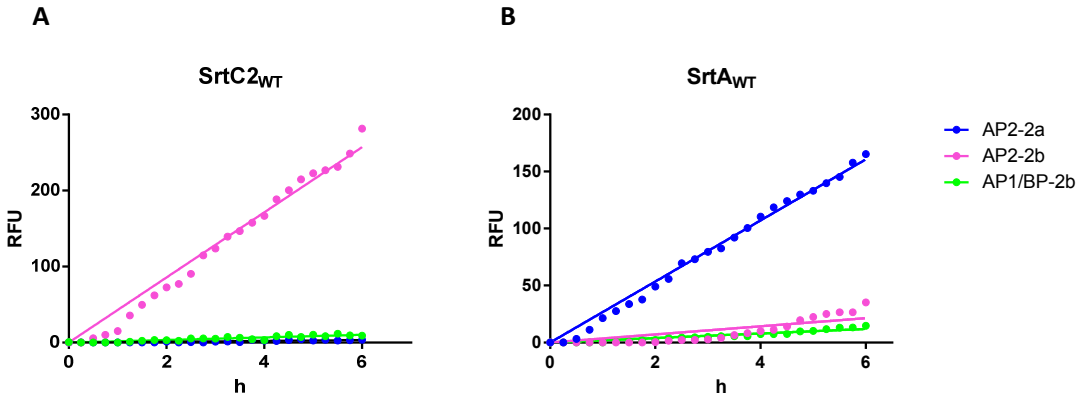

Figure 19. SrtC2 specifically cleaves AP2-2b fluorescent peptide. *In vitro* enzymatic activity assessed by FRET analysis of the recombinant wild-type SrtC2 (**A**) or SrtA (**B**) proteins using fluorogenic peptides (64 µM) carrying the LPxTG-like motif of the minor ancillary protein 2 from pilus 2b (AP2-2b), of minor ancillary protein 2 from pilus 2a (AP2-2a) and the sorting motif of pilus 2b backbone protein overlapping with that of the major ancillary (AP1/BP-2b). Progress curves of the cleavage reactions of the fluorescent peptides catalyzed by recombinant SrtC2 wild-type ($SrtC2_{WT}$) or SrtA wild-type ($SrtA_{WT}$) show that SrtC2 is specific only for AP2-2b that instead can not be cleaved by housekeeping SrtA. Each assay was done in triplicate and the graphs report the mean values.

To further confirm these data we performed an *in vitro* cleavage assay by incubating the rSrtC2 or rSrtA enzyme with a recombinant C-terminal His-tagged protein (rAP2-2b) produced in *E. coli*. 50µM of rSrtC2 or rSrtA was incubated at 37°C over-night with 25µM of rAP2-2b. Reaction mixtures were then purified by IMAC and the fractions were analyzed by Western Blot using a mouse antiserum α-AP2-2b. The IMAC purification allowed eluting only His-tagged proteins or peptides and releasing in the flow through fraction any protein/peptide lacking the His-tag. Accordingly, if the C-terminal His-tagged AP2-2b protein is not cleaved by a sortase at its C-terminal sorting signal, AP2-2b will be collected only in the elute fraction. By contrast, the cleavage of its sorting signal will be proved by the presence of the cleaved AP2-2b protein in the flow through fraction. Antibodies specific for the AP2-2b protein revealed a band at a lower MW than the size of the full length AP2-2b in the flow through fraction only when the rAP2-2b protein was incubated with rSrtC2 (Fig. 20), meaning that the protein was cleaved only by SrtC2 with the consequent loss of the His-tagged sorting signal. Accordingly, the protein eluted completely full-length when incubated with the rSrtA (Fig. 20).

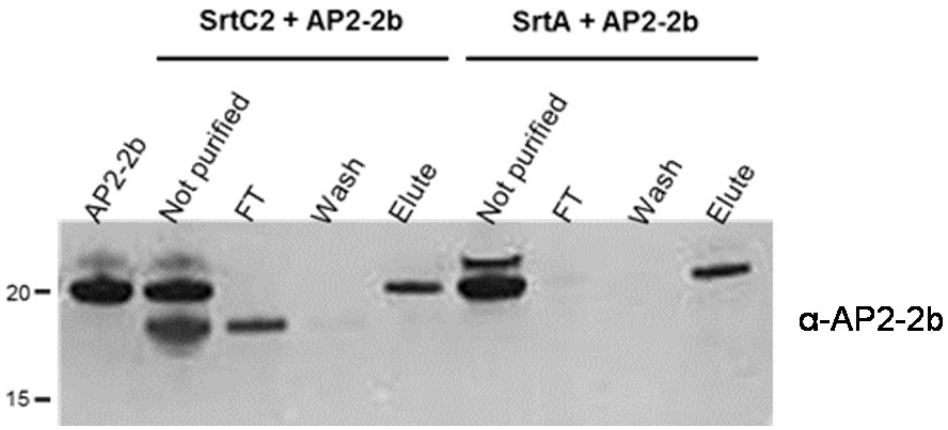

Figure 20. AP2-2b is cleaved only by SrtC2 and not by SrtA. *In vitro* cleavage assay of the recombinant C-terminal His-tagged AP2-2b protein incubated either with the recombinant SrtC2 or SrtA. Cleavage reactions were then purified by IMAC and the single fractions were analyzed by Western blot using a mouse serum anti AP2-2b.

These data, taken together with the above described experiments strongly suggest that pilus 2b is anchored to the cell wall through the minor ancillary protein AP2,

which is the specific target of the pilus-associated SrtC2. Moreover, FRET experiments confirmed genetic data indicating that SrtC2 is not involved in backbone protein polymerization, since it is not able to cleave its sorting motif.

2.1.8 C115 and C192 are not essential for the SrtC2 activity *in vivo*

Sequence analysis of SrtC2-2b by multiple alignment with other GBS sortase reveals the presence of two more cysteines (C115 and C192) in addition to the conserved canonical triad represented by H117, C180 and R187 (Fig. 14). Moreover, also SrtC2-2b (as SrtC1-2b) does not contain the canonical DPY\W\F lid motif. To investigate the possible involvement of those cysteines in the catalytic activity of SrtC2-2b, we generated complementation vectors expressing three mutated forms of SrtC2 ($SrtC2_{C115A}$, $SrtC2_{C180A}$ and $SrtC2_{C192A}$). Each cysteine residue was individually replaced by an alanine into the complementation vector pAM_*SrtC2* by the PIPE method and site-directed mutagenesis using synthetic oligonucleotide primers. The new vectors carrying the specific mutations were then used in restoring the activity of the enzyme by transforming the KO mutant strain Δ*srtC2*. After complementation, the effect of each mutation was analyzed by Western blot analysis, checking the release of polymerized pilus structures in the culture media supernatants from complemented strains. As expected, no high-molecular-weight polymerized pilus structures were found in the media supernatants of the complemented strains with the gene expressing the wild type ($SrtC2_{wt}$) and the mutated enzymes ($SrtC2_{C115A}$ and $SrtC2_{C192A}$), meaning that these sortase forms restored pilus 2b anchoring to the cell wall (Figure 21). By contrast, by complementing the KO Δ*SrtC2* strain with the plasmid expressing the sortase carrying the C180A substitution released polymerized pili could still be detected in the culture medium, confirming that Cys180 is the catalytic residue essential for sortase C2 activity (Figure 21).

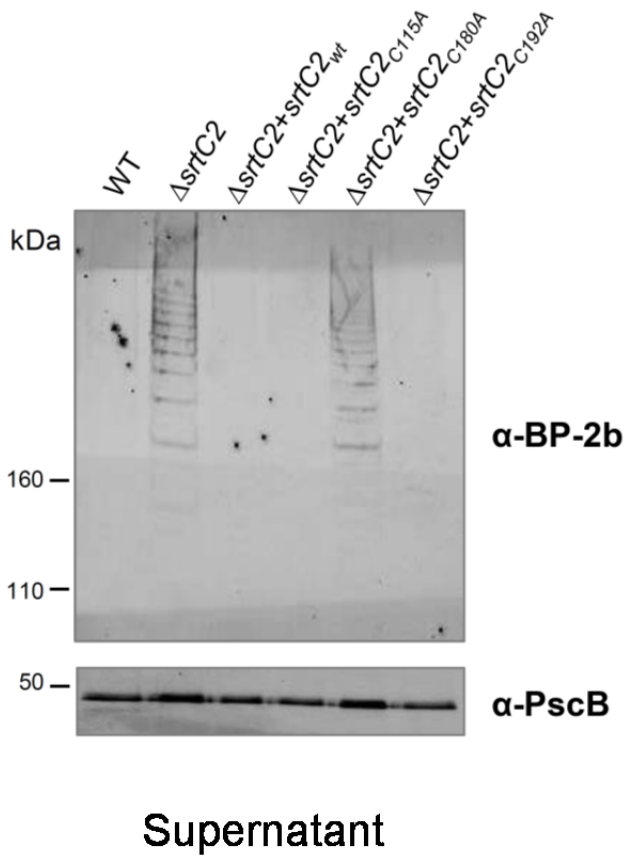

Figure 21. Cysteine 180 is responsible for catalytic activity of SrtC2-2b. Western Blot analysis of total proteins collected from culture media supernatants of GBS wild type strain (WT), GBS knock out strain deleted of *srtC2* gene (Δ*srtC2*) and Δ*srtC2* strain complemented with the plasmids pAM_$SrtC2_{WT}$ (Δ*srtC2*+$srtC2_{wt}$), pAM_$SrtC2_{C115A}$ (Δ*srtC2*+$srtC2_{C115A}$), pAM_$SrtC2_{C180A}$ (Δ*srtC2*+$srtC2_{C180A}$), pAM_$SrtC2_{C192A}$ (Δ*srtC2*+$srtC2_{C192A}$), expressing SrtC2 cysteine mutant enzymes. Nitrocellulose membrane was probed with a mouse antiserum raised against the backbone protein (α-BP-2b). The equal quantity loaded in each well was verified by immunoblotting the same gel with a control antiserum specific for the constitutive PcsB protein of 47 kDa (in the lower panel).

2.1.9 C115, C180 and C192 are not essential for the SrtC2 structural stability

Antibodies specific for SrtC1 or SrtC2 enzymes revealed that all the complemented strains expressed similar levels of the different forms of sortases, indicating that none of the introduced mutations had seriously affected the expression or the stability of the proteins (data not shown).

Moreover, to verify whether the Cys115 and Cys192 residues affected the general fold of SrtC2-2b, the mutant enzymes rSrtC2$_{C115A}$, and rSrtC2$_{C192A}$ were produced as recombinant ^{15}N-labeled proteins and analyzed by NMR spectroscopy.
The analysis of the HSQC spectra of the SrtC2 mutants showed that the signal dispersion is comparable to the WT meaning that each single mutation did not alter the overall structure of the proteins. Moreover, the spectra of the WT and of the mutants are highly superimposable with only few peaks showing chemical shift changes. Since peak position is very sensitive to chemical environment, this scenario is compatible with local modifications introduced around the mutation sites. Overall, it can be concluded that the mutated residues did not affect structural stability of the SrtC2 enzyme, as the native fold was preserved (Figure 22A).

2.1.10 Disulfide bonds formation between catalytic C180 and C192 suppress SrtC2 activity *in vitro*

To better investigate the contribution of the cysteines in SrtC2-2b activity the *in vitro* enzymatic activity of the SrtC2 mutants (rSrtC2$_{C115A}$, rSrtC2$_{C180A}$ and rSrtC2$_{C192A}$) compared with the rSrtC2wt was assessed by FRET assay and the presence of free thiols assessed by AMS assay
Recombinant sortases were generated by site-specific mutagenesis using as template the previously generated pET vector carrying the wild type *SrtC2* gene. Thus, the mutated SrtC2 were produced in *E. coli* as His-tagged recombinant proteins. The proteins were incubated at a concentration of 25 μM each with different concentrations of the fluorescent AP2-2b peptide and their activity was tested. In agreement with the above described data, the activity of SrtC2$_{C180A}$ enzyme was completely abolished, further confirming the catalytic role of this residue. Interestingly, the mutant SrtC2$_{C192A}$ showed an enhanced cleavage activity compared with the wild type enzyme, whereas the mutant SrtC2$_{C115A}$ revealed a highly reduced activity (Figure 22B).

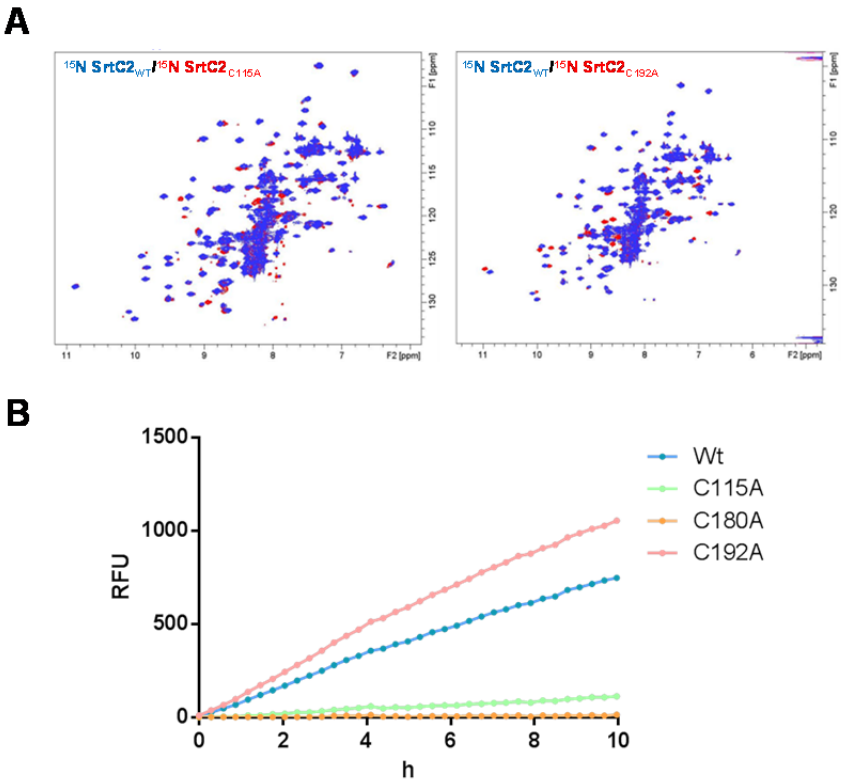

Figure 22. SrtC2 mutants characterization. SrtC2 differs from the other class C sortases because it has three cysteines needed for its activity and regulation. Recombinant SrtC2 with cysteines mutated one at the time, were cloned expressed and purified, and their correct folding was analyzed by NMR. A) Superimposition of NMR $_1$H-$_{15}$N HSQC spectra of SrtC2 wild-type and its mutants. Cyan, SrtC2 wild-type; red, SrtC2$_{C115A}$ or SrtC2C$_{192A}$. All samples are in 50 mM phosphate buffer, pH 6.5. B) FRET assay with rSrtC2 and its cysteine mutants at a concentration of 5 µM with 128 µM of the fluorescent peptide with the AP2-2b LPXTG motif. The assay was performed at 37°C in 50 mM Tris-HCl (pH 8), 300 mM NaCl, 1 mM DTT and was performed at least in triplicate. The graph shows that SrtC2$_{C192A}$ mutant is more active than the wild type sortase. Mutation of the catalyitic cysteine completely abrogates SrtC2 activity as expected, but also mutation of cysteine 115 leads to a decrease of fluorescence measured.

Interestingly, with the only exception of the C180 mutant, the activity of the other three samples correlated with the fluorescence values in the AMS assay (Fig.23). AMS specifically binds to free thiols and the sample fluorescence measured after the excess of AMS is removed is directly proportional to the number of free cysteines (108). In fact, the SrtC2$_{C192A}$ mutant that showed maximum cleavage activity revealed also the higher AMS fluorescence. In fact, the rSrtC2$_{C192A}$ that was characterized by maximum activity revealed also the higher AMS fluorescence. Pre-treatment of this protein with DTT did not modify the

fluorescence value, meaning that the number of its free cysteines does not change in the reduced form; the catalytic Cys180 remains free and thus active. On the contrary, the $SrtC2_{C115A}$ mutant characterized by low FRET activity showed in absence of DTT a low AMS fluorescence that increased when the sample was pre-treated with DTT. This observation indicates that the poor (almost no) enzymatic activity *in vitro* of $SrtC2_{C115A}$ is due to a disulfide bond formation between Cys192 and the catalytic Cys180, which thus results locked in its activity. As $SrtC2_{wt}$ showed an intermediate enzymatic activity and intermediate AMS fluorescence value, likely a balance between Cys192-Cys180 and Cys192-Cys115 disulfide bonds could exist. AMS results suggest that in $SrtC2_{wt}$ the Cys192 could be engaged in a disulfide bond with either Cys115 or Cys180, since both the mutants $SrtC2_{C115A}$ and $SrtC2_{C180A}$ after incubation with AMS resulted in the same fluorescence values. On the contrary, Cys115 and Cys180 are not able to directly interact to each other in a disulfide bond, and indeed the mutant $SrtC2_{C192A}$ seems to contain free cysteines in all tested conditions (Fig. 23).

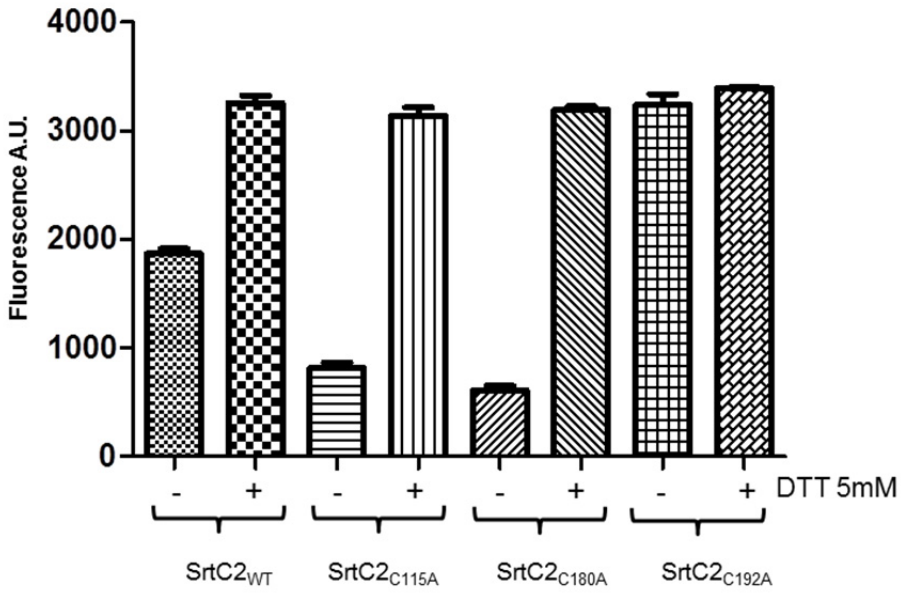

Figure 23. SrtC2 free cysteines quantification by AMS assay. 25 μM recombinant SrtC2 wt or cysteine mutated in both reduced and oxidized forms were incubated at 37°C for 30' with 250 μM AMS and SDS 1%. AMS binds to free cysteine thiols and the measurement of its fluorescence allow free cysteines quantification. $SrtC2_{C192A}$ is the only protein where the number of free cysteines does not change if reduced or not, meaning that the other two cysteines never interact between them, but only with cysteine 192 alternatively.

2.1.11 Overall folding of SrtC1-2b

To further elucidate the different roles of SrtC1-2b and SrtC2-2b in pilus 2b biogenesis we performed X-ray crystallography structural studies and solved the crystal structure of the sortase C1 (SrtC1-2b).

The ectodomains of SrtC1-2b and SrtC2-2b enzymes were produced in *E. coli* as soluble recombinant proteins containing via a TEV-cleavable N-terminal 6-His-tag and purified using standard chromatographic techniques as described in the Materials and Methods chapter and used in crystallization trials.

While all attempts to obtain crystals of SrtC2-2b enzyme failed, the crystal structure of SrtC1-2b was solved at 1.95 Å by molecular replacement in *molrep* (109), starting with a template made of coordinates of GBS SrtC1-1 (PDB ID 4g1j) (51.9% sequence identity) (Table 4, Fig. 24).

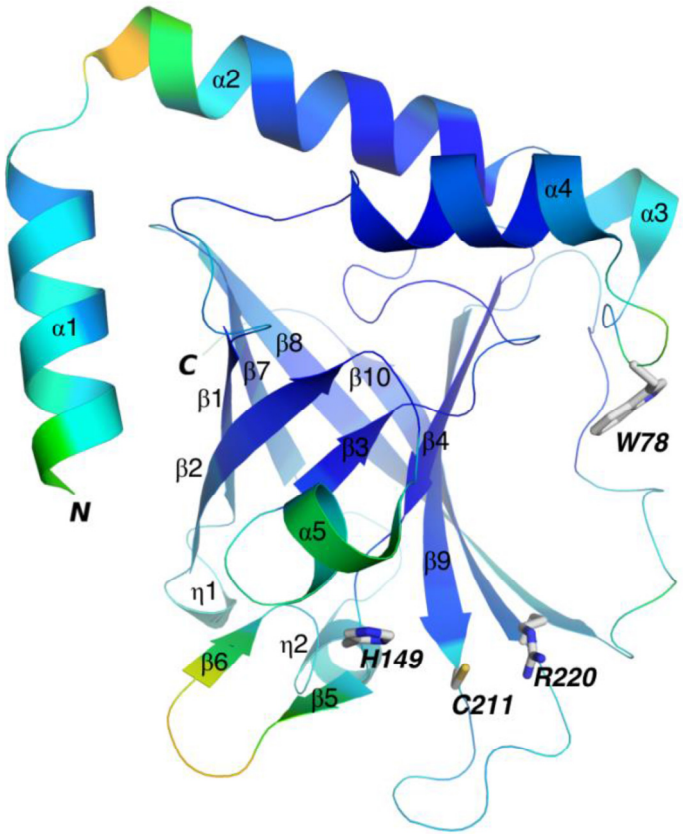

Figure 24. SrtC1-2b crystal structure. SrtC1-2b is depicted as cartoon colored according to B-factor distribution, using a gradient from blue (22 Å2) to red (120 Å2). Residues forming the catalytic triad and the Trp residue of the lid (W78) are shown with sticks and labelled.

Like for other sortase family members, the overall fold of SrtC1-2b exhibits a core made of a β-barrel compact structure with 10 β-sheets, surrounded by an α helical roof composed of 4 consecutive helices (Fig. 24). The first N-term helix (residues 39-51) runs parallel to the wall of the β-barrel core, whereas the second (residues 53-69), the third (residues 70-75) and the fourth helices (residues 81-90) run almost perpendicular to the first helix and flat on the top of the β-barrel (roof). The loop connecting helices 3 and 4 and carrying residues 76-80 corresponds to the "lid" region and includes a tryptophan residue (W78). The catalytic triad is made of the residues His149, Cys211, and Arg220 that belong to three different strands of the lower part of the β-barrel (Fig. 24).

To confirm the catalytic role of C211 in SrtC1 activity, this cysteine was replaced by site-directed mutagenesis with an alanine into the complementation plasmid pAM_*srtC1*. The generated new plasmid (pAM_$srtC1_{C211A}$) was used to transform the mutant strain *ΔsrtC1*. Western Blot analysis performed with total protein extracts from the complemented strain (*ΔsrtC1*+pAM_$srtC1_{C211A}$) and probed with an anti-backbone protein serum (α-BP-2b) showed that the polymerization of the major subunit of pilus 2b was completely abolished confirming the catalytic function of C211 (Fig. 25).

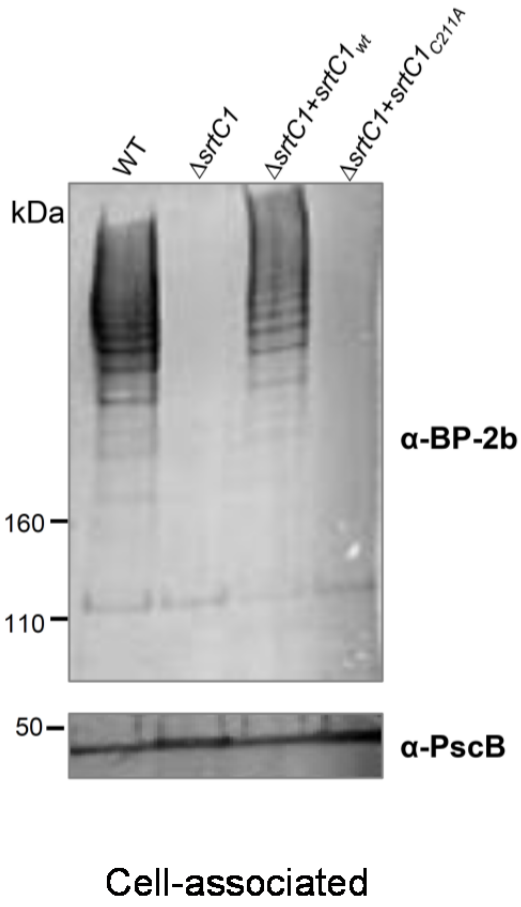

Figure 25. Cysteine 211 is responsible for catalytic activity of SrtC1-2b. Immunoblot of total protein extracts from GBS wild-type (WT), mutant strain lacking the sortase C1 gene (Δ*srtC1*) and Δ*srtC1* mutant strain complemented with the plasmid pAM_$SrtC1_{WT}$ (Δ*srtC1*+$srtC1_{wt}$) and the plasmid pAM_$SrtC1_{C211A}$ (Δ*srtC1*+$srtC1_{C211A}$) expressing the SrtC1 enzyme carrying the substitution of the cysteine 211 with an alanine. The equal quantity loaded in each well was verified by immunoblotting the same gel with a control antiserum that recognizes the protein PcsB of 47 kDa (in the lower panel).

2.1.12 Structural comparisons of SrtC1-2b with other sortases

A search of the Protein Data Bank (PDB) using the program DALI (110) revealed high structural similarities (Z-scores > 2) with more than 100 non-unique sortase family proteins. Among these, the highest Z-scores (>13) and lowest *rmsd* values unique entries (corresponding to class C or A sortases) were selected and analyzed by structural superposition onto the coordinates of SrtC1-2b (Suppl. Table 5). This analysis confirmed a highly conserved overall fold, but revealed how the lid

of SrtC1-2b assumes an apparent novel conformation. While for most structurally similar entries the lid is either not visible (likely because flexible and thus disordered), or closed to make interactions with the catalytic triad residues, in SrtC1-2b this assumes an "open" position. Although DALI also detected as highly similar two structures with an open lid conformation (PDB ID 3re9, which is the crystal structure of sortase C1 from *S. suis*, and PDB ID 3tb7 for GBS SrtC1-1 (type I), with Z-scores of 23.6 and 22.5, respectively), both these structures have a lid made of a long helix that does not superpose well with the lid of SrtC1-2b.

Coordinates of SrtC1 from *S. pneumoniae* (PDB 2w1j), the only sortase structure with electron density for the whole N-terminal region, and of GBS SrtC1-1 (PDB 4g1j) were used for further manual structural alignments and analyses. These revealed a β-barrel core structurally well conserved and a perfect superimposition of the catalytic triad residues, with *rmsd* values of 1.6 Å and 1.5 Å, for 2w1j and 4g1j, respectively (Fig. 26A-B). The N-terminal α helical portion, extending from S74 to D87, including the lid loop, revealed a significant difference. The putative regulatory lid tryptophan residue W78 in SrtC1-2b structure, which corresponds to residues W60 and Y92 in 2w1j and 4g1j, respectively (Fig. 26A-B) is displaced almost 15 Å away from the catalytic triad in the substrate binding active site. A multiple sequence alignment of SrtC1-2b and the other crystallized pilus-related sortases showed that only SrtC1-2b does not contain the canonical DPY\W\F lid motif, but just a tryptophan (W78) (Fig. 27).

To gain a better understanding of the open lid conformation of SrtC1-2b, we superimposed it onto the coordinates of the "open-form" structure of *S. suis* sortase C1 (PDB id 3re9). An overall good structural agreement was obtained (with *rmsd* value of 2Å), except for the lid region, where significant differences could be observed (Fig. 26C). While in *S. suis* SrtC1 the lid is made of 28 residues (N79-E107) that mainly form an α-helix, the lid of SrtC1-2b is made of a total of 14 residues (M76-Q90) and includes a loop (residues 76-80) and an α-helix (α4, residues 81-90). An angle of ~70º was measured between the helical lid of *S. suis* SrtC1 and α4 of SrtC1-2b (Fig 26C), resulting in the regulatory lid Y87 residue of SrtC1_suis positioned farther away from the catalytic triad, as well as from W78 of SrtC1-2b (Fig. 26C). This suggests that *S. suis* SrtC1 has an even more open

conformation than SrtC1-2b, thus supporting the notion of high flexibility of the lid (99).

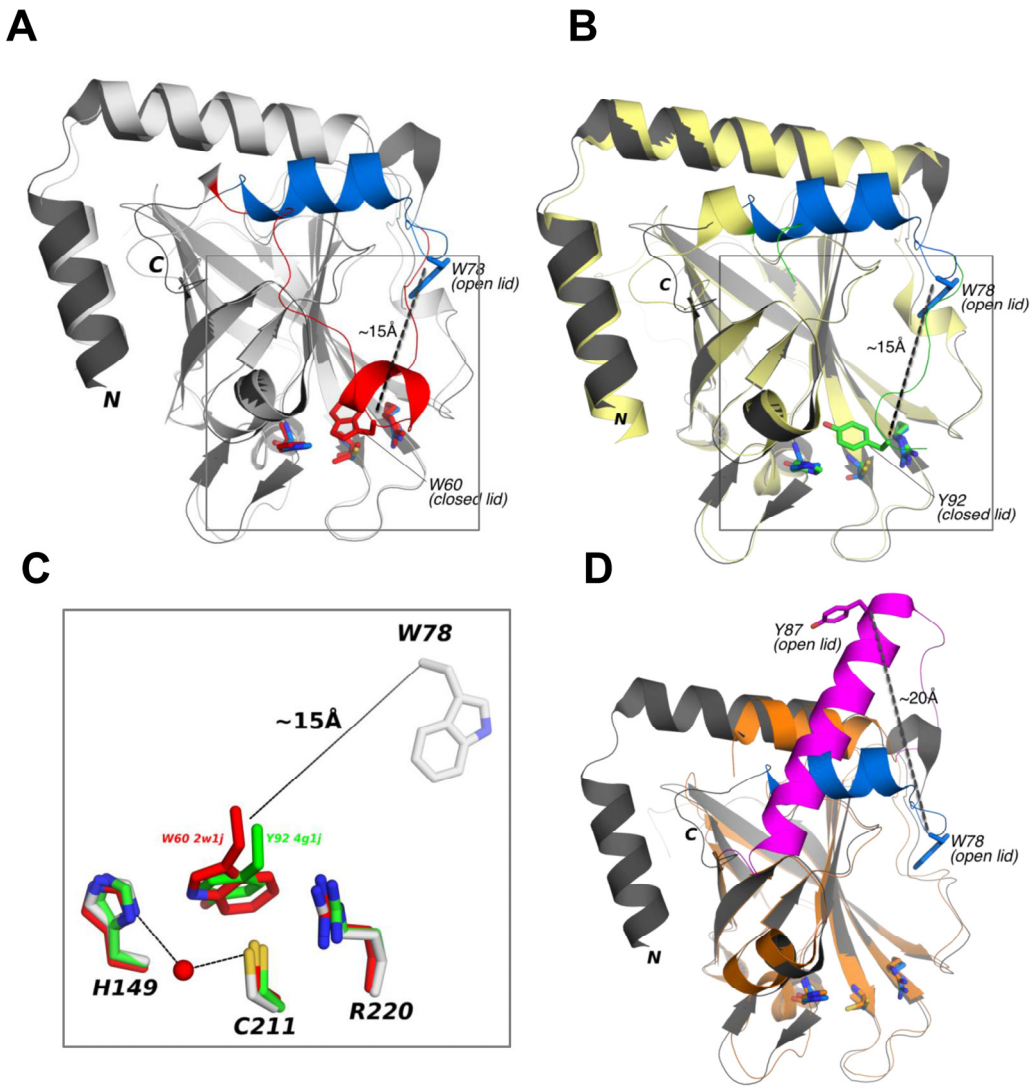

Figure 26. Open and closed lid of Sortase C structures. The structure of SrtC1-2b is depicted as dark gray cartoon in all panels, and the lid region colored in blue. Superposition of SrtC1-2b onto the structures of **(A)** SrtC1 *of S. pneumoniae* (PDB 2w1j, light gray cartoon), **(B)** GBS SrtC1-1 from pilus type 1 (PDB 4g1j, light yellow cartoon). **(C)** Zoom into the region of the catalytic triad and of the lid, showing with green sticks residues of SrtC1-1, with red sticks those of *S.pneumoniae* SrtC1. and with gray sticks those belonging to SrtC1-2b. The distance between Cα atoms of the aromatic lid residue is also shown, to highlight the displacement of the lid in SrtC1-2b. **(D)** Superposition of SrtC1-2b onto the SrtC1 from *S. suis* (PDB 3er9, orange cartoon). The lid regions of 2w1j, 4g1j, and 3er9 are colored in red, green, and magenta. Superimposed residues of the catalytic triads of all structures, as well as aromatic residues of the lids, are shown with sticks and colored accordingly to the structure or region to which they belong.

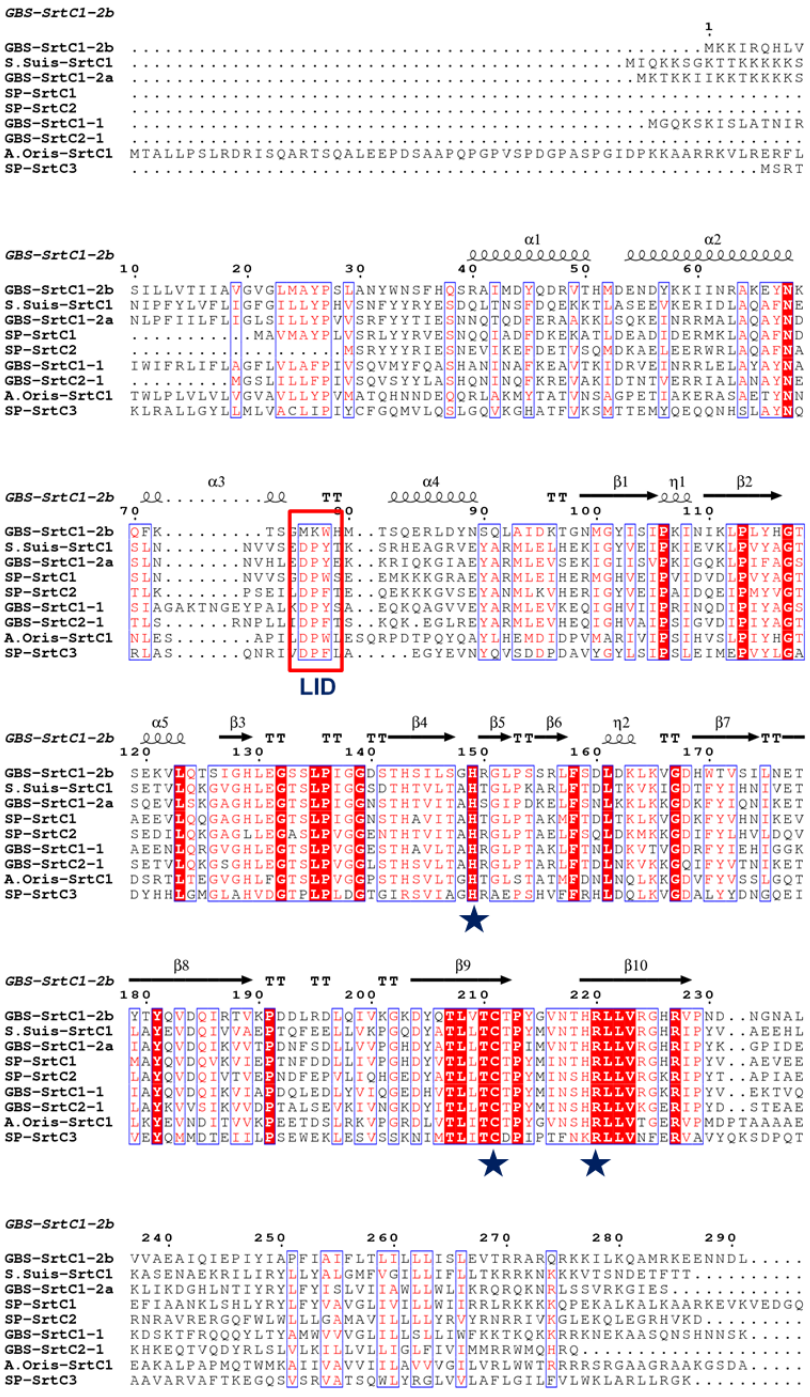

Figure 27. Multiple sequence alignment of the pilus-forming sortases deposited in the protein data bank (PDB). Structure-based sequence alignment by using ESPript of GBS SrtC1-2b (PDB 4D7W), GBS pilus 1 SrtC1-1 (PDB 4G1J) and Srt2-2b-1 (PDB 4G1H), GBS pilus 2a SrtC1-2a (PDB 3O0P), *S. pneumoniae* sortase C1 (PDB 2W1J), sortase C2 (PDB 3G69), and sortase C3 (PDB 2W1K), *S. suis* SrtC1 (PDB 3RE9) and *A. oris* SrtC1 (PDB 2XWG). Identical residues are shown with a red background, whereas similar residues are shown in red and highlighted with blue boxes. Residues located within the active site cleft (His, Cys and Arg) are conserved among all sortases and are highlighted with blue stars, whereas the lid residues DPF\Y\W are highlighted with a red box.

2.2 Pilus 2b functional characterization

2.2.1 The expressions of different pilus types in the same GBS strain are independent

To study the function of different pilus types in GBS pathogenesis we used two mutant strains previously generated in COH1 strain, a well-known serotype III-ST-17 isolate, which expresses pilus 1 and pilus 2b (50). Each mutant strain carried an in-frame deletion of the gene coding for the backbone protein (BP) of pilus 1 (Δ*BP-1*) or of pilus 2b (Δ*BP-2b*), respectively. Total proteins were extracted from each mutant strain and analyzed by immunoblot analysis using sera anti BP-1 or 2b. Total proteins from the wild type strain revealed the typical HMW laddering indicative of pilus-like structures, whereas this laddering was not present in the two deletion mutant strains, suggesting that protein polymerization was completely abrogated. Complementation of *BP* genes restored protein polymerization to levels comparable to those of the wild type strain (50), confirming that the presence of the backbone proteins is fundamental for pili polymerization.

Figure 28. Schematic representation of COH PI-1 and PI-2b. COH1 strain has two different pilus genomic islands. PI-1 and PI-2b and they both encode for the three structural pilins and for two class C sortases. In this study two different mutant strains were used, each deleted of a different BP protein.

To analyze if the deletion of a BP in one genomic pilus island (PI) could influence the expression of the other one, a FACS analysis on whole bacteria was performed using monoclonal antibodies anti BP-1 and BP-2b. Antibodies raised against the BP-2a of pilus 2a and anti-polysaccharide type-III were used as negative and positive control, respectively. As shown in figure 29, backbone protein expressions from different pilus islands are independent, meaning that the mutation of one pilus island does not affect the protein expression of the other

pilus island. These results confirm that these mutants as appropriate tools for our analysis.

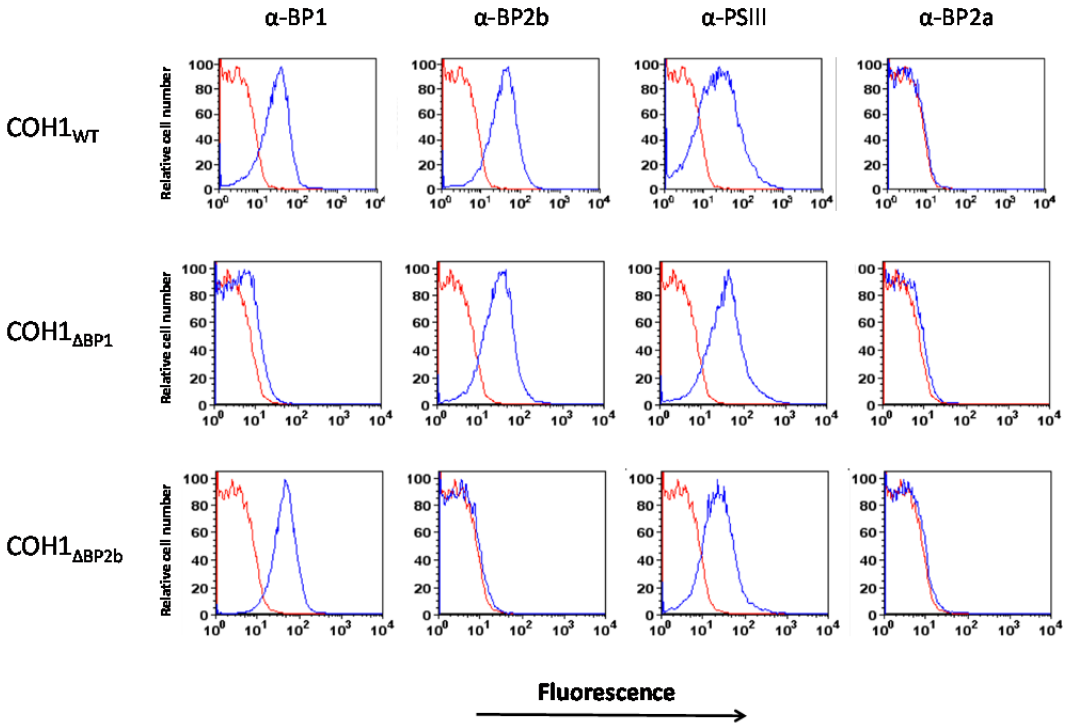

Figure 29. Different backbone protein expressions are independent. FACS analysis on COH1 wt and *BP* deletion mutant strains. Antibodies against BP1 and 2b were used to check the single deletion of each *BP* in the two mutant strains generated. It was used also to check if this single deletion could affect the expression of the other backbone protein. An antibody anti-serotype III was used as positive control and one against BP2a as negative control. As reported in the graph the deletion of one backbone protein do not influence the expression of the other one.

2.2.2 Pilus 2b is the one involved in COH1 adherence to host cells

The analysis of pili function upon host-cell interaction started with in vitro cell-based assays. Different cell lines were used, including human brain microvascular endothelial cells (hBMEC), vaginal epithelial cells (VK2/E6E7) and lung epithelial cells (A549). All the cell lines were incubated with bacteria at an MOI of 1 and all assays were done in triplicate. As shown in figure 30A, only when type 2b pilus is deleted, COH1 is significantly less adherent and therefore less invasive in hBMEC cells. The complemented strain expressing *BP-2b* restored

normal levels of adherence and invasion comparable to those of the wild type. The deletion of type 1 pilus did not result in any significant difference in terms of adherence and invasion from the wild type strain.

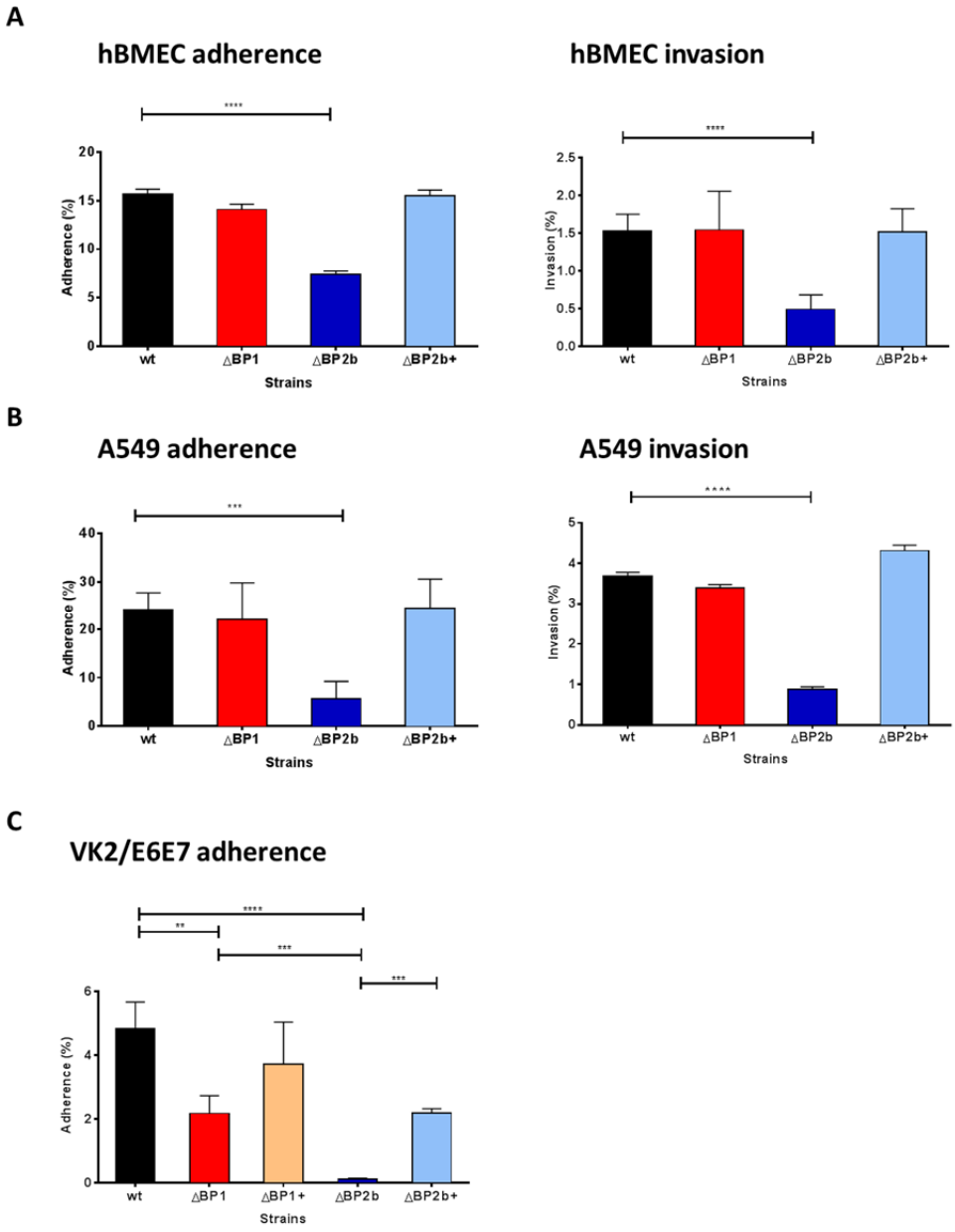

Figure 30. Pilus 2b backbone protein deletion affects GBS interaction with the host. COH1 wt and *BP* mutant and complemented strains were tested in adherence and invasion assays with human brain microvascular endothelial cells (hBMEC), vaginal epithelial (VK2/E6E7) and lung epithelial (A549) cells. A) Only the deletion of *BP-2b* causes a significant decrease in both adherence and invasion to hBMEC while instead the deletion of *BP-1* do not. Same results can be observed after GBS incubation with lung epithelial cells (18B). C) When GBS is incubated with vaginal epithelial cells both mutants result in a decrease in terms of adherence, but also in this case the deletion of *BP-2b* results in a dramatically decrease in adherence. All the complemented strains restored the wt phenotype.

Same results were obtained for lung epithelial cells (Fig. 30B). Cell adherence assay was done also with vaginal epithelial cells, and similar results were obtained but in this case also the *ΔBP-1* mutant caused decreased adherence to the cells. This suggests that this pilus type could be normally involved in more specific interaction with this kind of cells (Fig. 30C).

To further investigate how pili affect the adherence to host cells, we tested GBS binding abilities to Extracellular Matrix (ECM) components by using ECM proteins coated plates. As reported in figure 31, both mutants caused significant binding decreases to collagen, fibrinogen and laminin and fibronectin, which suggested that pili may contribute to GBS attachment to host cells through ECM binding. Especially the *ΔBP-2b* mutant resulted in a decreased binding ability to ECM components.

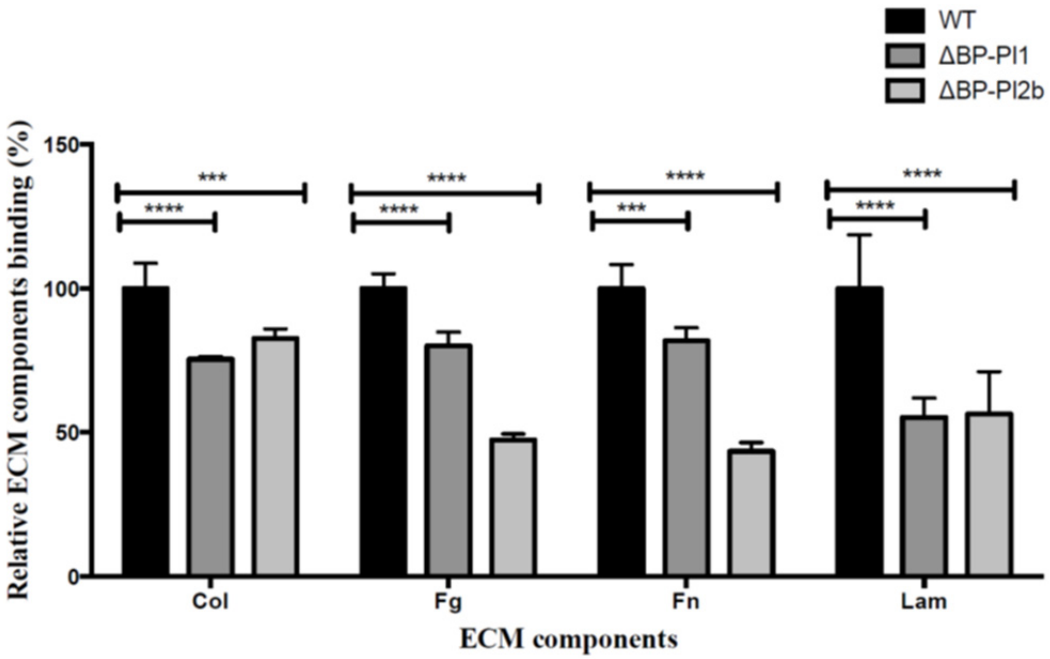

Figure 31. Pilus 2b is important for fibronectin binding. Wild-type GBS strain and Δ*BP* mutant strains were incubated with ECM components for and adherence assay. All the mutant strains tested gave significant differences in comparison to the wild-type. In particular BP-2b looks to be important for the binding to fibronectin. In fact when pilus 2b BP is deleted, GBS adherence significantly decrease; when instead is the only one present because BP-1 is deleted, GBS binding to fibronectin increase in a significant way.

2.2.3 Pilus 2b contributes to pathogenesis of meningitis in vivo

We have shown that type 2b pilus in *in vitro* assays resulted in a decreased adherence and invasion to all the cell lines tested and ECM components. To test if these findings could be confirmed also *in vivo*, we decided to examine different pili contribution to the pathogenesis of GBS CNS (central nervous system) infection *in vivo*.

Since ECM components and fibronectin have been demonstrated to be on brain endothelium (42) we thought that this binding could be an initial step for BBB penetration and meningitis development. We employed our mouse model of GBS hematogenous meningitis, as described previously (40,42,111,112). Ten mice per group (8-week, CD-1 male) were intravenously injected with either WT GBS or one of the two ΔBP mutants at a concentration of $1.5x10^8$ CFU. They were monitored for survival every three hours and they were sacrificed after 48 hours. After collecting and homogenizing brain and lungs in PBS, tissues were serial diluted and plated on THA plates. Also blood was collected, diluted and plated.

Bacterial loads found in different tissues in wt- and Δ*BP-1*-injected groups were similar, while instead there was a significant decrease in bacterial load in both the tissues and blood of mice infected with BP-PI-2b mutant (Fig. 32A). These findings demonstrated the important role of type 2b pilus in *in vivo* infection since its deletion affected GBS ability to survive and infect host tissues.

In order to better clarify different pili contribution to BBB penetration, an *in vitro* blood survival assay was performed. In this way we could understand if the differences of bacterial load found in blood and tissues of infected mice were due to different strains growth defects.

Fresh mice blood was collected and heparinized and it was then incubated at 37°C for 7 hours with bacteria at an MOI of 0.1. For each strain, three tubes were used for every time point collected.

Samples were then serial diluted in PBS and plated on THA every 30 min, and plates were then incubated over-night at 37°C. Mutant strains exhibited equivalent growth kinetics to the WT parent strain in murine whole blood ex vivo, thus

suggesting that the three strains tested did not have growth defects in blood (Fig. 32B).

Taken together these findings indicate that in COH1 strain type 2b pilus is the one mostly involved in host infection in *in vivo* model, confirming the in vitro results previously obtained.

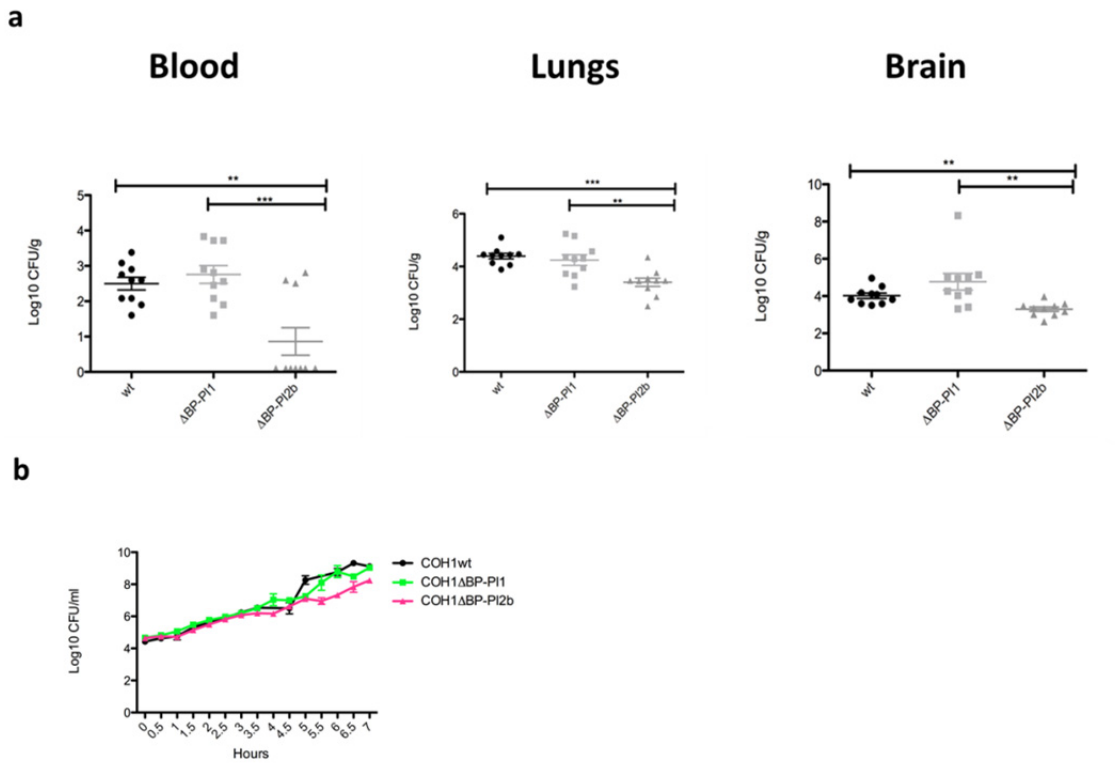

Figure 32. Pilus 2b contributes also to meningitis development in vivo. A) Mice were infected i.v. with COH1 wt or with one of the two mutant strains, each one deleted of a different BP. After 2 days mice were sacrificed and blood, brains and lungs were collected, homogenized and plated to quantify the bacterial load. As reported, the mutant strain deleted of BP-1 did not show any difference from the wild type strain in any of the tissues analyzed, while instead the deletion pf BP-2b lead to a significant decrease in the bacterial load in all the samples analyzed. B) This difference is not due to Δ*BP-2b* growth defects, since after in vitro blood survival assay, no significant differences among the tested strains could be observed.

2.2.4 Both pili are important for *in vivo* vaginal colonization

Our *in vitro* data indicates that both pilus types alter vaginal epithelial interactions (Fig. 30). To confirm these results *in vivo*, we used a mouse model of GBS vaginal colonization already described (113). In rodents, normal flora load and novel bacterial colonization ability appear to peak at estrus (114-116). We found this to be true in our model of GBS colonization (113). Consequently, we treated 8-week old CD1 mice with 17β-estradiol one day prior to bacterial inoculation. We inserted ~1×10^7 cfu GBS into the vagina, and on successive days, the vaginal lumen was swabbed and recovered bacteria quantified on agar plates to determine changes in bacterial load over time. The *ΔBP-2b* mutant exhibited decreased persistence in the vaginal tract by day 6 post-inoculation when compared to WT or *ΔBP-1* mutant strains, but not in a significant way (Fig. 33). Moreover, at day 10 we could not observe any difference between all the strains tested, suggesting that both the pilus types are important for vaginal colonization.

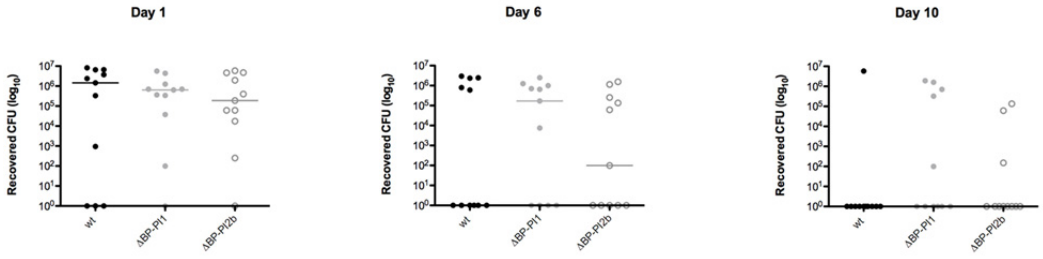

Figure 33. Both pilus types contribute to in vivo vaginal colonization. Mice were injected in the vaginal lumen with COH1 wt or with one of the two mutant strains, each one deleted of a different *BP* and swabbed everyday. After 10 days we could not detect any significant difference, even if a trend could be observed.

Chapter 3. Discussion

In Group B Streptococcus (GBS), a major cause of sepsis and meningitis in infants, pili have been associated to virulence and pathogenesis of the bacterium and discovered as highly immunogenic vaccine candidates (24,45,52). Pili are high-molecular-weight (HMW) polymers, visible by electron microscopy as long filamentous structures extending out from the bacterial surface. In GBS three structurally distinct pilus types have been identified and they are PI-1, PI-2a and PI-2b. These pili are heterotrimeric structures, constituted by a major pilus subunit, the backbone protein forming the pilus shaft, and two ancillary proteins (APs). These pilins are encoded by a pilus genomic island (PI) that includes also two class C sortases and a transcriptional regulator.
Sortase enzymes have a critical role in Gram-positive bacteria pathogenesis due to their function to covalently link to the bacterial cell-wall surface proteins or pilus polymers. Because of the importance of their substrates for a successful bacterial infection, sortases represent an attractive antivirulence/therapeutic target.

In this work we explored the sortase-mediated mechanism of pilus type 2b biogenesis in Group B *Streptococcus*, showing that it differs significantly from the current model of pilus assembly in Gram-positive pathogens.
Pilus-associated sortases, classified also as class C sortases (SrtC), are a family of membrane-associated cysteine transpeptidases, broadly distributed in Gram-positive bacteria that function as pilin polymerases that construct multi-subunit pili on the cell surface to promote bacterial adhesion (58,79). Unlike the constitutively expressed sortase A (SrtA), which normally anchors most surface LPXTG-containing proteins to the cell wall (117), SrtC enzymes are predicted to target a much smaller set of substrates. Their genes are present in several copies in a genome and differently from *srtA* gene, which is present in a monocistronic operon, occur typically in operons located in pathogenicity islands that also encode their substrates. The main novelty of this work is that the assembly mechanism that we propose for GBS pilus type 2b appears non-canonical. The genomic pilus 2b island (PI-2b) codes for two sortases (*SrtC1* and *SrtC2*) in addition to three structural subunits. We show that only SrtC1-2b is involved in

pilus protein polymerization, while SrtC2-2b does not act as a pilin polymerase, but it is involved in pilus anchoring process by recognizing the minor pilin subunit. This subunit (AP2-2b) is not conversely recognized by the housekeeping SrtA as happens for the pilus assembly in the majority of Gram-positive bacteria. By contrast, the classical model deriving from studies of the archetype SpaA-type pili in *Corynebacterium diphtheriae* (55) outlines two basic steps of pilin proteins polymerization catalyzed by a class C-sortase followed by the cell wall anchoring step of the resulting polymer by the housekeeping SrtA (56). Previous data indicated that also the other two pilus types of GBS (pilus 1 and 2a) follow this "canonical" assembly model and that both two sortases C (SrtC1 and SrtC2) coded by the genomic pilus islands 1 and 2a (PI-1 and PI-2a) can efficiently polymerize the backbone proteins *in vivo*, showing a certain level of redundancy. Their substrate specificity appeared to be related to their ability to predominantly incorporate into pili one of the two ancillary subunits, with significantly reduced ability to incorporate the other one (50). Accordingly, genetic and biochemical studies showed that the cell-wall anchoring of polymerized pili is completed by the housekeeping SrtA (59,92). Therefore, although the three GBS pili appear structurally highly similar as well as the overall gene organization of the genomic pilus islands, the only pilus type 2b follows a unique assembly mechanism. In *C. diphtheriae*, which produces three distinct pilus structures, SpaA-, SpaD- and SpaH-type pili, it has been demonstrated that the cell-wall attachment of Spa-type pili is mediated by the housekeeping sortase (named SrtF). Nevertheless, when the constitutive SrtF is absent, a class C sortase that is "normally" responsible for pilin polymerization, can be activated to catalyze the polymerized pili anchoring step, although less efficiently than SrtF (118). Not relatively to pili assembly, other studies reported that under specific environmental conditions class B or C sortases are activated for targeting proteins to the cell wall (80); for example, in sporulating *Bacillus anthracis* under iron starvation conditions a sortase B enzyme is activated for the cell-wall anchoring of a heme-binding protein involved in uptake of iron; or a sortase C enzyme can anchor a surface polypeptidide to the bacterial cell wall envelope for the formation of infectious spores (117,119,120). Similar evidences have been reported in *Streptococcus pyogenes*, where a class C sortase (SrtC2) is in competition with SrtA for protein cell wall anchoring (119).

However, the data reported so far on sortases action mechanism, sometimes apparently controversial and discrepant highlighted the universality of the transpeptidation mechanism of all sortase members belonging to different families and their redundancy and promiscuity in substrate recognition.

To better explore the different role of SrtC1 and SrtC2 in GBS pilus 2b assembly we conducted additional analysis by comparing these sortases with other characterized pilus-related sortases in Gram-positive species both at the sequence and structural level. Compared with GBS pilus 1 and pilus 2a sortases, pilus 2b sortases revealed a very low percentage of amino acid identity, forming a cluster far away from the others (91). However, at sequence level the most significant peculiarity of both SrtC1-2b and SrtC2-2b is the lack of the conserved DPY\W\F residues in the N-terminal regulatory lid motif. Moreover, in SrtC2-2b the N-terminal region is significantly shorter compared to the other, and more, this enzyme lacks also the predicted C-terminal transmembrane helix, that is known to be required for an efficient protein polymerization in pilus 2a formation (91). These observations led us to speculate different mechanisms of activation and regulation of these enzymes.

Currently, the presence of an N-terminal lid loop has been considered a characteristic feature of all pilus-specific sortases. Interestingly, except for SrtC1 from *S. pneumoniae* the poor electron density for most of the main and side chains of residues located within the lid (with the exception of the DPY\W\F residues) in the majority of SrtC structures indicated a high flexibility of this loop This flexibility has been correlated with an important role of the lid in enzyme activation, specifically in the regulation of substrate accessibility to the active site (91,93-96). Recent data on GBS pilus 2a sortase C1 strongly supported the hypothesis that SrtC are auto-inhibited by the presence of the lid and that their catalytic activity can be induced through a displacement of this loop from the enzyme active site probably as a result of the interaction with the substrate proteins and/or other unknown factors (121). It has been recently showed that an efficient polymerization of the backbone protein of pilus 2a can be achieved *in vitro* by using a recombinant mutant SrtC enzyme carrying a single residue

mutation in the lid region, whereas the wild type enzyme was totally inactive. This data suggested that a single residue in the lid can regulate the sortase catalytic activity through its interaction with the catalytic cysteine the in the active site. The absence of this lid residue might break this interaction, making the active site available for substrate binding. Additional analysis revealed that the lid confers thermodynamic and proteolytic stability to the sortase enzymes (121). SrtC1-2b has a tryptophan residue (W78) that could act as the putative regulatory residue by interacting with the catalytic cysteine in the enzyme active site. Interestingly, all the residues from S74 to D87 of the lid region in the N-terminal α helical roof surrounding the conserved β-barrel core could be included in SrtC1-2b structure, whereas other structures showed gaps. This might indicate that the conformation of SrtC1-2b N-terminal region is more stable. Moreover, this region is structurally different in terms of position relative to the β-barrel core; the lid loop is displaced from the active site and does not cover the substrate binding groove, thus resulting is in a wide-open state, suggesting a possible different mechanism for the substrate to gain access to the catalytic core. Except for the lid region, the overall fold of SrtC1-2b resembles the previously reported sortase C structures, particularly in the β-barrel core region, where the catalytic triad perfectly and spatially is overlapping among structures. However, since SrtC1-2b structure is in an open conformation, the role of the hypothetical lid residue W78 in enzyme regulation cannot be confirmed. Interestingly, superimposition of SrtC1-2b structure onto the "open-form" structure of sortase C1 from *S. suis* (98), indicated that *S. suis* SrtC1 is in an even more open conformation than SrtC1-2b. Hence, we could speculate that the lid region is capable of exploring wide conformational space, going from all the way up (*S. suis* SrtC1-like conformation) to a closed state (*S. pneumoniae* SrtC1-like or GBS SrtC1-1-like conformation) passing through an "open-intermediate" form as observed in SrtC2-2b conformation.

Another aspect on the sortase activity regulation *in vivo* takes into account the involvement of chaperone-like proteins in pilus assembly. An example is provided in pilus polymerization in *S. pyogenes*, where genetic evidences have demonstrated that the sortase is not sufficient alone to polymerize the backbone protein Spy0128, being the signal peptidase-like protein SipA, coded by the same

genomic pilus operon, also required for polymers formation (122). Interestingly, the crystal structure of Spy0129 revealed that it belongs to class B sortases, with a conserved β-barrel core, but lacking of the canonical lid motif as well as of the C-terminal transmembrane anchor, which is also considered a SrtC typical element. The flexibility of the β6/β7 loop is supposed to play a significant role in binding the sortase recognition motif of the substrate protein and conformational movements in this loop might correlate with the positions and orientations of the catalytic Cys and His residues, and be important for enzyme function (123). The need of a peptidase-like protein as chaperone for pilus assembly *in vivo* may be common to other pilus systems in the regulation of sortase activity. Interestingly, other pilus gene clusters contain genes encoding peptidase-like proteins, i.e. in *Actinomyces naeslundii* (124), in *S. pneumoniae* (125) and in *S. sui*s (126) as well as the genomic pilus island 2b contains a gene coding for a LepA-type signal peptidase. Further efforts will be necessary to understand the role of this protein in pilus 2b assembly.

An alternative mechanism could instead regulate the enzymatic activity of SrtC2-2b. As *S. pyogenes* Spy0129, SrtC2-2b does not contain a canonical lid region and the C-terminal TM, but it carries two additional cysteine residues that we speculated could be involved in the regulation of the enzymatic activity by disulfide bonds formation. FRET and AMS assays performed with cysteine single mutants of the recombinant SrtC2-2b protein suggested that disulfide bonds between the catalytic C180 and C115 could suppress the SrtC2 activity *in vitro*. Given that class C sortases are involved in a highly regulated process, we supposed that SrtC2-2b activation could be controlled by a redox regulation mechanism involving its three cysteines. We could speculate a model where C192 act as a sortase regulator, since it could be involved alternatively in disulfide bonds both with C180 and with C115. Although this hypothesis fits also with the SrtC2 structure model obtained by homology modeling, it remains to be further confirmed by additional structural studies.

In conclusion, sortase enzymes have a critical role in Gram-positive bacteria due to their function to covalently link to the cell-wall surface proteins or pilus

polymers, associated to virulence and pathogenesis of the bacterium (52). Importantly, in GBS pilin structural components have been discovered as highly immunogenic vaccine candidates and all epidemiologically relevant clinical isolates express at least one pilus type (24,45,52,127). Therefore, because of the importance of their substrates for a successful bacterial infection, sortases could represent an attractive antivirulence/therapeutic target. Thus, fully understanding the molecular basis of the mechanism of pilus biogenesis at the membrane environment during the establishment and persistence of infections by Gram-positive microorganisms, trying to solve open issues, for example why some pili are associated with multiple sortases and what determines sortase substrate specificity remains of great scientific interest.

Pilus type 2b remained uncharacterized so far, although it has been associated to a hypervirulent clone (ST17-serotype III) responsible of the majority of neonatal invasive diseases (24) (28,34,48,49,128).

The host-pathogen interaction upon GBS infection and invasion of BBB is still incompletely understood. Previous studies have identified several GBS virulence factors contributing to GBS adherence to and invasion of host cells, including pili, Fibronectin binding protein SfbA, Serine rich repeat protein Srr, lipoteichoic acid-anchoring protein IagA, HvgA and the alpha C protein (APC) (40,42,111,112,129-132). But their role at molecular level needs to be further determined.

The importance of pili for GBS virulence has already been demonstrated by several studies both *in vitro* and *in vivo*, where their subunits have been shown to be important for the initial bacterial attachment to the host cell promoting an efficient colonization (11,12,40,133-136). In particular pili are important for bacterial invasion that can lead to invasive diseases and then they play also a role in promoting resistance to phagocytic clearance (135,137). GBS in fact can cause meningitis crossing the BBB after adhesion and invasion of brain endothelium (42).

It has been demonstrated that the three different pilin subunits constituting GBS pili have different roles in bacterial infection.

The major pilin subunit, the backbone protein, has been shown to contribute to invasion by promoting resistance to phagocyte killing, thus increasing GBS bloodstream survival (135,137).

The tip ancillary protein (AP1) on the other hand has been demonstrated to be involved in adhesion to human pulmonary epithelial cells (11,134,138) or to human brain endothelial cells (40,75,137). In particular AP1 binds to collagen which promotes GBS interaction with the host thus activating the immune system and promoting bacterial entry into the CNS (40). However, the majority of these studies have been carried out on pilus types 1 or 2a.

In this study, we investigated the function of both type 1 and type 2b pilus using COH1 as background, a strain belonging to the serotype III-ST 17 lineage. COH1 expresses both pilus 1 and 2b and deleting individually BPs, we obtained two different strains expressing just one pilus. (62). In this way these knockout mutants represented a perfect tool to analyze the role of each pilus in host adherence and invasion.

Previous studies have shown that the capacity of a COH1 Δ*BP-1* mutant strain, not expressing pilus 1 on its surface, to adhere to epithelial cells was not affected. The COH1 *ΔAP1-1* mutant strain lacking the gene coding for the AP1 protein instead bound significantly less to epithelial cells compared to the wild type, suggesting that in pilus type 1 the ancillary protein AP1 seems to have a role for pili adhesion to host cells. Type 2b pilus subunits role in adherence were never investigated in a ST-17 background (139).

Our findings demonstrate that the *ΔBP-2b* mutant resulted in a dramatic decrease in adherence and invasion to different cell lines, whereas the *ΔBP1* mutant strain did not show any significant difference in adherence and invasion compared with the wild-type strain in hBMEC and lung epithelial cells. Accordingly with our results, it was previously reported that the Δ*BP-1* mutant did not impair GBS adherence not only to lung epithelial cells, but also to intestinal cell line (Caco2) and human cervical epithelial cells (ME180) (139).

However, Δ*BP-1* mutant strain does show significant differences in adherence to vaginal epithelial cells compared with the wild-type strain, suggesting that pilus proteins function may depend on specific characteristics of host cells (42) since

these results were also confirmed by the *in vivo* vaginal colonization model. Indeed it has been reported that the acidic pH of the vaginal tract enhances type 1 pilus expression [51].

Another study instead showed that a *ΔBP-1* mutant did not appear to contribute significantly to vaginal epithelial cell adherence (140), however, this analysis was not performed on a COH1 background, suggesting that results could be influenced also by the tested GBS strain.

In previous studies the *ΔBP-2b* mutant strain resulted in a decreased adherence and invasion to A549, ME-180, C2Bbe1 colonic, and HeLa cervical epithelial cells (135,136), in agreement to our evidences.

Our data also show that both type 1 and type 2b pilus are involved in ECM components binding suggesting that pili promote GBS attachment to host cells through binding to ECM components. Indeed it has been previously reported that PI-AP1 interacts with fibronectin and fibrinogen (75), but also with collagen, which engages integrins and the integrin-signaling machinery that contributes to the pathogenesis of meningitis *in vivo* (141).

Since ECM components and fibronectin have been demonstrated to be on brain endothelium (42) we investigated if this binding could be an initial step for BBB penetration and meningitis development.

From our *in vivo* studies we observed that type 2b pilus contributes to GBS virulence and BBB penetration *in vivo*. In the mouse meningitis model, bacterial counts in blood and tissues from mice injected with *ΔBP-2b* mutant were significantly lower in comparison with those from mice injected with the wild-type or *ΔBP-1* mutant. Of note, *ex vivo* blood survival did not show difference among GBS wild-type strain and the two mutant strains indicating the reduced virulence from *ΔBP-2b* mutant is not due to growth defect.

In summary our data highlight importance of type 2b pilus in GBS attachment and invasion of host cell and its contribution to GBS virulence in vivo, suggesting that this pilus type so far poorly characterized, should be further investigated.

Chapter 4. Experimental procedures

4.1 Bioinformatics

The complete genome sequences of *Streptococcus agalactiae* strain COH1 are available in NCBI GenBank under the Accession Number HG939456.1. The primary sequences of SrtC1 protein (accession number CDN66744) and SrtC2 protein (accession number CDN66742) were used in TMHMM Server (http://www.cbs.dtu.dk/services/TMHMM/) to predict transmembrane helices and membrane topology of protein sequences. Multiple sequence alignments were performed using ClustalW and alignment analyses were done with ESPript (http://espript.ibcp.fr/ESPript/ESPript/) (142).

4.2 Bacterial strains, media, and growth conditions

Group B *Streptococcus* strains (Suppl. Table 1) were grown in Todd Hewitt Broth (THB) or trypticase soy agar (TSA) plates or chemically defined RPMI-1640 medium (Sigma-Aldrich) at 37°C in 5% CO_2. *Escherichia coli* cells were grown aerobically at 37°C in Luria-Bertani medium. When required, antibiotics were added to the medium at the following concentrations: erythromycin, 1 µg/ml (*S. agalactiae*) or 100 µg/ml (*E. coli*); chloramphenicol, 10 µg/ml (*S. agalactiae*) or 20 µg/ml (*E. coli*), ampicillin 100 µg/ml (*E. coli*).

4.3 DNA manipulation

Genomic DNA was isolated from GBS strains by a standard protocol for Gram-Positive bacteria, by mutanolysin-treatment of bacterial cells using a GeneElute Bacterial Genomic DNA kit (Sigma-Aldrich) according to the manufacturer's instructions. Plasmids (Suppl. Table 1) were purified from *E. coli* cells using a HP Plasmid Miniprep Kit (Omega Bio-Tek, VWR). DNA restriction and modification enzymes were used under the conditions specified by the manufacturer (NEB,

Ipswich, MA). Oligonucleotides used in this study were synthesized in-house or by Sigma-Aldrich. PCR experiments were performed using Kapa HiFi DNA polymerase (KapaBiosystems) and PCR products were purified using the Wizard SV Gel/PCR Clean-Up System (Promega).

4.4 Construction of in-frame deletion mutant strains, complementation vectors and site-specific mutagenesis

In-frame deletion mutant strains, listed in Suppl. Table 1, were generated in GBS strain ABC020017623 carrying only pilus island 2b, using Splicing by Overlap Extension (SOE) PCR as described previously (50,143). For each mutant strain generated, two PCR products comprising the flanking sequences of the target gene and a 30 bp overlapping region, were ligated via the overlap sequence and cloned into the temperature-sensitive allelic exchange vector pJRS233 (gift of June Scott, Emory University, Atlanta, GA), generating pJRS233-derived plasmids carrying overlapping flanking sequences of each target gene to knock out. Transformation and allelic exchange were then performed as described previously (144) and confirmation of the predicted insertions was obtained by PCR amplification and sequencing.

Complementation vectors (Suppl. Table 1) were generated into the *E. coli*-streptococcal shuttle vector pAM401/gbs80P_T, previously described (50,145) containing the promoter and terminator regions of the *gbs80* gene (TIGR annotation SAG_0645). For the generation of vectors pAM_srtC1, pAM_srtC2 and pAM_AP2-2b, DNA fragments corresponding to *srtC1*, *srtC2* and *ap2* genes were PCR amplified from GBS strain ABC020017623 genomic DNA and the products were cloned into the shuttle vector pAM401/gbs80P_T.

For the generation of the complementation vector pAM_BP-2b, a DNA fragment corresponding to *BP-2b* gene (locus tag SAK_1440) was PCR amplified from GBS A909 genome, and the product was cloned into the same shuttle vector.

Site-directed mutagenesis was performed by the polymerase incomplete primer extension (PIPE) method (146), using the complementation vectors pAM_SrtC1, pAM_SrtC2 and pAM_BP-2b as templates for the introduction of specific

mutations. The method was improved using Kapa HiFi polymerase and digesting DNA template with DpnI enzyme to optimize the protocol for large plasmids. Mutations were confirmed by DNA sequencing. All complementation vectors expressing mutated forms of sortases were electroporated into the corresponding knock-out (KO) strains. Complementation was confirmed by checking protein expression by Western blot analysis.

4.5 Antibodies

Antisera specific for the pilus 2b subunits, backbone protein (BP-2b), major and minor ancillary proteins (AP1-2b and AP2-2b) and sortases C were produced by immunizing CD1 mice with the purified recombinant proteins as previously reported (24,50). Animal treatments were performed in compliance with current Italian legislation on the care and use of animals in experimentation (Legislative Decree 116/92) and with the Novartis Animal Welfare Policy and Standards. Protocols were approved by the Italian Ministry of Health (authorization 21/2009-B) and by the local Novartis Animal Ethical Committee (authorization AEC 200825).

Mouse monoclonal antibodies (mAbs) anti BP-1, anti BP-2a, anti BP-2b and anti polysaccharide III (PS-III) were generated by Areta International (Varese, Italy) using standard protocols. Briefly, B-cell hybridoma clones were isolated from spleen cells of immunized CD1 mice with the purified recombinant proteins (BP-1, BP-2a and BP-2b) and the purified tetanus toxoid (TT)-conjugated serotype III polysaccharide. Hybridoma clones were screened by enzyme-linked immunosorbent assay (ELISA). Positive clones were then tested for binding to the surface of GBS by flow cytometry. The selected mAbs were finally purified by protein G affinity chromatography. and the MAbs were purified by protein G affinity chromatography.

4.6 GBS proteins extraction and immunoblot analysis

For the preparation of total soluble proteins GBS mid-exponential-phase cells, grown in THB or RPMI, were harvested by centrifugation, washed in phosphate-buffered saline (PBS) and re-suspended in 50mM Tris-HCl (pH 6.8), containing mutanolysin (Sigma-Aldrich, St. Louis, MO, USA) and complete protease inhibitors (Roche, Basel, Switzerland). Cell suspensions were incubated at 37°C for 2 hours. After 3 cycles of freeze and thaw, total soluble proteins were separated from insoluble materials by centrifugation at 15000 g at 4°C for 10 min. The pellet corresponding to the membrane-enriched fraction was solubilized in 2% SDS buffer and used for assessing sortase expression. To visualize proteins released during bacterial growth, supernatants from cultures in RPMI medium were harvested by centrifugation at 4,000 g for 20 min, filtered with a 0,22 μm syringe filter and 10-fold concentrated. Protein concentration was measured using BCA protein assay (Pierce; Thermo Scientific, Rockford, IL, USA).

Equal amounts of bacterial proteins from each strain were separated by sodium dodecyl sulfate–polyacrylamide gel electrophoresis (SDS-PAGE) and transferred to nitrocellulose membranes using iBlot transfer (Dry blot system, Lifetechnologies). Membranes were probed with mouse antisera directed against structural pilus proteins or against sortase C enzymes (1:1000 dilution), followed by a rabbit anti-mouse horseradish peroxidase-conjugated secondary antibody (Dako, Glostrup, Denmark). Bands were then visualized using an Opti-4CN substrate kit (Bio-Rad) or SuperSignal West Pico chemiluminescent substrate (Pierce; Thermo Scientific, Rockford, IL, USA).

4.7 Cloning, expression, and purification of recombinant proteins

PCR fragments encoding $SrtC1_{38\text{-}245}$ (locus tag GBSCOH1_1278) and $SrtC2_{32\text{-}199}$ (locus tag GBSCOH1_1276) domains were amplified by PCR from genomic DNA extracted from the COH1 GBS strain and cloned into pET15-TEV vector (modified in house from Novagen to adapt to PIPE cloning) using the polymerase incomplete primer extension (PIPE) method (146) to produce N-terminal HIS-

tagged (TEV cleavable) proteins. The $SrtC2_{C115A}$, $SrtC2_{C180A}$, and $SrtC2_{C192A}$ mutants were generated by PIPE site-directed mutagenesis using as template the HIS-tagged $SrtC2_{32-199}$ wild type plasmid. The recombinant SrtA was produced as previously reported (92) and AP2-2b (locus tag GBSCOH1_1277) was cloned in pET21b(+) vector to produce a C-terminal HIS-tagged protein following the same strategy reported for AP2-2a (92).

Protein expression was performed in Escherichia coli Rosetta2(DE3) cells (Novagen) using the EnPresso Tablet Cultivation Set (BioSilta) supplemented with 100 μg/mL ampicillin. Bacteria were first grown at 30°C, 160rpmfor 12 hours and afterwards target protein production was induced by the addition of 1mM IPTG at 25°C, 160rpm for 24 hours. Cells were harvested by centrifugation (4000 rpm, 30 min, 4°C), and then cell lysis were performed using Cell Lytic Express (Sigma Aldrich). Protein purification was performed by a first immobilized metal affinity chromatography (IMAC) step followed by a second IMAC step after TEV cleavage to remove the N-terminal 6XHis-tag.

For the purification of $SrtC1_{WT}$ and $SrtC2_{WT}$ used for crystallization trials the last IMAC purification step was followed by size-exclusion chromatography (SEC) using HiLoad 26/60 Superdex 200 (GE Healthcare; Life Sciences, Piscataway, NJ, USA) equilibrated in 25 mM HEPES,75 mM NaCl pH7 at a flow rate of 2 ml/min. The fractions containing the pure protein, which showed a single band by SDS-PAGE, were quantified with the bicinchoninic acid (BCA) assay (Pierce; Thermo Scientific, Rockford, IL, USA).

For NMR experiments cells were grown in M9 minimal medium containing 1 g/l of $(15NH_4)2SO_4$ for the expression of 15N labeled samples, at 37°C until OD_{600} ~ 0.8 and then induced with 1 mM isopropyl-β-d-thiogalactoside for 16 h at 25°C. The soluble proteins were extracted using CelLytic B (Sigma-Aldrich) and DNase and then purified by a FF-Crude His-Trap HP nickel chelating column (Amersham Biosciences, Piscataway, NJ, USA). The recombinant SrtC2 mutants were eluted with 300 mM imidazole, and the buffer was exchanged with TEV cleavage buffer (50 mM Tris-HCl, pH 8; 1 mM DTT, and 0.5 mM EDTA) using a PD-10 desalting coloumn (GE healthcare). HIS-tag was cleaved by incubation with AcTEV protease (12h at RT) and then removed by a subtractive IMAC

purification step. The proteins were then concentrated by ultrafiltration to 20 mg/ml, and the buffer was exchanged using a PD-10 desalting column (Amersham Biosciences) equilibrated with 50mM NaH_2PO_4 pH 6.5.

4.8 Crystallization, data collection and structure determination

Crystallization experiments were performed by the sitting-drop method, mixing 0.2 µL of protein at 30 mg/ml and 0.1 µL of reservoir solutions in 96-well low-profile crystallization plates and using a Crystal Gryphon robot (Art Robbins Instruments). Crystals of SrtC1-2b were obtained in condition H2 of the Hampton Research PEG/ION screen, containing 0.05M tri-Sodium Citrate (pH 2.3), 16% PEG3,350, 0.05M Bis-Tris propane (pH 9.7). Before data collection, crystals of SrtC1-2b were first soaked in 10% ethylene glycol as cryoprotectant, and then cooled to 100 K in liquid nitrogen.

Diffraction data were measured at 100K on beamline ID29 of the European Synchrotron Radiation Facility (ESRF) in Grenoble, and processed with XDS (147) and the CCP4 suite of programs (148). The structure of SrtC1-2b was solved by molecular replacement in molrep (149), using coordinates of the sortase C1 of the pilus island 1 of GBS (pdb ID 4g1j) as input template model. Structure refinement and rebuilding were performed by Phenix (150), and Coot (151), with final model Rwork and Rfree statistics of 18.0 and 22.3 %, respectively. The final refined coordinates of SrtC1 includes residues 39-232, and were deposited in the PDB with accession code 4d7w. Data collection and refinement statistics are summarized in Table 4.

4.9 Nuclear magnetic resonance (NMR) spectroscopy

^{15}N labeled recombinant protein sample were buffer exchanged using a PD-10 desalting column (Amersham Biosciences, Arlington Heights, IL, USA), equilibrated with 50 mM phosphate buffer (pH 6.5), and finally concentrated by ultrafiltration to 0.3 mM.

Next, ^{1}H-^{15}N heteronuclear single-quantum coherence (HSQC) spectra were recorded at 25°C on a Bruker Avance III spectrometer (Bruker, Karlsruhe, Germany) operating at 600.13 MHz proton Larmor frequency, equipped with a cryogenic probe. A standard ^{1}H-^{15}N HSQC pulse sequence was used, with pulsed field gradients for suppression of the solvent signal and cancellation of artifacts. Next, 2048 (^{1}H) × 256 (^{15}N) complex data points were acquired with spectral windows of 8196.935 Hz (^{1}H) ×2432.718 Hz (^{15}N), 8 transients, and 1.2-s relaxation delay. Proton T_2 measurements were performed with the 1D oneone echo sequence (152) using variable delays of 0.2 and 5.2 ms and evaluating the corresponding signal intensities [$T_2 = 2 \times (5.2 - 0.2)/\ln (I_{0.2}/I_{5.2})$]. Processing of all the spectra was performed with Topspin2.1 (Bruker, Karlsruhe, Germany).

4.10 Fluorescence resonance energy transfer (FRET) assay

The Fluorescence resonance energy transfer (FRET) assay was used to monitor the *in vitro* activity of the recombinant sortase enzymes by using fluorescently self-quenched peptides, tagged with EDANS as fluorophore and DABCYL as quencher, containing the LPXTG-like motif of pilin subunits (Table 3). The synthetic fluorogenic peptides were purchased from Thermo Scientific Biopolymers (Waltham, MA, USA) and were dissolved in 50% DMSO.
The activity test was performed in 300 mM NaCl, 50 mM Tris-HCl (pH 8), 5 or 25 μM sortase enzymes, and 64 or 128 μM fluorogenic peptide. Reaction was started by the addition of enzyme and was monitored by measuring the increase in fluorescence every 20 min (λex=336 nm, λem=490 nm) at 37°C using an InfiniteM200 spectrophotometer microplate reader (Tecan, Mannedorf, Switzerland). Measurements of fluorogenic peptides incubated at the same conditions, but without sortases were used as blank.

4.11 In vitro cleavage assay

The *in vitro* cleavage assay was performed by mixing 50 μM of the recombinant $SrtC2_{WT}$ or $SrtA_{WT}$ with 25 μM of the recombinant His-tagged AP2-2b protein.

The volume of reaction was 1 ml in buffer containing 50 mM Tris-HCl, 300 mM NaCl, and 1 mM DTT (pH 8). DTT was added just to prevent the formation of potential disulfide bridges leading to aspecific SrtC2 dimerization during the incubation time. As control each protein was incubated alone at the same conditions.

The incubation was performed at 37°C, and the reaction samples were purified by IMAC and eluted with 300 mM imidazole. The concentration of the purified fractions was then measured with BCA assay and then equal amount of each sample was analyzed by Western blot analysis using sera anti-AP2-2b.

4.12 Free-cysteines quantification

Estimation of free thiols was performed by AMS (4-acetamido-4_-maleimidylstilbene-2,2_disulfonic Acid) to study if the cysteines oxidation state is or not involved in disulphide bonds formation. AMS has high water solubility and readily is conjugated to free thiols (108).

Recombinant SrtC2 wt and $SrtC2_{C115A}$, $SrtC2_{C180A}$, and $SrtC2_{C192A}$ mutants were purified by two steps of IMAC and TEV cleavage. All the protein samples were quantified through BCA assay and checked by SDS_PAGE. Half of the samples (reduced form) were incubated with 5 mM DTT for 15' at 37°C, buffer was then exchanged through PD-10 to remove the DTT. The other half of the samples (non-reduced form) was directly incubated incubated with AMS without any DTT treatment.

Samples of 1 ml of the reaction mixture in 50 mM Tris-HCl, 300 mM NaCl buffer (pH 8) containing 25 μM protein, 250 μM AMS, and 1% SDS were incubated for 30 min at 37°C to complete the reaction. The excess of AMS was removed by dialysis.

AMS shows a typical UV absorption at ≈328 nm and emission maximum at 408 nm. Fluorescence measurements (λ excitation=322 nm; λ emission=406 nm) were performed to detect the AMS bounded to the free thiols present in each protein samples at the moment of the AMS addiction to evaluate the difference in the number of free thiols between reduced and native forms of the wild type and

cysteine-mutated sortases. The same buffer only with AMS and without sortase was used as blank.

4.13 Flow cytometry

GBS was grown in THB and stopped at OD 0.5 and after a wash with PBS, harvested bacterial cells were resuspended in PBS containing 0.1% (wt/vol) paraformaldehyde. Cell suspensions were incubated at 37°C for 1 h. Fixed cells were then washed in PBS/1% BSA and incubated at RT for 20 min in newborn calf serum (Sigma, St. Louis, MO). Bacteria were then incubated for 30 min at RT with primary antibodies diluted 1:200 in dilution buffer (PBS, 0.1% [wt/vol] bovine serum albumin, 20% [vol/vol] newborn calf serum). Monoclonal antibodies used were anti BP-1, anti BP-2a, anti BP-2b and anti polysaccharide III (PS-III). Cells were washed in PBS–0.1% (wt/vol) bovine serum albumin and incubated for a further 30 min with R-phycoerythrin-conjugated F(ab)2 goat anti-mouse immunoglobulin G (1:100 dilution) (Jackson ImmunoResearch Laboratories, West Grove, PA) diluted 1:100 in PBS containing 0.1% BSA. Cells were washed again, resuspended in PBS, and analyzed with a BD FACS Calibur (BD Bioscience) by acquiring 15,000 events. FlowJo software (v.8.6, Tree Star, Ashland, OR) was used.

4.14 Cell lines

GBS infection assays were performed in both endothelial and epithelial cell lines. Immortalized human brain microvascular endothelial cell line (hBMEC) was kindly provided by professor Kwang Sik Kim at Johns Hopkins University and cells were cultured in RPMI1640 containing 10% FBS, 10% Nu-serum and 1% nonessential amino acids. Immortalized human vaginal (VK2/E6E7) epithelial cell line was obtained from the American Type Culture Collection (ATCC CRL-2616) and was cultured in keratinocyte serum-free medium (KSFM) (Invitrogen) containing 0.1 ng.ml_1 human recombinant epidermal growth factor (EGF), 0.05 mg.ml_1 bovine pituitary extract, and 0.4 nM calcium chloride . Human A549

lung carcinoma cell line was obtained from the American Type Culture Collection (ATCC CCL-185) and was cultured in RPMI1640 Human A549 lung carcinoma cell line was containing 10% FBS, and 1% nonessential amino acids. All cells lines were maintained at 37°C with 5% CO2.

4.15 Adherence and invasion assays

For the infection assays mid-log grown bacteria were added to confluent cell monolayers at a multiplicity of infection (MOI) of 1. Total cell-associated GBS bacteria were recovered after an incubation of 30 minutes, while intracellular GBS were recovered after 2-h infection and 2-h incubation with 100 μg of gentamicin (Sigma) and 5μg of penicillin (Sigma) to kill all extracellular bacteria. After washing, monolayers were trypsinized with 0.1 ml of 0.25% trypsin-EDTA solution and lysed with addition of 0.4 ml of 0.025% Triton X-100 by vigorous pipetting and the number of invasive bacteria was quantified by serial dilution plating on THA. Parallel invasion experiments were performed in hBMEC, vaginal epithelial cells and A549 lung epithelial cells. Bacterial adherence (total cell-associated) and invasion was calculated as (recovered CFU/initial inoculum CFU) x100%.

All cellular adherence and invasion assays were performed in triplicate and repeated at least three times.

4.16 Binding of GBS to ECM components

96 well plates were coated with human fibronectin (Sigma), rat tail collagen type I (Sigma), human fibrinogen (Acris Antibodies) and laminin from human placenta (Sigma) respectively at a concentration of 5μg.ml^{-1}. The assay was performed as described previously (42). Briefly ~1×10^5 CFU of GBS were added into each well and incubate for 30 min at 37°C. The wells were then washed with PBS to remove unbound bacteria, and adherent bacteria were treated with 50 μL 0.25% trypsin-EDTA solution for 10 min at 37°C to release the attached bacteria. Bacteria were quantified by plating serial dilutions onto THB agar. The percentage of GBS

binding to ECM components was calculated as (recovered CFU/initial inoculum) ×100%.

4.17 Mouse model of meningitis

Animal experiments were approved by the committee on the use and care of animals at San Diego State University (SDSU) protocol APF 13-07-011D and performed using accepted veterinary standards. We utilized a mouse model of hematogenous GBS meningitis that has already been used in Kelly Doran's lab at SDSU (42). Briefly, 8-week-old male CD-1 mice (Charles River Laboratories, Wilmington, MA, USA) were injected via tail vein (i.v.) with 1.5×10^8 CFU of GBS. At the experimental endpoint (day 2 p.i.) blood, brain and lungs were collected upon euthanasia. Tissues were homogenized and homogenates as well as blood were plated on THB agar for enumeration of bacterial CFU.

4.18 Bacteria blood survival assay

4×10^3 CFU of mid log phase GBS were added into 0.2 ml of heparinized mice fresh blood and incubated at 37°C with rotation. The number of viable bacteria in the mixture was determined by plating serial dilutions on THA every 30 min up to 7 hr. Each GBS strain was run in triplicate for each time point.

4.19 In vivo mouse model of vaginal colonization

Female CD1 mice, 8 weeks of age were used for colonization assays (10 mice per group) as described previously (113). They were injected intraperitoneally (i.p.) with 0.5mg β-estradiol valerate in 100uL of sesame oil (Sigma) to synchronize estrus and optimize bacterial colonization 24h prior to GBS inoculation.Mice were inoculated with a total ~1x107 CFU of GBS in 10μL of PBS in the vaginal vault.WT and the two BP mutant strains were used. In the following days the bacterial load was determined by swabbing the vaginal lumen with ultrafine calcium alginate-tipped swabs and serial dilution plating of swab samples on

CHROMagarStrepBagar (DRGInternational Inc.). These plates allow to identify GBS and native Enterococcus strains by the presence of pink- and blue-pigmented colonies, respectively.

4.20 Statistical analysis

The significance of differences in bacterial counts between mice groups or in hBMEC adherence and invasion was determined using one-way ANOVA. $P < 0.05$ was considered to be significant.
GraphPad Prism (GraphPad Software, San Diego, CA, USA) was used for all the analyses.

Supplementary tables

Table 1. Bacterial strains and plasmids used in this study

Strain or plasmid	Relevant characteristic(s)	Source or reference
Strains		
E. coli		
Rosetta	F– ompT hsdSB(rB– mB–) gal dcm pRARE2 (CamR)	Novagen
DH5α	F- φ80lacZΔM15 Δ(lacZYA-argF) U169 recA1 endA1 hsdR17 (rk-, mk+) phoA supE44 λ- thi-1 gyrA96 relA1	Invitrogen
Mach1™-T1R	F- φ80(lacZ)ΔM15 ΔlacX74 hsdR(rK-mK+) ΔrecA1398 endA1 tonA	Invitrogen
S. agalactiae		
ABC020017623	Wild type	(24)
ABC020017623Δ*BP*	GBS knockout (KO) deleted of pilus 2b backbone protein gene	(153)
ABC020017623Δ*BP* + BPwt	ΔBP complemented with pAM401_BP_{WT}	This study
ABC020017623Δ*BP* + $BP_{\Delta LPXTG}$	ΔBP complemented with pAM401_$BP_{\Delta LPXTG}$	This study
ABC020017623Δ*BP* + BP_{E423A}	ΔBP complemented with pAM401_BP_{E423A}	This study
ABC020017623Δ*BP* + BP_{K77A}	ΔBP complemented with pAM401_BP_{K77A}	This study
ABC020017623Δ*BP* + BP_{K82A}	ΔBP complemented with pAM401_BP_{K82A}	This study
ABC020017623Δ*BP* + BP_{K118A}	ΔBP complemented with pAM401_BP_{K118A}	This study
ABC020017623Δ*BP* + BP_{K175A}	ΔBP complemented with pAM401_BP_{K175A}	This study
ABC020017623Δ*SrtC1*	GBS knockout (KO) deleted of pilus 2b sortase C1 gene	This study
ABC020017623Δ*SrtC1* + SrtC1wt	ΔSrtC1 complemented with pAM401_$SrtC1_{WT}$	This study
ABC020017623Δ*SrtC1* + $SrtC1_{C188A}$	ΔSrtC1 complemented with pAM401_$SrtC1_{C188A}$	This study
ABC020017623Δ*SrtC2*	GBS knockout (KO) deleted of pilus 2b sortase C2 gene	This study
ABC020017623Δ*SrtC2* + SrtC2wt	ΔSrtC2 complemented with pAM401_$SrtC2_{WT}$	This study
ABC020017623Δ*SrtC2* + $SrtC2_{C115A}$	ΔSrtC2 complemented with pAM401_$SrtC1_{C115A}$	This study

ABC020017623Δ*SrtC2* + $SrtC2_{C180A}$	ΔSrtC2 complemented with pAM401-SrtC1C180A	This study
ABC020017623Δ*SrtC2* + $SrtC2_{C192A}$	ΔSrtC2 complemented with pAM401-SrtC1C192A	This study
ABC020017623Δ*AP2*	ΔAP2	Unpublished data
ABC020017623Δ*AP2* + AP2	ΔAP2 complemented with pAM401-AP2	This study
COH1	Wild type	(50)
COH1Δ*BP-1*	GBS knockout (KO) deleted of pilus 1 backbone protein gene	(50)
COH1Δ*BP-1* + BP-1	ΔBP-1 complemented with pAM401-BP-1	(50)
COH1Δ*BP-2b*	GBS knockout (KO) deleted of pilus 2b backbone protein gene	Unpublished data
COH1Δ*BP-2b* + BP-2b	ΔBP-2b complemented with pAM401-BP-2b	This study
Plasmids		
pJRS233	6.0 kb; ColE1 *ori*; temperature-sensitive *E. coli*-streptococcal shuttle vector	(154)
pJRS233_Δ*SrtC1*	pJRS233-derived containing overlapping flanking sequences of *SrtC1* gene	This study
pJRS233_Δ*SrtC2*	pJRS233-derived containing overlapping flanking sequences of *SrtC2* gene	This study
pAM401/gbs80P+T	11.5 kb; Cmr; ColE1 *ori; E. Coli*-streptococcal shuttle vector pAM401 containing promoter of gbs80	(50)
. . pAM401_$SrtC1_{WT}$	pAM401/gbs80P+T-derived containing entire $SrtC1_{WT}$ coding sequence	This study
. . pAM401_$SrtC_{C188A}$	pAM401/gbs80P+T-derived containing entire $SrtC1_{C188A}$ coding sequence	This study
.. pAM401_$SrtC2_{WT}$	pAM401/gbs80P+T-derived containing entire $SrtC2_{WT}$ coding sequence	This study
pAM401_$SrtC2_{C115A}$	pAM401/gbs80P+T-derived containing entire $SrtC2_{C115A}$ coding sequence	This study
.. pAM401_$SrtC2_{C180A}$	pAM401/gbs80P+T-derived containing entire $SrtC2_{C180A}$ coding sequence	This study
.. pAM401_$SrtC2_{C192A}$	pAM401/gbs80P+T-derived containing entire $SrtC2_{C192A}$ coding sequence	This study
.. pAM401_*AP2*	pAM401/gbs80P+T-derived containing entire *AP2* coding sequence	This study

pAM401_*BP-2b*	pAM401/gbs80P+T-derived containing entire *BP-2b* coding sequence	This study
pAM401_*BP-2b*$_{\Delta LPXTG}$	pAM401/gbs80P+T-derived containing *BP-2b*$_{\Delta LPXTG}$ coding sequence	This study
pAM401_*BP-2b*$_{E423A}$	pAM401/gbs80P+T-derived containing entire *BP-2b*$_{E423A}$ coding sequence	This study
pAM401_*BP-2b*$_{K77A}$	pAM401/gbs80P+T-derived containing entire *BP-2b*$_{K77A}$ coding sequence	This study
pAM401_*BP-2b*$_{K82A}$	pAM401/gbs80P+T-derived containing entire *BP-2b*$_{K82A}$ coding sequence	This study
pAM401_*BP-2b*$_{K118A}$	pAM401/gbs80P+T-derived containing entire *BP-2b*$_{K118A}$ coding sequence	This study
pAM401_*BP-2b*$_{K175A}$	pAM401/gbs80P+T-derived containing entire *BP-2b*$_{K175A}$ coding sequence	This study
pET15-TEV	5708bp; Bacterial expression vector with T7 promoter and N-terminal TEV-cleavable 6xHis- tag; ampicillin resistance in bacteria; restriction enzyme cloning	Novagen
pET15-TEV-*Srtc2*$_{32-199}$	pET15TEV-derived containing *SrtC2*$_{32-199}$ coding sequence	This study
pET15-TEV-*Srtc2*$_{C115A}$	pET15TEV-derived containing *SrtC2*$_{C115A}$ coding sequence	This study
pET15-TEV-*Srtc2*$_{C180A}$	pET15TEV-derived containing *SrtC2*$_{C180A}$ coding sequence	This study
pET15-TEV-*Srtc2*$_{C192A}$	pET15TEV-derived containing *SrtC2*$_{C192A}$ coding sequence	This study
pET15-TEV-*Srtc1*$_{38-245}$	pET15TEV-derived containing *SrtC1* coding sequence lacking of the N- and C-term transmembrane regions	This study

Table 2. Primers used in this study

	Sequence	
petTEVfor	TAACGCGACTTAATTCTAGCATAACCCCTTGGGGCCTCAAACGG	Sequencing after cloning in pet15 vector
petTEVrev	GCCCTGGAAGTACAGGTTTTCGTGATGATGATGATGATGGCTGCTGCCCATGGTATATC	Sequencing after cloning in pet15 vector
seqpetrev	GATATCCGGATATAGTTCCTC	Sequencing after cloning in pet15 vector
npet	CGCGAAATTAATACGACTCAC	Sequencing after cloning in pet15 vector
MSrtC2C115F	GTGATTGCGGCGCATAATTTTCCTTATCATTTTGAT	Site-directed mutagenesis for C115A in SrtC2
MSrtC2C115R	ATGCGCCGCAATCACCATGTTATTAGTTAAATAAGA	Site-directed mutagenesis for C115A in SrtC2
MSrtC2C180F	TTTACTGCGACAAAGGCAGGAGTAGCTAGAGTATTA	Site-directed mutagenesis for C180A in SrtC2
MSrtC2C180R	CTTTGTCGCAGTAAACAAGCTTAAGTCCCAATCATT	Site-directed mutagenesis for C180A in SrtC2
MSrtC2C192F	GTGCGCGCGCAATTAATTGATGTTAAAAATTAA	Site-directed mutagenesis for C192A in SrtC2
MSrtC2C192R	TAATTGCGCGCGCACTAATACTCTAGCTACTCCTGC	Site-directed mutagenesis for C192A in SrtC2
MSrtC1C188F	GTGACGGCGACACCATATGGCGTTAATACCCATCGG	Site-directed mutagenesis for C188A in SrtC1
MSrtC1C188R	TGGTGTCGCCGTCACCAAAGTTTGGTAGTCTTTACC	Site-directed mutagenesis for C188A in SrtC1
SeqSrtC2F	ACAAGGTATTATGGTTCTTAT	Sequencing of SrtC2
SeqAP2F	ACAAAAGCTGTTCATAAAACT	Sequencing of AP2
SeqSrtC1F	TTAAAAGTTGGAGACCACTGG	Sequencing of SrtC1
PSrtC2R	AATTAAGTCGCGTTAATTTTTAACATCAATTAATTG	Cloning of SrtC2 in pet15tev
PSrtC1F	CTGTACTTCCAGGGCGCTTATCCTTCACTTGCTAAT	Cloning of SrtC1 in pet15tev
PSrtC1R22	AATTAAGTCGCGTTACTCTATTTGTATTGCCTCTGC	Cloning of SrtC2 in

2		pet15tev
SanSrtC1REV	CTCTCTCTGAGATCTTTATAAATCATTGTTCTCTTCCTTTCT	Cloning of SrtC1 in PAM
P5pjrsF	GCTATGACCATGATTACGCCAAGC	Sequencing of insertion in Pjrs
P6pjrsR	GCTTAAATCGGGCCATTTTGCG	Sequencing of insertion in Pjrs
P1FSrtC1	CGCGGATCCATGCCATCTGCTTCTGTAGTTGATTTGAAC	SrtC1 Ko construction
P2R SrtC1	ATCGCTCGAGATTGGTGAAATGAATTC	SrtC1 Ko construction
P3F SrtC1	TCACCAATCTCGAGCGATAACGTAAGAAAATTTTAAAACAAGCA	SrtC1 Ko construction
SrtC1R4sal	CCGGTCGACTTAAGTTCGGAATATCCAGAGTTCCCAAG	SrtC1 Ko construction
P7seq SrtC1F	ATGCCATCTGCTTCTGTAGTTGATTTGAAC	SrtC1 Ko construction
P8seq SrtC1R	TTTAAAACAAATATAGCACCTTGTAATGAA	SrtC1 Ko construction
P9seq SrtC1F	GAATGCTACGGGTCAATTTCTAAACTTTAA	SrtC1 Ko construction
P10seq SrtC1R	TAAATGTTGTCTTATTTTTTTCATATATTT	SrtC1 Ko construction
P11seq SrtC1F	GTATCCATTTTGCTTGTCACTATAATTGCA	SrtC1 Ko construction
P12seq SrtC1R	AAAGCCTTGAAGAGGGTAAACCTCTATGTC	SrtC1 Ko construction
P13seq SrtC1F	TTTCTGATTTGGATAAGTTAAAAGTTGGAG	SrtC1 Ko construction
P14seq SrtC1R	TACTTAGACTAAATAATAAGAGAAGAGTTA	SrtC1 Ko construction
P15seq SrtC1F	CTCAACTTGTGTCTGCTGATACCAATGATC	SrtC1 Ko construction
P16seq SrtC1R	AGGGCTCATTTTCTCAAATGCTGTAATATC	SrtC1 Ko construction
P17seq SrtC1F	TTAAATGCTAAACCTAAAAAAGAAGAGACA	SrtC1 Ko construction

P18seq SrtC1R	TTAAGTTCGGAATATCCAGAGTTCCCAAGT	SrtC1 Ko construction
P19ext SrtC1F	ATCATGGTACAGAAAAAGTGTATCAATATG	SrtC1 Ko construction
P20ext SrtC1R	ACAGTTGTTCAAAACTATAATTAGCAGCTA	SrtC1 Ko construction
P1F SrtC2	CGCGGATCCATATGGCGTTAATACCCATCGGTTACTAGT	SrtC2 Ko construction
P2R SrtC2	TAGATTCCAGAACTTACCAGAATAATTCCG	SrtC2 Ko construction
P3F SrtC2	AGGAGTAGCTAGAGTATTCGGAATTATTCTGGTAAGTTCTGGAA	SrtC2 Ko construction
P4R SrtC2	CCGCTCGAGTCAAATGCGATTACAGTGTCGGGCCAATAT	SrtC2 Ko construction
P5seq SrtC2F	ATATGGCGTTAATACCCATCGGTTACTAGT	SrtC2 Ko construction
P6seq SrtC2R	TATAGTAATAGAACCCGTTTTCATCTGATC	SrtC2 Ko construction
P7seq SrtC2F	AGGTATTGGAATAAAAGACGATGATCTAAC	SrtC2 Ko construction
P8seq SrtC2R	TAATCACGTCTTCTTCTCCATTTTAAAGCT	SrtC2 Ko construction
P9seq SrtC2F	GAAGATATTCAGCAAATTTTTTAGCTATAC	SrtC2 Ko construction
P10seq SrtC2R	TCTATTACTGATTTTGTAGTGATAGATTTG	SrtC2 Ko construction
P11seq SrtC2F	GAAATTATTGAACCAACAGCGATTGAAAAA	SrtC2 Ko construction
P12seq SrtC2R	CATTTTACGTGTATTTGTCATAAAAAAATT	SrtC2 Ko construction
P13seq SrtC2F	GTGACAATCGCCATTCTTTCTGCCTTATCT	SrtC2 Ko construction
P14seq SrtC2R	TTTATATCTTTCTAATATTGGCAAACAAGCCA	SrtC2 Ko construction
P15ext SrtC2F	ATTGTTAAAGGTAAAGACTACCAAACTTTG	SrtC2 Ko construction
P16ext SrtC2R	TAGAAAGATTTGGCAACTGTCCTCTAACAC	SrtC2 Ko construction

SrtC1 Not for	CACCTGTCATGCGGCCGCATTTTAGTAATAGGAGCAG GTA	Cloning of SrtC1 into Pam
SrtC1 BglII-rev	CTCTCTCTGAGATCTTTATAAATCATTGTTCTCTTCC TTTCT	Cloning of SrtC1 into Pam
SrtC2 Not for	CACCTGTCATGCGGCCGCTAATTATGTCAGGACTTC	Cloning of SrtC2 into Pam
SrtC2 Bgl rev	CACCTGTCATAGATCTTTAATTTTTAACATCAATTAA	Cloning of SrtC2 into Pam
AP2 Not for	CACCTGTCATGCGGCCGCAGCAATGAGAAAGGAAGAG AACAA	Cloning of AP2 into Pam
AP2 Bgl rev	CACCTGTCATAGATCTCTAATCACGTCTTCTTCTCCA T	Cloning of AP2 into Pam
pAM-F	CGTGACATGACTGAAATAGGTAGTTGAG	Sequencing after cloning into pam vector
pAM-R	CATCGCCATCTTCAGTTGATTTTAATTGG	Sequencing after cloning into pam vector
AP2 Not for	CACCTGTCATGCGGCCGCAGCAATGAGAAA GGAAGAGAACAA	Cloning of AP2 into Pam
AP2 Bgl rev	CACCTGTCATAGATCTCTAATCACGTCTTC TTCTCCAT	Cloning of AP2 into Pam
BP-2b Not for	CACCTGTCATGCGGCCGCGCTTTAGCTCTA CCATCAGGA	Cloning of BP-2b into Pam
BP-2b Bgl rev	CACCTGTCATAGATCTTTAAGAACGTAAAC GACGACGA	Cloning of BP-2b into Pam
M-BP-LPXTG-F	AACAAAGGTACTGAGGGTATTGGTACAACA ATTTTC	Site-directed mutagenesis for LPXTG in BP-2b
M-BP-LPXTG-R	CTCAGTACCTTTGTTATTTTCAACAGTTGG	Site-directed mutagenesis for LPXTG in BP-2b
M-BP-E423-F	GTAGTTGCGGCGAACGCGGGGTCTTA TGAAGTAACT	Site-directed mutagenesis for E423A in BP-2b
M-BP-E423-F	AGACCCCGCGTTCGCCGCAACTACAG AAGCAGATGG	Site-directed mutagenesis for E423A in BP-2b
M-BP-K77-	CAAGGTGCGGAAGCTGAGTATAAAGC	Site-directed mutagenesis for K77A

F	TTCAACTGAT	in BP-2b
M-BP-K77-R	AGCTTCCGCACCTTGAGGAATTAAATAAGAAGCTCC	Site-directed mutagenesis for K77A in BP-2b
M-BP-K82-F	GAGTATGCGGCTTCAACTGATTTTAATTCTCTTTTT	Site-directed mutagenesis for K82A in BP-2b
M-BP-K82-R	TGAAGCCGCATACTCAGCTTCTTTACCTTGAGGAAT	Site-directed mutagenesis for K82A in BP-2b
M-BP-K118-F	TGGGCT**GCG**TCTATATCAGCTAATACTACACCAGTT	Site-directed mutagenesis for K118A in BP-2b
M-BP-K118-R	TATAGACGCAGCCCATGTCGCAATCTCATTTGCTGA	Site-directed mutagenesis for K118A in BP-2b
M-BP-K175-F	CATGAA**GCG**AATACTGATGCGACATGGGGAGATGGT	Site-directed mutagenesis for K175A in BP-2b
M-BP-K175-R	AGTATT**CGC**TTCATGAATAGTAGCATTTGGAGTTAC	Site-directed mutagenesis for K175A in BP-2b

Table 3. Peptides used in this study

PEPTIDE	SEQUENCE
BP-2b = AP1-2b	Dabsyl-KGTELPSTGGIGT-Edans
AP2-2b	Dabsyl-QTKGKLPFTGQV-Edans
AP2-2a	Dabsyl-SFLPKTGM-Edans
AP2-1	Dabsyl-RGGLIPKTGEQQ-Edans

Table 4. Data collection and refinement statistics

	SrtC1-2b
Wavelength	1.072
Resolution range	45.92 - 1.95 (2.02 - 1.95)
Space group	P 21 21 2
Unit cell	37.56 124.76 45.92 90 90 90
Total reflections	56716 (5190)
Unique reflections	16211 (1538)
Multiplicity	3.5 (3.4)
Completeness (%)	0.99 (0.96)
Mean I/sigma(I)	15.73 (1.59)
Wilson B-factor	34.81
R-merge	0.04989 (0.6619)
R-meas	0.0588 (0.7852)
CC1/2	0.999 (0.695)
CC*	1 (0.906)
Reflections used in refinement	16202 (1534)
Reflections used for R-free	811 (77)
R-work1	0.1809 (0.2825)
R-free2	0.2230 (0.3374)
CC(work)	0.966 (0.836)
CC(free)	0.973 (0.614)
Number of non-hydrogen atoms	1645
macromolecules	1551
ligands	4
Protein residues	193
RMS(bonds)	0.008

RMS(angles)	1.03
Ramachandran favored (%)	97
Ramachandran allowed (%)	3.1
Ramachandran outliers (%)	0
Rotamer outliers (%)	0.57
Clashscore	3.54
Average B-factor	44.04
macromolecules	44.08
ligands	41.29
solvent	43.47
Number of TLS groups	9

Statistics for the highest-resolution shell are shown in parentheses.

1 Rwork = Σ||F(obs)|- |F(calc)||/Σ|F(obs)|

2 Rfree = as for Rwork, but calculated for 5.0% of the total reflections that were chosen at random and omitted from refinement.

Table 5. Multiple structural alignment of SrtC1-2b (pdb 4d7w) with other known sortase structures using the DALI server

PDB-Chain	Z score	rmsd	length alignment	number of residues	sequence identity (%)	SORTASE FAMILY	description	reference
3g69-A	29	1,3	183	192	43	SORTASE C	*Streptococcus pneumoniae* Sortase C2 (SRTC-2)	1
4g1j-B	28,6	1,5	185	199	42	SORTASE C	Sortase C1 of GBS Pilus Island 1 (SrtC1-1)	2
2w1j-B	27,6	1,6	182	195	47	SORTASE C	*Streptococcus pneumoniae* Sortase C1 (SRTC-1)	3
2xwg-B	27,3	1,4	174	185	44	SORTASE C	*Actinomyces oris* sortase C1	4
3o0p-A	27	1,5	178	194	46	SORTASE C	Sortase C1 of GBS Pilus Island 2a (SrtC1-2a)	5
4g1h-A	25,8	1,4	167	176	49	SORTASE C	Sortase C2 of GBS Pilus Island 1 (SrtC2-1)	6
3re9-A	23,6	2	161	179	50	SORTASE C	*Streptococcus suis* sortase C1	7
3tb7-A	22,5	1,7	176	188	43	SORTASE C	Type I *Streptococcus agalactiae* sortase C1	8
2w1k-A	22,2	2,4	181	208	30	SORTASE C	*Streptococcus pneumoniae* Sortase C3 (SRTC-3)	9
3fn5-B	16,6	2	135	163	27	SORTASE A	*S. pyogenes* serotype M1 sortase A (Spy1154)	10
2kid-A	14,5	2,6	139	148	28	SORTASE A	*S. aureus* Sortase A-substrate Complex	11
3rcc-G	14,4	2,5	128	132	27	SORTASE A	*Streptococcus agalactiae* Sortase A	12
2kw8-A	14	2,9	130	158	30	SORTASE A	*Bacillus anthracis* Sortase A	13

Hits are ranked by Z-Score with best hits at the top of the table.
PDB: Protein Data Bank
rmsd: root-mean-square deviation of Cα atoms of superimposed proteins in Angstroms
length alignment: number of structurally equivalent positions
number of residues: number of structurally equivalent aligned residues
sequence identity (%): percentage of amino acid identity in aligned positions

Table References

1. Neiers, F., et al., Two crystal structures of pneumococcal pilus sortase C provide novel insights into catalysis and substrate specificity. J Mol Biol, 2009. 393(3): p. 704-16.
2. Cozzi, R., et al., Structural basis for group B streptococcus pilus 1 sortases C regulation and specificity. PLoS One, 2012. 7(11): p. e49048.
3. Manzano, C., et al., Sortase-mediated pilus fiber biogenesis in Streptococcus pneumoniae. Structure, 2008. 16(12): p. 1838-48.
4. Persson, K., Structure of the sortase AcSrtC-1 from Actinomyces oris. Acta Crystallogr D Biol Crystallogr, 2011. 67(Pt 3): p. 212-7.
5. Cozzi, R., et al., Structure analysis and site-directed mutagenesis of defined key residues and motives for pilus-related sortase C1 in group B Streptococcus. Faseb j, 2011. 25(6): p. 1874-86.
6. Cozzi, R., et al., Structural basis for group B streptococcus pilus 1 sortases C regulation and specificity. PLoS One, 2012. 7(11): p. e49048.
7. Lu, G., et al., A novel "open-form" structure of sortaseC from Streptococcus suis. Proteins, 2011. 79(9): p. 2764-9.
8. Khare, B., et al., The crystal structure analysis of group B Streptococcus sortase C1: a model for the "lid" movement upon substrate binding. J Mol Biol, 2011. 414(4): p. 563-77.

9. Manzano, C., et al., Sortase-mediated pilus fiber biogenesis in Streptococcus pneumoniae. Structure, 2008. 16(12): p. 1838-48.
10. Race, P.R., et al., Crystal structure of Streptococcus pyogenes sortase A: implications for sortase mechanism. J Biol Chem, 2009. 284(11): p. 6924-33.
11. Suree, N., et al., The structure of the Staphylococcus aureus sortase-substrate complex reveals how the universally conserved LPXTG sorting signal is recognized. J Biol Chem, 2009. 284(36): p. 24465-77.
12. Khare, B., et al., Structural differences between the Streptococcus agalactiae housekeeping and pilus-specific sortases: SrtA and SrtC1. PLoS One, 2011. 6(8): p. e22995.
13. Weiner, E.M., et al., The Sortase A enzyme that attaches proteins to the cell wall of Bacillus anthracis contains an unusual active site architecture. J Biol Chem, 2010. 285(30): p. 23433-43.

Bibliography

1. Gibbs, R. S., Schrag, S., and Schuchat, A. (2004) Perinatal infections due to group B streptococci. *Obstet Gynecol* **104**, 1062-1076
2. Johri, A. K., Paoletti, L. C., Glaser, P., Dua, M., Sharma, P. K., Grandi, G., and Rappuoli, R. (2006) Group B Streptococcus: global incidence and vaccine development. *Nature reviews. Microbiology* **4**, 932-942
3. Kogan, G., Uhrin, D., Brisson, J. R., Paoletti, L. C., Blodgett, A. E., Kasper, D. L., and Jennings, H. J. (1996) Structural and immunochemical characterization of the type VIII group B Streptococcus capsular polysaccharide. *J Biol Chem* **271**, 8786-8790
4. Mitchell, T. J. (2003) The pathogenesis of streptococcal infections: from tooth decay to meningitis. *Nat Rev Microbiol* **1**, 219-230
5. Baker, C. J. (1997) Group B streptococcal infections. *Clin Perinatol* **24**, 59-70
6. Maisey, H. C., Doran, K. S., and Nizet, V. (2008) Recent advances in understanding the molecular basis of group B Streptococcus virulence. *Expert Rev Mol Med* **10**, e27
7. Hansen, S. M., Uldbjerg, N., Kilian, M., and Sorensen, U. B. R. (2004) Dynamics of Streptococcus agalactiae colonization in women during and after pregnancy and in their infants. *J Clin Microbiol* **42**, 83-89
8. Yamamoto, Y., Pargade, V., Lamberet, G., Gaudu, P., Thomas, F., Texereau, J., Gruss, A., Trieu-Cuot, P., and Poyart, C. (2006) The Group B Streptococcus NADH oxidase Nox-2 is involved in fatty acid biosynthesis during aerobic growth and contributes to virulence. *Mol Microbiol*
9. Betz, A. L. (1985) Epithelial properties of brain capillary endothelium. *Fed Proc* **44**, 2614-2615
10. Betz, A. L. (1992) An overview of the multiple functions of the blood-brain barrier. *NIDA Res Monogr* **120**, 54-72
11. Dramsi, S., Caliot, E., Bonne, I., Guadagnini, S., Prevost, M. C., Kojadinovic, M., Lalioui, L., Poyart, C., and Trieu-Cuot, P. (2006) Assembly and role of pili in group B streptococci. *Mol Microbiol* **60**, 1401-1413
12. Maisey, H. C., Hensler, M., Nizet, V., and Doran, K. S. (2007) Group B streptococcal pilus proteins contribute to adherence to and invasion of brain microvascular endothelial cells. *J Bacteriol* **189**, 1464-1467
13. Baker, C. J. (2013) The spectrum of perinatal group B streptococcal disease. *Vaccine* **31 Suppl 4**, D3-6
14. Skoff, T. H., Farley, M. M., Petit, S., Craig, A. S., Schaffner, W., Gershman, K., Harrison, L. H., Lynfield, R., Mohle-Boetani, J., Zansky, S., Albanese, B. A., Stefonek, K., Zell, E. R., Jackson, D., Thompson, T., and Schrag, S. J. (2009) Increasing burden of invasive group B streptococcal disease in nonpregnant adults, 1990-2007. *Clinical infectious diseases : an official publication of the Infectious Diseases Society of America* **49**, 85-92
15. Schuchat, A. (1998) Epidemiology of group B streptococcal disease in the United States: shifting paradigms. *Clin Microbiol Rev* **11**, 497-513
16. Doran, K. S., and Nizet, V. (2004) Molecular pathogenesis of neonatal group B streptococcal infection: no longer in its infancy. *Mol Microbiol* **54**, 23-31
17. Rubens, C. E., Raff, H. V., Jackson, J. C., Chi, E. Y., Bielitzki, J. T., and Hillier, S. L. (1991) Pathophysiology and histopathology of group B streptococcal sepsis in Macaca nemestrina primates induced after intraamniotic inoculation: evidence for bacterial cellular invasion. *J Infect Dis* **164**, 320-330
18. **Edwards, M. S., and C. J. Baker**. (2001) *Group B streptococcal infections*, *In* J. S. Remington and J. O. Klein (ed.)

19. Puopolo, K. M., Madoff, L. C., and Eichenwald, E. C. (2005) Early-onset group B streptococcal disease in the era of maternal screening. *Pediatrics* **115**, 1240-1246
20. Schrag, S. J., Zywicki, S., Farley, M. M., Reingold, A. L., Harrison, L. H., Lefkowitz, L. B., Hadler, J. L., Danila, R., Cieslak, P. R., and Schuchat, A. (2000) Group B streptococcal disease in the era of intrapartum antibiotic prophylaxis. *N Engl J Med* **342**, 15-20
21. Korzeniowska-Kowal, A., Witkowska, D., and Gamian, A. (2001) [Molecular mimicry of bacterial polysaccharides and their role in etiology of infectious and autoimmune diseases]. *Postepy Hig Med Dosw* **55**, 211-232
22. Martin, D., Rioux, S., Gagnon, E., Boyer, M., Hamel, J., Charland, N., and Brodeur, B. R. (2002) Protection from group B streptococcal infection in neonatal mice by maternal immunization with recombinant Sip protein. *Infection and immunity* **70**, 4897-4901
23. Maione, D., Margarit, I., Rinaudo, C. D., Masignani, V., Mora, M., Scarselli, M., Tettelin, H., Brettoni, C., Iacobini, E. T., Rosini, R., D'Agostino, N., Miorin, L., Buccato, S., Mariani, M., Galli, G., Nogarotto, R., Dei, V. N., Vegni, F., Fraser, C., Mancuso, G., Teti, G., Madoff, L. C., Paoletti, L. C., Rappuoli, R., Kasper, D. L., Telford, J. L., and Grandi, G. (2005) Identification of a Universal Group B Streptococcus Vaccine by Multiple Genome Screen. *Science* **309**, 148-150
24. Margarit, I., Rinaudo, C. D., Galeotti, C. L., Maione, D., Ghezzo, C., Buttazzoni, E., Rosini, R., Runci, Y., Mora, M., Buccato, S., Pagani, M., Tresoldi, E., Berardi, A., Creti, R., Baker, C. J., Telford, J. L., and Grandi, G. (2009) Preventing bacterial infections with pilus-based vaccines: the group B streptococcus paradigm. *J Infect Dis* **199**, 108-115
25. Jones, N., Bohnsack, J. F., Takahashi, S., Oliver, K. A., Chan, M. S., Kunst, F., Glaser, P., Rusniok, C., Crook, D. W., Harding, R. M., Bisharat, N., and Spratt, B. G. (2003) Multilocus sequence typing system for group B streptococcus. *Journal of clinical microbiology* **41**, 2530-2536
26. Musser, J. M., Mattingly, S. J., Quentin, R., Goudeau, A., and Selander, R. K. (1989) Identification of a high-virulence clone of type III Streptococcus agalactiae (group B Streptococcus) causing invasive neonatal disease. *Proc Natl Acad Sci U S A* **86**, 4731-4735
27. Jones, N., Oliver, K. A., Barry, J., Harding, R. M., Bisharat, N., Spratt, B. G., Peto, T., Crook, D. W., and Oxford Group, B. S. C. (2006) Enhanced invasiveness of bovine-derived neonatal sequence type 17 group B streptococcus is independent of capsular serotype. *Clin Infect Dis* **42**, 915-924
28. Lamy, M. C., Dramsi, S., Billoet, A., Reglier-Poupet, H., Tazi, A., Raymond, J., Guerin, F., Couve, E., Kunst, F., Glaser, P., Trieu-Cuot, P., and Poyart, C. (2006) Rapid detection of the "highly virulent" group B Streptococcus ST-17 clone. *Microbes Infect* **8**, 1714-1722
29. Manning, S. D., Springman, A. C., Lehotzky, E., Lewis, M. A., Whittam, T. S., and Davies, H. D. (2009) Multilocus sequence types associated with neonatal group B streptococcal sepsis and meningitis in Canada. *Journal of clinical microbiology* **47**, 1143-1148
30. Bisharat, N., Jones, N., Marchaim, D., Block, C., Harding, R. M., Yagupsky, P., Peto, T., and Crook, D. W. (2005) Population structure of group B streptococcus from a low-incidence region for invasive neonatal disease. *Microbiology (Reading, England)* **151**, 1875-1881
31. Luan, S. L., Granlund, M., Sellin, M., Lagergard, T., Spratt, B. G., and Norgren, M. (2005) Multilocus sequence typing of Swedish invasive group B streptococcus isolates indicates a neonatally associated genetic lineage and capsule switching. *Journal of clinical microbiology* **43**, 3727-3733

32. Jones, N., Oliver, K. A., Barry, J., Harding, R. M., Bisharat, N., Spratt, B. G., Peto, T., and Crook, D. W. (2006) Enhanced invasiveness of bovine-derived neonatal sequence type 17 group B streptococcus is independent of capsular serotype. *Clinical infectious diseases : an official publication of the Infectious Diseases Society of America* **42**, 915-924
33. Martins, E. R., Pessanha, M. A., Ramirez, M., and Melo-Cristino, J. (2007) Analysis of group B streptococcal isolates from infants and pregnant women in Portugal revealing two lineages with enhanced invasiveness. *Journal of clinical microbiology* **45**, 3224-3229
34. Poyart, C., Reglier-Poupet, H., Tazi, A., Billoet, A., Dmytruk, N., Bidet, P., Bingen, E., Raymond, J., and Trieu-Cuot, P. (2008) Invasive group B streptococcal infections in infants, France. *Emerg Infect Dis* **14**, 1647-1649
35. Lin, F. Y., Whiting, A., Adderson, E., Takahashi, S., Dunn, D. M., Weiss, R., Azimi, P. H., Philips, J. B., 3rd, Weisman, L. E., Regan, J., Clark, P., Rhoads, G. G., Frasch, C. E., Troendle, J., Moyer, P., and Bohnsack, J. F. (2006) Phylogenetic lineages of invasive and colonizing strains of serotype III group B Streptococci from neonates: a multicenter prospective study. *Journal of clinical microbiology* **44**, 1257-1261
36. Bohnsack, J. F., Whiting, A., Gottschalk, M., Dunn, D. M., Weiss, R., Azimi, P. H., Philips, J. B., 3rd, Weisman, L. E., Rhoads, G. G., and Lin, F. Y. (2008) Population structure of invasive and colonizing strains of Streptococcus agalactiae from neonates of six U.S. Academic Centers from 1995 to 1999. *Journal of clinical microbiology* **46**, 1285-1291
37. Brochet, M., Couve, E., Zouine, M., Vallaeys, T., Rusniok, C., Lamy, M. C., Buchrieser, C., Trieu-Cuot, P., Kunst, F., Poyart, C., and Glaser, P. (2006) Genomic diversity and evolution within the species Streptococcus agalactiae. *Microbes and infection / Institut Pasteur* **8**, 1227-1243
38. Mandlik, A., Swierczynski, A., Das, A., and Ton-That, H. (2008) Pili in Gram-positive bacteria: assembly, involvement in colonization and biofilm development. *Trends Microbiol* **16**, 33-40
39. Konto-Ghiorghi, Y., Mairey, E., Mallet, A., Dumenil, G., Caliot, E., Trieu-Cuot, P., and Dramsi, S. (2009) Dual role for pilus in adherence to epithelial cells and biofilm formation in Streptococcus agalactiae. *PLoS pathogens* **5**, e1000422
40. Banerjee, A., Kim, B. J., Carmona, E. M., Cutting, A. S., Gurney, M. A., Carlos, C., Feuer, R., Prasadarao, N. V., and Doran, K. S. (2011) Bacterial Pili exploit integrin machinery to promote immune activation and efficient blood-brain barrier penetration. *Nat Commun* **2**, 462
41. Baeten, K. M., and Akassoglou, K. (2011) Extracellular matrix and matrix receptors in blood-brain barrier formation and stroke. *Dev Neurobiol* **71**, 1018-1039
42. Mu, R., Kim, B. J., Paco, C., Del Rosario, Y., Courtney, H. S., and Doran, K. S. (2014) Identification of a group B streptococcal fibronectin binding protein, SfbA, that contributes to invasion of brain endothelium and development of meningitis. *Infection and immunity* **82**, 2276-2286
43. Soriani, M., Santi, I., Taddei, A., Rappuoli, R., Grandi, G., and Telford, J. L. (2006) Group B Streptococcus crosses human epithelial cells by a paracellular route. *J Infect Dis* **193**, 241-250
44. Nallapareddy, S. R., Singh, K. V., Sillanpaa, J., Garsin, D. A., Hook, M., Erlandsen, S. L., and Murray, B. E. (2006) Endocarditis and biofilm-associated pili of Enterococcus faecalis. *J Clin Invest* **116**, 2799-2807
45. Nuccitelli, A., Cozzi, R., Gourlay, L. J., Donnarumma, D., Necchi, F., Norais, N., Telford, J. L., Rappuoli, R., Bolognesi, M., Maione, D., Grandi, G., and Rinaudo, C. D. (2011) Structure-based approach to rationally design a chimeric protein for

an effective vaccine against Group B Streptococcus infections. *Proc Natl Acad Sci U S A* **108**, 10278-10283
46. Tettelin, H., Masignani, V., Cieslewicz, M. J., Donati, C., Medini, D., Ward, N. L., Angiuoli, S. V., Crabtree, J., Jones, A. L., Durkin, A. S., Deboy, R. T., Davidsen, T. M., Mora, M., Scarselli, M., Margarit, Y. R. I., Peterson, J. D., Hauser, C. R., Sundaram, J. P., Nelson, W. C., Madupu, R., Brinkac, L. M., Dodson, R. J., Rosovitz, M. J., Sullivan, S. A., Daugherty, S. C., Haft, D. H., Selengut, J., Gwinn, M. L., Zhou, L., Zafar, N., Khouri, H., Radune, D., Dimitrov, G., Watkins, K., O'Connor K, J., Smith, S., Utterback, T. R., White, O., Rubens, C. E., Grandi, G., Madoff, L. C., Kasper, D. L., Telford, J. L., Wessels, M. R., Rappuoli, R., and Fraser, C. M. (2005) Genome analysis of multiple pathogenic isolates of Streptococcus agalactiae: Implications for the microbial "pan-genome". *Proc Natl Acad Sci U S A* **102**, 13950-13955
47. Jiang, S., Park, S. E., Yadav, P., Paoletti, L. C., and Wessels, M. R. (2012) Regulation and function of pilus island 1 in group B streptococcus. *J Bacteriol* **194**, 2479-2490
48. Springman, A. C., Lacher, D. W., Waymire, E. A., Wengert, S. L., Singh, P., Zadoks, R. N., Davies, H. D., and Manning, S. D. (2014) Pilus distribution among lineages of group b streptococcus: an evolutionary and clinical perspective. *BMC microbiology* **14**, 159
49. Madzivhandila, M., Adrian, P. V., Cutland, C. L., Kuwanda, L., and Madhi, S. A. (2013) Distribution of pilus islands of group B streptococcus associated with maternal colonization and invasive disease in South Africa. *Journal of medical microbiology* **62**, 249-253
50. Rosini, R., Rinaudo, C. D., Soriani, M., Lauer, P., Mora, M., Maione, D., Taddei, A., Santi, I., Ghezzo, C., Brettoni, C., Buccato, S., Margarit, I., Grandi, G., and Telford, J. L. (2006) Identification of novel genomic islands coding for antigenic pilus-like structures in Streptococcus agalactiae. *Mol Microbiol* **61**, 126-141
51. Waksman, G., and Hultgren, S. J. (2009) Structural biology of the chaperone-usher pathway of pilus biogenesis. *Nat Rev Microbiol* **7**, 765-774
52. Telford, J. L., Barocchi, M. A., Margarit, I., Rappuoli, R., and Grandi, G. (2006) Pili in gram-positive pathogens. *Nature reviews. Microbiology* **4**, 509-519
53. Kang, H. J., and Baker, E. N. Structure and assembly of Gram-positive bacterial pili: unique covalent polymers. *Curr Opin Struct Biol* **22**, 200-207
54. Mandlik, A., Das, A., and Ton-That, H. (2008) The molecular switch that activates the cell wall anchoring step of pilus assembly in gram-positive bacteria. *Proc Natl Acad Sci U S A* **105**, 14147-14152
55. Ton-That, H., and Schneewind, O. (2003) Assembly of pili on the surface of Corynebacterium diphtheriae. *Mol Microbiol* **50**, 1429-1438
56. Ton-That, H., and Schneewind, O. (2004) Assembly of pili in Gram-positive bacteria. *Trends Microbiol* **12**, 228-234
57. Ton-That, H., Marraffini, L. A., and Schneewind, O. (2004) Protein sorting to the cell wall envelope of Gram-positive bacteria. *Biochim Biophys Acta* **1694**, 269-278
58. Kang, H. J., and Baker, E. N. (2012) Structure and assembly of Gram-positive bacterial pili: unique covalent polymers. *Curr Opin Struct Biol* **22**, 200-207
59. Nobbs, A. H., Rosini, R., Rinaudo, C. D., Maione, D., Grandi, G., and Telford, J. L. (2008) Sortase A utilizes an ancillary protein anchor for efficient cell wall anchoring of pili in Streptococcus agalactiae. *Infection and immunity* **76**, 3550-3560
60. Ton-That, H., Marraffini, L. A., and Schneewind, O. (2004) Sortases and pilin elements involved in pilus assembly of Corynebacterium diphtheriae. *Mol Microbiol* **53**, 251-261

61. Yeates, T. O., and Clubb, R. T. (2007) Biochemistry. How some pili pull. *Science* **318**, 1558-1559
62. Cozzi, R., Nuccitelli, A., D'Onofrio, M., Necchi, F., Rosini, R., Zerbini, F., Biagini, M., Norais, N., Beier, C., Telford, J. L., Grandi, G., Assfalg, M., Zacharias, M., Maione, D., and Rinaudo, C. D. (2012) New insights into the role of the glutamic acid of the E-box motif in group B Streptococcus pilus 2a assembly. *Faseb j* **26**, 2008-2018
63. Hendrickx, A. P., Budzik, J. M., Oh, S. Y., and Schneewind, O. Architects at the bacterial surface - sortases and the assembly of pili with isopeptide bonds. *Nat Rev Microbiol* **9**, 166-176
64. Kang, H. J., and Baker, E. N. Intramolecular isopeptide bonds: protein crosslinks built for stress? *Trends Biochem Sci* **36**, 229-237
65. Kang, H. J., Coulibaly, F., Clow, F., Proft, T., and Baker, E. N. (2007) Stabilizing isopeptide bonds revealed in gram-positive bacterial pilus structure. *Science* **318**, 1625-1628
66. Kang, H. J., Paterson, N. G., Gaspar, A. H., Ton-That, H., and Baker, E. N. (2009) The Corynebacterium diphtheriae shaft pilin SpaA is built of tandem Ig-like modules with stabilizing isopeptide and disulfide bonds. *Proc Natl Acad Sci U S A* **106**, 16967-16971
67. Kang, H. J., Paterson, N. G., Kim, C. U., Middleditch, M., Chang, C., Ton-That, H., and Baker, E. N. (2014) A slow-forming isopeptide bond in the structure of the major pilin SpaD from Corynebacterium diphtheriae has implications for pilus assembly. *Acta crystallographica* **70**, 1190-1201
68. Mishra, A., Devarajan, B., Reardon, M. E., Dwivedi, P., Krishnan, V., Cisar, J. O., Das, A., Narayana, S. V., and Ton-That, H. (2011) Two autonomous structural modules in the fimbrial shaft adhesin FimA mediate Actinomyces interactions with streptococci and host cells during oral biofilm development. *Mol Microbiol* **81**, 1205-1220
69. Persson, K., Esberg, A., Claesson, R., and Stromberg, N. (2012) The pilin protein FimP from Actinomyces oris: crystal structure and sequence analyses. *PLoS One* **7**, e48364
70. Spraggon, G., Koesema, E., Scarselli, M., Malito, E., Biagini, M., Norais, N., Emolo, C., Barocchi, M. A., Giusti, F., Hilleringmann, M., Rappuoli, R., Lesley, S., Covacci, A., Masignani, V., and Ferlenghi, I. (2010) Supramolecular organization of the repetitive backbone unit of the Streptococcus pneumoniae pilus. *PLoS One* **5**, e10919
71. Gentile, M. A., Melchiorre, S., Emolo, C., Moschioni, M., Gianfaldoni, C., Pancotto, L., Ferlenghi, I., Scarselli, M., Pansegrau, W., Veggi, D., Merola, M., Cantini, F., Ruggiero, P., Banci, L., and Masignani, V. (2011) Structural and functional characterization of the Streptococcus pneumoniae RrgB pilus backbone D1 domain. *J Biol Chem* **286**, 14588-14597
72. El Mortaji, L., Contreras-Martel, C., Moschioni, M., Ferlenghi, I., Manzano, C., Vernet, T., Dessen, A., and Di Guilmi, A. M. (2012) The full-length Streptococcus pneumoniae major pilin RrgB crystallizes in a fibre-like structure, which presents the D1 isopeptide bond and provides details on the mechanism of pilus polymerization. *The Biochemical journal* **441**, 833-841
73. Paterson, N. G., and Baker, E. N. (2011) Structure of the full-length major pilin from Streptococcus pneumoniae: implications for isopeptide bond formation in gram-positive bacterial pili. *PLoS One* **6**, e22095
74. Izore, T., Contreras-Martel, C., El Mortaji, L., Manzano, C., Terrasse, R., Vernet, T., Di Guilmi, A. M., and Dessen, A. (2010) Structural basis of host cell recognition by the pilus adhesin from Streptococcus pneumoniae. *Structure* **18**, 106-115

75. Krishnan, V., Dwivedi, P., Kim, B. J., Samal, A., Macon, K., Ma, X., Mishra, A., Doran, K. S., Ton-That, H., and Narayana, S. V. (2013) Structure of Streptococcus agalactiae tip pilin GBS104: a model for GBS pili assembly and host interactions. *Acta crystallographica. Section D, Biological crystallography* **69**, 1073-1089
76. Krishnan, V., Gaspar, A. H., Ye, N., Mandlik, A., Ton-That, H., and Narayana, S. V. (2007) An IgG-like domain in the minor pilin GBS52 of Streptococcus agalactiae mediates lung epithelial cell adhesion. *Structure* **15**, 893-903
77. Vengadesan, K., Ma, X., Dwivedi, P., Ton-That, H., and Narayana, S. V. (2011) A model for group B Streptococcus pilus type 1: the structure of a 35-kDa C-terminal fragment of the major pilin GBS80. *J Mol Biol* **407**, 731-743
78. Budzik, J. M., Poor, C. B., Faull, K. F., Whitelegge, J. P., He, C., and Schneewind, O. (2009) Intramolecular amide bonds stabilize pili on the surface of bacilli. *Proc Natl Acad Sci U S A* **106**, 19992-19997
79. Spirig, T., Weiner, E. M., and Clubb, R. T. (2011) Sortase enzymes in Gram-positive bacteria. *Molecular microbiology* **82**, 1044-1059
80. Marraffini, L. A., Dedent, A. C., and Schneewind, O. (2006) Sortases and the art of anchoring proteins to the envelopes of gram-positive bacteria. *Microbiology and molecular biology reviews : MMBR* **70**, 192-221
81. Mazmanian, S. K., Ton-That, H., and Schneewind, O. (2001) Sortase-catalysed anchoring of surface proteins to the cell wall of Staphylococcus aureus. *Molecular microbiology* **40**, 1049-1057
82. Ton-That, H., Liu, G., Mazmanian, S. K., Faull, K. F., and Schneewind, O. (1999) Purification and characterization of sortase, the transpeptidase that cleaves surface proteins of Staphylococcus aureus at the LPXTG motif. *Proc Natl Acad Sci U S A* **96**, 12424-12429
83. Nguyen, H. D., Phan, T. T., and Schumann, W. Analysis and application of Bacillus subtilis sortases to anchor recombinant proteins on the cell wall. *AMB Express* **1**, 22
84. Comfort, D., and Clubb, R. T. (2004) A comparative genome analysis identifies distinct sorting pathways in gram-positive bacteria. *Infection and immunity* **72**, 2710-2722
85. Dramsi, S., Trieu-Cuot, P., and Bierne, H. (2005) Sorting sortases: a nomenclature proposal for the various sortases of Gram-positive bacteria. *Res Microbiol* **156**, 289-297
86. Papadopoulos, J. S., and Agarwala, R. (2007) COBALT: constraint-based alignment tool for multiple protein sequences. *Bioinformatics (Oxford, England)* **23**, 1073-1079
87. Naik, M. T., Suree, N., Ilangovan, U., Liew, C. K., Thieu, W., Campbell, D. O., Clemens, J. J., Jung, M. E., and Clubb, R. T. (2006) Staphylococcus aureus Sortase A transpeptidase. Calcium promotes sorting signal binding by altering the mobility and structure of an active site loop. *J Biol Chem* **281**, 1817-1826
88. Maresso, A. W., Chapa, T. J., and Schneewind, O. (2006) Surface protein IsdC and Sortase B are required for heme-iron scavenging of Bacillus anthracis. *J Bacteriol* **188**, 8145-8152
89. Pallen, M. J., Lam, A. C., Antonio, M., and Dunbar, K. (2001) An embarrassment of sortases - a richness of substrates? *Trends Microbiol* **9**, 97-102
90. Pallen, M. J., Chaudhuri, R. R., and Henderson, I. R. (2003) Genomic analysis of secretion systems. *Curr Opin Microbiol* **6**, 519-527
91. Cozzi, R., Malito, E., Nuccitelli, A., D'Onofrio, M., Martinelli, M., Ferlenghi, I., Grandi, G., Telford, J. L., Maione, D., and Rinaudo, C. D. (2011) Structure analysis and site-directed mutagenesis of defined key residues and motives for pilus-related sortase C1 in group B Streptococcus. *Faseb j* **25**, 1874-1886

92. Necchi, F., Nardi-Dei, V., Biagini, M., Assfalg, M., Nuccitelli, A., Cozzi, R., Norais, N., Telford, J. L., Rinaudo, C. D., Grandi, G., and Maione, D. (2011) Sortase A substrate specificity in GBS pilus 2a cell wall anchoring. *PloS one* **6**, e25300
93. Manzano, C., Contreras-Martel, C., El Mortaji, L., Izore, T., Fenel, D., Vernet, T., Schoehn, G., Di Guilmi, A. M., and Dessen, A. (2008) Sortase-mediated pilus fiber biogenesis in Streptococcus pneumoniae. *Structure (London, England : 1993)* **16**, 1838-1848
94. Neiers, F., Madhurantakam, C., Falker, S., Manzano, C., Dessen, A., Normark, S., Henriques-Normark, B., and Achour, A. (2009) Two crystal structures of pneumococcal pilus sortase C provide novel insights into catalysis and substrate specificity. *J Mol Biol* **393**, 704-716
95. Cozzi, R., Prigozhin, D., Rosini, R., Abate, F., Bottomley, M. J., Grandi, G., Telford, J. L., Rinaudo, C. D., Maione, D., and Alber, T. (2012) Structural basis for group B streptococcus pilus 1 sortases C regulation and specificity. *PloS one* **7**, e49048
96. Khare, B., Fu, Z. Q., Huang, I. H., Ton-That, H., and Narayana, S. V. (2011) The crystal structure analysis of group B Streptococcus sortase C1: a model for the "lid" movement upon substrate binding. *J Mol Biol* **414**, 563-577
97. Persson, K. (2011) Structure of the sortase AcSrtC-1 from Actinomyces oris. *Acta Crystallogr D Biol Crystallogr* **67**, 212-217
98. Lu, G., Qi, J., Gao, F., Yan, J., Tang, J., and Gao, G. F. (2011) A novel "open-form" structure of sortaseC from Streptococcus suis. *Proteins* **79**, 2764-2769
99. Manzano, C., Izore, T., Job, V., Di Guilmi, A. M., and Dessen, A. (2009) Sortase activity is controlled by a flexible lid in the pilus biogenesis mechanism of gram-positive pathogens. *Biochemistry* **48**, 10549-10557
100. Zong, Y., Bice, T. W., Ton-That, H., Schneewind, O., and Narayana, S. V. (2004) Crystal structures of Staphylococcus aureus sortase A and its substrate complex. *J Biol Chem* **279**, 31383-31389
101. Zong, Y., Mazmanian, S. K., Schneewind, O., and Narayana, S. V. (2004) The structure of sortase B, a cysteine transpeptidase that tethers surface protein to the Staphylococcus aureus cell wall. *Structure* **12**, 105-112
102. Weiner, E. M., Robson, S., Marohn, M., and Clubb, R. T. The Sortase A enzyme that attaches proteins to the cell wall of Bacillus anthracis contains an unusual active site architecture. *J Biol Chem* **285**, 23433-23443
103. Khare, B., Krishnan, V., Rajashankar, K. R., H, I. H., Xin, M., Ton-That, H., and Narayana, S. V. (2011) Structural differences between the Streptococcus agalactiae housekeeping and pilus-specific sortases: SrtA and SrtC1. *PLoS One* **6**, e22995
104. Wu, C., Mishra, A., Reardon, M. E., Huang, I. H., Counts, S. C., Das, A., and Ton-That, H. Structural determinants of Actinomyces sortase SrtC2 required for membrane localization and assembly of type 2 fimbriae for interbacterial coaggregation and oral biofilm formation. *J Bacteriol* **194**, 2531-2539
105. Viguera, A. R., and Serrano, L. (1995) Side-chain interactions between sulfur-containing amino acids and phenylalanine in alpha-helices. *Biochemistry* **34**, 8771-8779
106. Guttilla, I. K., Gaspar, A. H., Swierczynski, A., Swaminathan, A., Dwivedi, P., Das, A., and Ton-That, H. (2009) Acyl enzyme intermediates in sortase-catalyzed pilus morphogenesis in gram-positive bacteria. *J Bacteriol* **191**, 5603-5612
107. Nakata, M., Koller, T., Moritz, K., Ribardo, D., Jonas, L., McIver, K. S., Sumitomo, T., Terao, Y., Kawabata, S., Podbielski, A., and Kreikemeyer, B. (2009) Mode of expression and functional characterization of FCT-3 pilus region-encoded proteins in Streptococcus pyogenes serotype M49. *Infect Immun* **77**, 32-44

108. Banci, L., Bertini, I., Durazo, A., Girotto, S., Gralla, E. B., Martinelli, M., Valentine, J. S., Vieru, M., and Whitelegge, J. P. (2007) Metal-free superoxide dismutase forms soluble oligomers under physiological conditions: a possible general mechanism for familial ALS. *Proc Natl Acad Sci U S A* **104**, 11263-11267
109. Vagin, A., and Teplyakov, A. (1997) MOLREP: an automated program for molecular replacement. *Journal of Applied Crystallography* **30**, 1022-1025
110. Holm, L., and Rosenstrom, P. (2010) Dali server: conservation mapping in 3D. *Nucleic Acids Res* **38**, W545-549
111. Doran, K. S., Liu, G. Y., and Nizet, V. (2003) Group B streptococcal beta-hemolysin/cytolysin activates neutrophil signaling pathways in brain endothelium and contributes to development of meningitis. *J Clin Invest* **112**, 736-744
112. Doran, K. S., Engelson, E. J., Khosravi, A., Maisey, H. C., Fedtke, I., Equils, O., Michelsen, K. S., Arditi, M., Peschel, A., and Nizet, V. (2005) Blood-brain barrier invasion by group B Streptococcus depends upon proper cell-surface anchoring of lipoteichoic acid. *J Clin Invest* **115**, 2499-2507
113. Patras, K. A., Wang, N. Y., Fletcher, E. M., Cavaco, C. K., Jimenez, A., Garg, M., Fierer, J., Sheen, T. R., Rajagopal, L., and Doran, K. S. (2013) Group B Streptococcus CovR regulation modulates host immune signalling pathways to promote vaginal colonization. *Cellular microbiology* **15**, 1154-1167
114. Furr, P. M., Hetherington, C. M., and Taylor-Robinson, D. (1989) The susceptibility of germ-free, oestradiol-treated, mice to Mycoplasma hominis. *Journal of medical microbiology* **30**, 233-236
115. Koiter, T. R., Hazenberg, M. P., and van der Schoot, P. (1977) Regulation of the bacterial microflora of the vagina in cyclic female rats. *The Journal of experimental zoology* **202**, 121-128
116. Larsen, B., Markovetz, A. J., and Galask, R. P. (1977) Role of estrogen in controlling the genital microflora of female rats. *Applied and environmental microbiology* **34**, 534-540
117. Marraffini, L. A., and Schneewind, O. (2007) Sortase C-mediated anchoring of BasI to the cell wall envelope of Bacillus anthracis. *J Bacteriol* **189**, 6425-6436
118. Swaminathan, A., Mandlik, A., Swierczynski, A., Gaspar, A., Das, A., and Ton-That, H. (2007) Housekeeping sortase facilitates the cell wall anchoring of pilus polymers in Corynebacterium diphtheriae. *Mol Microbiol* **66**, 961-974
119. Barnett, T. C., Patel, A. R., and Scott, J. R. (2004) A novel sortase, SrtC2, from Streptococcus pyogenes anchors a surface protein containing a QVPTGV motif to the cell wall. *J Bacteriol* **186**, 5865-5875
120. Marraffini, L. A., and Schneewind, O. (2006) Targeting proteins to the cell wall of sporulating Bacillus anthracis. *Mol Microbiol* **62**, 1402-1417
121. Cozzi, R., Zerbini, F., Assfalg, M., D'Onofrio, M., Biagini, M., Martinelli, M., Nuccitelli, A., Norais, N., Telford, J. L., Maione, D., and Rinaudo, C. D. (2013) Group B Streptococcus pilus sortase regulation: a single mutation in the lid region induces pilin protein polymerization in vitro. *FASEB journal : official publication of the Federation of American Societies for Experimental Biology* **27**, 3144-3154
122. Zahner, D., and Scott, J. R. (2008) SipA is required for pilus formation in Streptococcus pyogenes serotype M3. *Journal of bacteriology* **190**, 527-535
123. Kang, H. J., Coulibaly, F., Proft, T., and Baker, E. N. (2011) Crystal structure of Spy0129, a Streptococcus pyogenes class B sortase involved in pilus assembly. *PloS one* **6**, e15969
124. Mishra, A., Das, A., Cisar, J. O., and Ton-That, H. (2007) Sortase-catalyzed assembly of distinct heteromeric fimbriae in Actinomyces naeslundii. *Journal of bacteriology* **189**, 3156-3165

125. Bagnoli, F., Moschioni, M., Donati, C., Dimitrovska, V., Ferlenghi, I., Facciotti, C., Muzzi, A., Giusti, F., Emolo, C., Sinisi, A., Hilleringmann, M., Pansegrau, W., Censini, S., Rappuoli, R., Covacci, A., Masignani, V., and Barocchi, M. A. (2008) A second pilus type in Streptococcus pneumoniae is prevalent in emerging serotypes and mediates adhesion to host cells. *Journal of bacteriology* **190**, 5480-5492
126. Okura, M., Osaki, M., Fittipaldi, N., Gottschalk, M., Sekizaki, T., and Takamatsu, D. (2011) The minor pilin subunit Sgp2 is necessary for assembly of the pilus encoded by the srtG cluster of Streptococcus suis. *Journal of bacteriology* **193**, 822-831
127. Maione, D., Margarit, I., Rinaudo, C. D., Masignani, V., Mora, M., Scarselli, M., Tettelin, H., Brettoni, C., Iacobini, E. T., Rosini, R., D'Agostino, N., Miorin, L., Buccato, S., Mariani, M., Galli, G., Nogarotto, R., Nardi-Dei, V., Vegni, F., Fraser, C., Mancuso, G., Teti, G., Madoff, L. C., Paoletti, L. C., Rappuoli, R., Kasper, D. L., Telford, J. L., and Grandi, G. (2005) Identification of a universal Group B streptococcus vaccine by multiple genome screen. *Science* **309**, 148-150
128. Tazi, A., Bellais, S., Tardieux, I., Dramsi, S., Trieu-Cuot, P., and Poyart, C. (2012) Group B Streptococcus surface proteins as major determinants for meningeal tropism. *Curr Opin Microbiol* **15**, 44-49
129. Tazi, A., Disson, O., Bellais, S., Bouaboud, A., Dmytruk, N., Dramsi, S., Mistou, M. Y., Khun, H., Mechler, C., Tardieux, I., Trieu-Cuot, P., Lecuit, M., and Poyart, C. (2010) The surface protein HvgA mediates group B streptococcus hypervirulence and meningeal tropism in neonates. *The Journal of experimental medicine* **207**, 2313-2322
130. Seo, H. S., Mu, R., Kim, B. J., Doran, K. S., and Sullam, P. M. (2012) Binding of glycoprotein Srr1 of Streptococcus agalactiae to fibrinogen promotes attachment to brain endothelium and the development of meningitis. *PLoS pathogens* **8**, e1002947
131. van Sorge, N. M., Quach, D., Gurney, M. A., Sullam, P. M., Nizet, V., and Doran, K. S. (2009) The group B streptococcal serine-rich repeat 1 glycoprotein mediates penetration of the blood-brain barrier. *The Journal of infectious diseases* **199**, 1479-1487
132. Chang, Y. C., Wang, Z., Flax, L. A., Xu, D., Esko, J. D., Nizet, V., and Baron, M. J. (2011) Glycosaminoglycan binding facilitates entry of a bacterial pathogen into central nervous systems. *PLoS pathogens* **7**, e1002082
133. Brittan, J. L., and Nobbs, A. H. (2015) Group B Streptococcus pili mediate adherence to salivary glycoproteins. *Microbes Infect*
134. Sharma, P., Lata, H., Arya, D. K., Kashyap, A. K., Kumar, H., Dua, M., Ali, A., and Johri, A. K. (2013) Role of pilus proteins in adherence and invasion of Streptococcus agalactiae to the lung and cervical epithelial cells. *J Biol Chem* **288**, 4023-4034
135. Chattopadhyay, D., Carey, A. J., Caliot, E., Webb, R. I., Layton, J. R., Wang, Y., Bohnsack, J. F., Adderson, E. E., and Ulett, G. C. (2011) Phylogenetic lineage and pilus protein Spb1/SAN1518 affect opsonin-independent phagocytosis and intracellular survival of Group B Streptococcus. *Microbes and infection / Institut Pasteur* **13**, 369-382
136. Adderson, E. E., Takahashi, S., Wang, Y., Armstrong, J., Miller, D. V., and Bohnsack, J. F. (2003) Subtractive hybridization identifies a novel predicted protein mediating epithelial cell invasion by virulent serotype III group B Streptococcus agalactiae. *Infection and immunity* **71**, 6857-6863
137. Maisey, H. C., Quach, D., Hensler, M. E., Liu, G. Y., Gallo, R. L., Nizet, V., and Doran, K. S. (2008) A group B streptococcal pilus protein promotes phagocyte resistance and systemic virulence. *Faseb j* **22**, 1715-1724

138. Tamura, G. S., Kuypers, J. M., Smith, S., Raff, H., and Rubens, C. E. (1994) Adherence of group B streptococci to cultured epithelial cells: roles of environmental factors and bacterial surface components. *Infection and immunity* **62**, 2450-2458
139. Pezzicoli, A., Santi, I., Lauer, P., Rosini, R., Rinaudo, D., Grandi, G., Telford, J. L., and Soriani, M. (2008) Pilus backbone contributes to group B Streptococcus paracellular translocation through epithelial cells. *J Infect Dis* **198**, 890-898
140. Sheen, T. R., Jimenez, A., Wang, N. Y., Banerjee, A., van Sorge, N. M., and Doran, K. S. (2011) Serine-rich repeat proteins and pili promote Streptococcus agalactiae colonization of the vaginal tract. *Journal of bacteriology* **193**, 6834-6842
141. Tamura, G. S., and Rubens, C. E. (1995) Group B streptococci adhere to a variant of fibronectin attached to a solid phase. *Molecular microbiology* **15**, 581-589
142. Robert, X., and Gouet, P. (2014) Deciphering key features in protein structures with the new ENDscript server. *Nucleic acids research* **42**, W320-324
143. Horton, R. M., Hunt, H. D., Ho, S. N., Pullen, J. K., and Pease, L. R. (1989) Engineering hybrid genes without the use of restriction enzymes: gene splicing by overlap extension. *Gene* **77**, 61-68
144. Framson, P. E., Nittayajarn, A., Merry, J., Youngman, P., and Rubens, C. E. (1997) New genetic techniques for group B streptococci: high-efficiency transformation, maintenance of temperature-sensitive pWV01 plasmids, and mutagenesis with Tn917. *Applied and environmental microbiology* **63**, 3539-3547
145. Lauer, P., Rinaudo, C. D., Soriani, M., Margarit, I., Maione, D., Rosini, R., Taddei, A. R., Mora, M., Rappuoli, R., Grandi, G., and Telford, J. L. (2005) Genome analysis reveals pili in Group B Streptococcus. *Science* **309**, 105
146. Klock, H. E., and Lesley, S. A. (2009) The Polymerase Incomplete Primer Extension (PIPE) method applied to high-throughput cloning and site-directed mutagenesis. *Methods Mol Biol* **498**, 91-103
147. Kabsch, W. (2010) Xds. *Acta Crystallographica D* **66**, 125-132
148. 4, C. C. P. N. (1994) The CCP4 suite: programs for protein crystallography. *Acta Crystallographica D* **50**, 760-763
149. Vagin, A., and Teplyakov, A. (1997) MOLREP: an automated program for molecular replacement. *Journal of Applied Crystallography* **30**, 1022-1025
150. Adams, P. D., Afonine, P. V., Bunkóczi, G., Chen, V. B., Davis, I. W., Echols, N., Headd, J. J., Hung, L. W., Kapral, G. J., Grosse-Kunstleve, R. W., Mccoy, A. J., Moriarty, N. W., Oeffner, R., Read, R. J., Richardson, D. C., Richardson, J. S., Terwilliger, T. C., and Zwart, P. H. (2010) PHENIX: a comprehensive Python-based system for macromolecular structure solution. *Acta Crystallographica D* **66**, 213-221
151. Emsley, P., Lohkamp, B., Scott, W. G., and Cowtan, K. (2010) Features and development of Coot. *Acta Crystallographica D* **66**, 486-501
152. Sklenar, V., Brooks, B. R., Zon, G., and Bax, A. (1987) Absorption mode two-dimensional NOE spectroscopy of exchangeable protons in oligonucleotides. *FEBS Lett* **216**, 249-252
153. Rinaudo, C. D., Rosini, R., Galeotti, C. L., Berti, F., Necchi, F., Reguzzi, V., Ghezzo, C., Telford, J. L., Grandi, G., and Maione, D. (2010) Specific involvement of pilus type 2a in biofilm formation in group B Streptococcus. *PloS one* **5**, e9216
154. Perez-Casal, J. F., Dillon, H. F., Husmann, L. K., Graham, B., and Scott, J. R. (1993) Virulence of two Streptococcus pyogenes strains (types M1 and M3) associated with toxic-shock-like syndrome depends on an intact mry-like gene. *Infection and immunity* **61**, 5426-5430
155. Cozzi R., Malito E., Lazzarin M., Nuccitelli A., Castagnetti A., Bottomley M. J.,

Margarit I., Maione D., Rinaudo C. D. (2015) Structure and assembly of Group B Streptococcus pilus 2b backbone protein. *Manuscript submitted for publication*

Acknowledgments

Finally this PhD has come to an end and I have to thank all the people without which this PhD would not have been possible.
First of all I would like to thank Prof. Vincenzo Scarlato and the University of Bologna, for giving me the opportunity to take a PhD in Cell and Molecular Biology and my supervisor Daniela Rinaudo for her constant help, support and patience.
I would like to thank Roberta Cozzi and Manuele Martinelli for always helping me and answering to all my questions whenever I needed it.
I thank also Enrico Malito for the X-ray experiments and Mariapina D'Onofrio from the University of Verona for having performed NMR experiments.

I also want to thank the project leader Immaculada Margarit Y Ros for having supervised my work and for giving me the opportunity to spend three months at San Diego State University.
It was an amazing experience both from a scientific and personal point of view, and I thank Professor Kelly Doran for having welcomed me into her wonderful group and having helped me during that period.
Many thanks to Rong Mu for the huge help in the lab, the infinite patience that she had in explaining and teaching to me everything in the lab and in helping me writing down the paper, but especially for her great friendship since the early days.
Special thanks also to the guys in the SDSU group for helping me in many things, not only in the lab: many thanks to Thomas, Katy, Berenice, Lauryn, Andres, Bryan and especially to Brandon Kim for being also a great friend.

Then I would like to thank all the people who have supported me everyday in Novartis starting from the lab mates Roberto Rosini and Edmondo Campisi. I thank the coolest office mates ever Emiliano Chiarot and Alessia Corrado for their help with Evil&Graphpad (of which I can now proudly declare myself a proficient user) and for all the good times we had together. Finally, a special thanks goes to those two girls that made me learn and love the Neapolitan dialect and have

always helped me and cheered me up: many thanks to Maria Giuliani and Francesca Zerbini.

But a huge thanks goes to all the friends, PhD students and not, that in these three years became my family here in Siena and that I love. I would like to thank for their friendship and for all the moments of joy and despair shared together Cristina Bruno, Sandra Lazzaro, Valentina Agnolon, Chiara Toniolo, Pasquale Marrazzo, Luigi Scietti, Lorenzo Argante, Alberto Nilo, Giuseppe Lofano, Serafina Guadagnuolo and Simona Castellana.

Finally, I have to thank for the constant presence and love obviously my family, mom dad and Vasco , my special friends Fiore, Fra and Laura that despite being so far away I feel as if we had never separated, and Enrico because some things never change (cit.) .